Metals and Methanotrophs: 1. Genetic and Biochemical Characterization of the Uptake and Synthesis of Methanobactin; 2. Bioinformatic Analyses of the Effect of Rare Earth Elements on Gene Expression.

by

Wenyu Gu

A dissertation submitted in partial fulfillment
of the requirements for the degree of
Doctor of Philosophy
(Environmental Engineering)
in The University of Michigan
2017

Doctoral Committee:

Professor Jeremy D. Semrau, Chair
Associate Professor Christian M. Lastoskie
Professor J. Colin Murrell, University of East Anglia, UK
Associate Professor Patrick D. Schloss

Wenyu Gu

gwenyu@umich.edu

ORCID iD: 0000-0001-8370-1715

ACKNOWLEDGEMENTS

I would like to thank Professor Jeremy D. Semrau for all his teaching, motivation and financial support, via the Department of Energy. I am grateful for his constant encouragement, patience, and invaluable suggestions. This work could not be possible without his help.

I would also like to thank my committee members, Professor Christian M. Lastoskie, J. Colin Murrell, and Patrick D. Schloss, for the teachings and comments they provided in my progress toward the doctoral degree. I would also like to especially thank Professor Alan A. Dispirito and his Ph.D. student Bipin S. Baral for providing priceless advice and help on the development of this study.

My gratitude also goes to my colleagues and friends in Semrau Lab with whom I had the privilege to work and spend time together. I am thankful to Alexey Vorobev and Bhagyalakshmi Kalidass, for helping me settle down in the laboratory, teaching me experimental techniques, and providing useful discussions. I am especially thankful to Muhammad Farhan Ul Haque, for his patience and excellent training of me on RT-qPCR and genetic cloning. I sincerely thank Thomas Yavaraski for all the help he provided with the analytical instruments. I am grateful to my friends for their moral support. My time at

UM was made enjoyable in large part due to the many friends that became a part of my life.

I am most indebted to my parents, Kebin Gu and Qing Yang, for their continuous understanding, motivation, and support at all times.

Finally, I want to thank the University of Michigan, where I met all these nice people and had a wonderful time.

TABLE OF CONTENTS

LIST OF TABLES

LIST OF FIGURES

ABSTRACT

Methanotrophs are a group of bacteria that use methane as their sole carbon and energy source. These microbes have various applications including methane removal, biodegradation of halogenated hydrocarbons, and valorization of methane to various products including biofuels, bioplastics, and single cell protein. Current obstacles for the application of aerobic methanotrophs include our incomplete understanding of their metabolism and genetics. This work studies the methanotrophic response to metals, i.e., copper and rare earth elements, with the goal of achieving better control of methanotrophic activity.

The expression and activities of alternative forms of methane monooxygenases in methanotrophs are regulated by the availability of copper. The genetic regulation by copper in methanotrophs involves in a copper-chelating molecule called methanobactin (mb) produced by methanotrophs. First, the uptake mechanism of mb was investigated. *mbnT,* encoding for TonB-dependent transporter, was knocked-out in *Methylosinus trichosporium* OB3b. The mutant was able to synthesize and secrete mb but not take it up as evidenced by significant decrease in copper uptake when grown at presence of exogenous mb. The mutant was, however, still able to take up free copper, indicating that there is (are) alternative copper uptake pathway(s) in *M. trichosporium* OB3b. Second, the biosynthesitic pathway of mb was investigated. Specifically, *mbnN,* encoding for an

aminotransferase, was disrupted in *M. trichosporium* OB3b. mb produced by this mutant has only one of the two oxazolone rings and the C-terminal methionine was missing. This study lays the foundation for achieving fine-tuning mb structure and for enhancing its production for potential applications.

In addition to copper, it was found that cerium also regulates key enzymes in methanotrophs, i.e., alternative forms of methanol dehydrogenases (MeDHs). This finding was first extended to consider the effect of other rare earth elements (REEs). It was found that lanthanum, praseodymium, neodymium and samarium also regulate the expression of MeDHs in *M. trichosporium* OB3b. These effects, however, were only observed in the absence of copper, indicating cross-regulation by copper and REEs. Second, the whole transcriptomic response to copper and/or cerium in *M. trichosporium* OB3b was studied using transcriptomic analyses. Interestingly, the largest difference in gene expression was observed when both copper and cerium were present. Many genes were upregulated, most notably multiple steps of the central methane oxidation pathway, the serine cycle, and the ethylmalonyl-CoA pathway, indicating more efficient carbon assimilation.

Lastly, attempts were made to elucidate alternative mechanism(s) of copper uptake in *M. trichosporium* OB3b. Specifically, *copCD,* putatively encoding for a periplasmic copper-binding protein and an inner membrane protein, respectively, were knocked out in

wildtype and a mb-defective mutant of *M. trichosporium* OB3b. Our results showed that these genes are not critical for copper uptake nor were they basis of copper-regulation in *M. trichosporium* OB3b.

CHAPTER I INTRODUCTION

I.1 Ecological and phylogenetic diversity of methanotrophs

Methanotrophs are an intriguing group of microorganisms that utilize methane as their sole source of carbon and energy. Two key functional groups of microorganisms, i.e., aerobic methane-oxidizing bacteria, and anaerobic methane-oxidizing archaea (ANME), fall into this definition. This study focuses on aerobic methane-oxidizing bacteria. There is great deal of interest in these microbes as they: (1) are ubiquitously distributed in the nature and are phylogenetically diverse; (2) play important roles in the global carbon cycle, e.g., they can remove methane from the atmosphere (Holmes et al., 1999; Roslev & Iversen, 1999, Dunfield et al., 1999, Knief & Dunfield, 2005, Kolb et al., 2005); (3) have been extensively used for biodegradation of halogenated hydrocarbons (Westrick et al., 1984, Wilson & Wilson, 1985, Semprini, 1997, Semrau et al., 2010); and (4) have great potential in promoting sustainability by valorizing methane to biofuels, bioplastics, and osmo-protectants, amongst other products (Fei et al., 2014, Stron et al., 2014, Kalyuzhnaya et al., 2015, Khmelenina et al., 2015).

Aerobic methane-oxidizing bacteria have been studied for over a century since being first described in 1906 (Söhngen, 1906). Most commonly, aerobic methane-oxidizing bacteria are found at oxic/anoxic interfaces of environments such as wetlands, aquatic sediments,

and landfills, where they feed on methane produced by methanogenic activities in anoxic zones (Wartiainen et al., 2006, Ettwig et al., 2010, Geymonat et al., 2011). Interestingly, methanotrophic bacteria are also found in "extreme" environments. One example is *Methylacidiphilum fumariolicum* Strain SolV isolated from acidic, geothermal environments. *M. fumariolicum* SolV has an optimal growth pH of 2 and has an optimal growth temperature of 60 °C. (Castaldi & Tedesco, 2005, Dunfield et al., 2007, Pol et al., 2007, Islam et al., 2008, Op den Camp et al., 2009) Another example is the psychrophilic methanotroph, *Methylosphaera hansonii,* isolated from Antarctic, marine-salinity lakes. It can grow at 0 °C with an optimal growth temperature of 10°C and can survive NaCl concentrations as high as 12% (w/v). (Bowman, 1998) There are also alkaliphilic methanotrophs isolated from Siberian soda lakes that can tolerate pH as high as 11. (Kaluzhnaya et al., 2001) Methanotrophic bacteria have also been identified and isolated from the rhizosphere and phyllosphere (Knief et al., 2012; Bao et al., 2014; Khalifa, et al., 2015).

Corresponding to their wide geographical distribution, methanotrophs are taxonomically diverse. Methanotrophs were initially grouped into three taxonomic groups, or types I, II, and X based on their morphology, structure of intracytoplasmic membrane and pathways for carbon assimilation (Whittenbury et al., 1970). With the rise of advanced sequencing technology in the 1990s, phylogenetic analyses based on 16S rRNA sequences were applied. In the review by Hanson & Hanson (1996) , methanotrophs were grouped into six genera in the Proteobacteria, with four genera, *Methylobacter, Methylococcus, Methylomicrobium*, and *Methylomonas* in the Gammaproteobacteria (*Methylococcaceae*

family), and two genera, *Methylocystis* and *Methylosinus,* in the Alphaproteobacteria (*Methylocystaceae* family). Twenty years later, 25 genera have now been described within the Proteobacteria. 20 are in the Gammaproteobacteria and five in the Alphaproteobacteria. New genera within the Gammaproteobacteria include *Methylocaldum, Methylosarcina, Methylosoma, Methylosphaera, Methylomagnum, Methyloglobulus, Methylogaea, Methylovulum, Methyloparacoccus, Methyloprofundus,* and *Methylomarinum*, which belong to the *Methlococcaceae* family, and *Methylohalobius, Methylomarinovum,* and *Methylothermus* that belong to the *Methylothermaceae* family. There are also filamentous methanotrophs under the *Clonothrix* and *Crenothrix* genera in the Gammaproteobacteria. New genera within the Alphaproteobacteria include *Methylocella, Methylocapsa*, and *Methyloferula*, which belong to the *Beijerinkiaceae* family.

Until 2007, all known species of methanotrophic bacteria belonged to the phylum Proteobacteria phylum. However, in 2007–2008, three research groups independently described the isolation of thermoacidophilic methanotrophs as mentioned previously that represented a distinct lineage within the Verrucomicrobia phylum. (Dunfield et al., 2007, Pol et al., 2007, Islam et al., 2008, Op den Camp et al., 2009) Although these strains were isolated from distinct geographical locations (i.e., New Zealand, Italy, and Russian), their 16S rRNA gene sequences are very similar (> 98.4% identical) and are considered to represent a single genus, *Methylacidiphilum* (Op den Camp et al., 2009). Another exciting new member is *Candidatus* Methylomirabilis oxyfera, which belongs to bacterial NC10 phylum. From the genome assembled from an enrichment culture from agricultural

runoff. *C.* Methylomirabilis oxyfera was characterized and drew attention in its unique ability to couple methane oxidation to nitrite reduction, and in so doing generate oxygen required for the initial turnover of methane to methanol (Ettwig et al., 2010).

I.2 Methanotrophic metabolism

I.2.1 Methane oxidation

The diversity of methanotrophs is reflected in the diversity of their metabolism. Methanotrophs were initially considered to be obligate aerobes. It is generally accepted that they oxidize methane to carbon dioxide and water via four central steps as shown in Figure 1.1. The initial and rate-limiting step is the conversion of methane to methanol by methane monooxygenase (MMO) (Hanson & Hanson, 1996). Methanol is subsequently oxidized to formaldehyde by a periplasmic pyrroloquinoline quinine (PQQ)-linked methanol dehydrogenase (MDH). Conversion of formaldehyde to formic acid and formic acid to carbon dioxide is catalyzed by formaldehyde dehydrogenase (FADH) and formate dehydrogenase (FDH), respectively. (Hanson & Hanson, 1996)

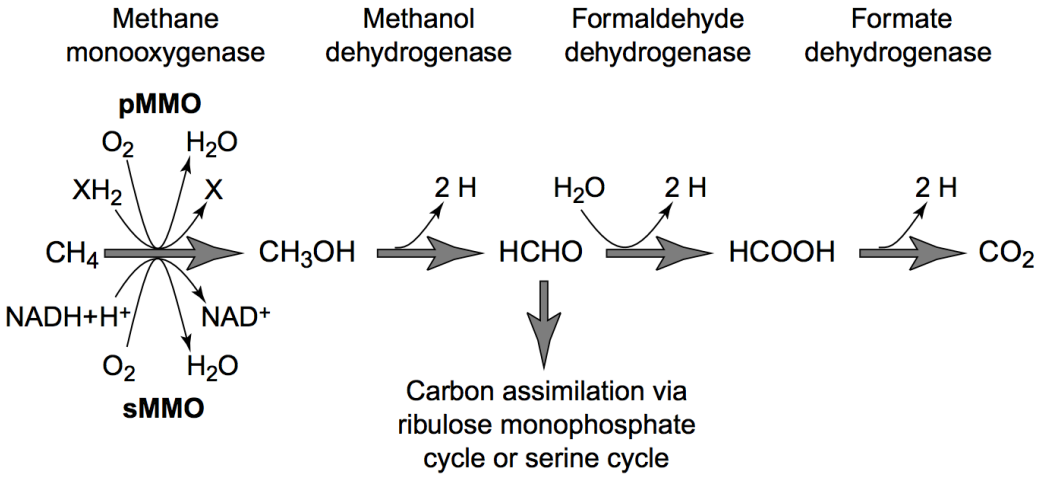

Figure 1.1. The pathway of methane oxidation by aerobic methanotrophs. NADH is the electron donor for the sMMO, but not the pMMO. X represents the unknown electron donor for the pMMO (Murrell et al. 2000).

However, anaerobic oxidation of methane has been shown to occur via three different microbial processes. First, geochemical evidence suggests a coupling of anaerobic methane oxidation with sulfate (Boetius et al., 2000, Orphan, et al., 2001), manganese, or iron reduction (Beal et al., 2009, Ettwig et al., 2016) by a consortium of archaea (i.e., ANME) and bacteria. Second, as mentioned above, *Candidatus* Methylomirabilis oxyfera of the bacterial NC10 phylum couples methane oxidation to nitrite reduction (Ettwig et al., 2010). M. oxyfera bypasses the denitrification intermediate nitrous oxide by the conversion of nitric oxide to dinitrogen and dioxygen, the latter then used to oxidize methane. This explains the biochemical mechanism of poorly understood freshwater methane sinks and shows a novel pathway for oxygen production. Third, the archaean *Candidatus* Methanoperedens nitroreducens can anaerobically oxidize methane through reverse methanogenesis with nitrate as the terminal electron acceptor (Haroon et al., 2013). The following discussion will focus on the methane oxidation pathways of aerobic methane-oxidizing bacteria.

I.2.1.1 Methane monooxygenase

The methane monooxygenase (MMO) catalyzes the oxidation of CH_4 to CH_3OH. Two distinct types of MMO are known- a cytoplasmic, soluble form (sMMO) and a membrane-bound particulate form (pMMO). pMMO is found in most methanotrophs, with exceptions of *Methylocella* and *Methyloferula* species (Dedysh et al., 2000, Dunfield et al., 2003, Vorobev et al., 2011). Some methanotrophs, such as *Methylococcus capsulatus* (Bath) and *Methylosinus trichosporium* OB3b, can express both sMMO and pMMO. (Table 1.1)

sMMO consists of three components- a hydroxylase (MMOH, 251 kDa), a reductase (MMOR, 38.6 kDa), and a regulatory protein (MMOB, 15.9 kDa) (Stirling & Dalton, 1979, Lee et al., 2013) (Figure 1.2). Methane oxidation occurs at a glutamate-bridged di-iron active site within MMOH, which has an $\alpha_2\beta_2\gamma_2$ polypeptide arrangement comprised of MmoX (α), MmoY (ß), and MmoZ (γ) subunits (Rosenzweig et al., 1993, Dalton, 2005). MMOR is a Fe-S flavoprotein that transfers electrons from NADH to MMOH (Merkx et al., 2001). The regulatory polypeptide MMOB is essential for the activity of MMOH and triggers the transformation of the enzyme from an NADH oxidase to a hydroxylase (Green & Dalton, 1985, Lee et al., 2013).

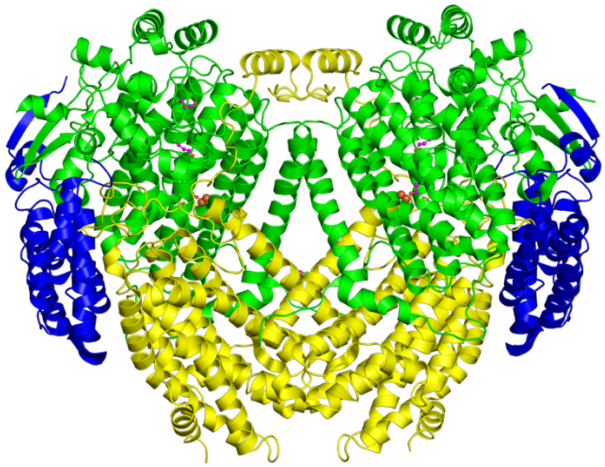

Figure 1.2. Structure of the hydroxylase component of sMMO from *Methylococcus capsulatus* Bath.
The α,β and γ subunits, encoded by the *mmoX*, *Y* and *Z* genes, are colored green, yellow and blue, respectively. The iron atoms of the binuclear iron centers are shown as pink spheres. (Sazinsky & Lippard, 2005)

pMMO is an integral membrane metalloenzyme composed of three polypeptides- PmoB, PmoA, PmoC- with molecular masses of approximately 45kDa , 26kDa, and 23kDa, respectively (Lieberman & Rosenzweig, 2005, Hakemian & Rosenzweig, 2007). Crystal structures of pMMOs from *M. capsulatus* Bath (Lieberman & Rosenzweig, 2005), *M.*

Table 1.1 Occurrence of select enzymes in the genomes of methanotrophs.

Strain	Phylum	Genera	*pmoA*	*mmoX*	*pxmA*	*mxaFI*	*xoxF*	*mbnB/C*
Methylobacter tundripaludum SV96	Gammaproteobacteria	*Methylobacter*	Yes	No	Yes	Yes	Yes	No
Methylobacter marinus A45	Gammaproteobacteria	*Methylobacter*	Yes	No	Yes	Yes	Yes	No
Methylobacter tundripaludum 21/22	Gammaproteobacteria	*Methylobacter*	Yes	No	Yes	Yes	Yes	No
Methylobacter luteus IMV-B-3098	Gammaproteobacteria	*Methylobacter*	Yes	No	Yes	Yes	Yes	No
Methylobacter tundripaludum 31/32	Gammaproteobacteria	*Methylobacter*	Yes	No	Yes	Yes	Yes	No
Methylobacter whittenburyi strain ACM	Gammaproteobacteria	*Methylobacter*	Yes	No	Yes	Yes	Yes	No
Methylobacter sp. BBA5.1	Gammaproteobacteria	*Methylobacter*	Yes	No	Yes	Yes	Yes	No
Methylocaldum szegediense O-12	Gammaproteobacteria	*Methylocaldum*	Yes	No	No	Yes	Yes	No
Methylococcus capsulatus str. Bath	Gammaproteobacteria	*Methylococcus*	Yes	Yes	No	Yes	Yes	No
Methyloglobulus morosus KoM1	Gammaproteobacteria	*Methyloglobulus*	Yes	No	Yes	Yes	Yes	No
Methylohalobius crimeensis 10Ki	Gammaproteobacteria	*Methylohalobius*	Yes	No	No	Yes	Yes	No
Methylomarinum vadi strain IT-4	Gammaproteobacteria	*Methylomarinum*	Yes	No	No	Yes	Yes	No
Methylomicrobium alcaliphilum	Gammaproteobacteria	*Methylomicrobium*	Yes	No	No	Yes	Yes	No
Methylomicrobium album BG8	Gammaproteobacteria	*Methylomicrobium*	Yes	No	Yes	Yes	Yes	No
Methylomicrobium buryatense 5G	Gammaproteobacteria	*Methylomicrobium*	Yes	Yes	No	Yes	Yes	No
Me*thylomicrobium agile* strain ATCC 35068	Gammaproteobacteria	*Methylomicrobium*	Yes	No	Yes	Yes	Yes	No
Methylomonas methanica MC09	Gammaproteobacteria	*Methylomonas*	Yes	Yes	No	Yes	Yes	No
Methylomonas sp. MK1	Gammaproteobacteria	*Methylomonas*	Yes	Yes	Yes	Yes	Yes	No
Methylomonas sp. 11b	Gammaproteobacteria	*Methylomonas*	Yes	Yes	Yes	Yes	Yes	No
Methylomonas sp. LW13	Gammaproteobacteria	*Methylomonas*	Yes	Yes	Yes	Yes	Yes	No
Methylomonas denitrificans strain FJG1	Gammaproteobacteria	*Methylomonas*	Yes	No	Yes	Yes	Yes	No
Methylosarcina fibrata AML-C10	Gammaproteobacteria	*Methylosarcina*	Yes	No	No	Yes	Yes	No
Methylosarcina lacus LW14	Gammaproteobacteria	*Methylosarcina*	Yes	No	No	Yes	Yes	No
Methylovulum miyakonense HT12	Gammaproteobacteria	*Methylovulum*	Yes	Yes	No	Yes	Yes	No

Table 1.1 Continued

Strain	Phylum	Genera	*pmoA*	*mmoX*	*pxmA*	*mxaF*	*xoxF*	*mbnB/C*
Methylocapsa acidiphila B2	Alphaproteobacteria	*Methylocapsa*	Yes	No	No	Yes	Yes	No
Methylocapsa aurea KYG	Alphaproteobacteria	*Methylocapsa*	Yes	No	No	Yes	Yes	No
Methylocella silvestris BL2	Alphaproteobacteria	*Methylocella*	No	Yes	No	Yes	Yes	No
Methylocystis sp. SB2	Alphaproteobacteria	*Methylocystis*	Yes	No	Yes	Yes	Yes	Yes
Methylocystis sp. SC2	Alphaproteobacteria	*Methylocystis*	Yes	No	No	Yes	Yes	Yes
Methylocystis rosea SV97	Alphaproteobacteria	*Methylocystis*	Yes	No	No	Yes	Yes	Yes
Methylocystis sp. ATCC 49242 strain Rockwell	Alphaproteobacteria	*Methylocystis*	Yes	No	No	Yes	Yes	No
Methylocystis parvus strain OBBP	Alphaproteobacteria	*Methylocystis*	Yes	No	No	Yes	Yes	Yes
Methyloferula stellata AR4 strain AR4T	Alphaproteobacteria	*Methyloferula*	No	Yes	No	Yes	Yes	No
Methylosinus sp. LW4	Alphaproteobacteria	*Methylosinus*	Yes	Yes	No	Yes	Yes	Yes
Methylosinus trichosporium OB3b	Alphaproteobacteria	*Methylosinus*	Yes	Yes	No	Yes	Yes	Yes
Methylosinus sp. LW3	Alphaproteobacteria	*Methylosinus*	Yes	Yes	No	Yes	Yes	Yes
Methylosinus sp. PW1	Alphaproteobacteria	*Methylosinus*	Yes	Yes	No	Yes	Yes	Yes
Methylocystis sp. LW5	Alphaproteobacteria	*Methylosystis*	Yes	Yes	No	Yes	Yes	Yes
Candidatus Methylomirabilis oxyfera	NC10	*Candidatus*	Yes	No	No	Yes	Yes	No
Methylacidiphilum fumariolicum SolV	Verrucomicrobia	*Methylacidiphilum*	Yes	No	No	No	Yes	No
Verrucomicrobia bacterium LP2A	Verrucomicrobia	*Verrucomicrobia*	Yes	No	No	No	Yes	No
Verrucomicrobium sp. 3C	Verrucomicrobia	*Verrucomicrobium*	Yes	No	No	No	Yes	No

trichosporium OB3b (Hakemian et al., 2008), and *Methylocystis* sp. strain M (Smith et al., 2011) have been determined and reveal that three copies each of the PmoB, PmoA, and PmoC subunits are arranged in an $\alpha_3\beta_3\gamma_3$ trimer (Figure 1.3). The PmoB subunit contains both periplasmic and transmembrane domains, while the PmoA and PmoC subunits are composed primarily of transmembrane helices. The metal content of pMMO is controversial, with reported values of 2-15 copper ions and 0-2 iron atoms per ~100-kDa purified pMMO (Nguyen et al., 1998, Basu et al., 2003, Choi et al., 2003, Yu et al., 2003). For the activity of this enzyme, methanobactin (mb) is postulated as a "Cu-shuttle" to scavenge copper from the environment. The involvement of this molecule will be discussed more in later sections. With multiple conflicting models proposed for the active site of this enzyme, the mechanism of pMMO for methane oxidation is still not clear (Semrau et al., 2010).

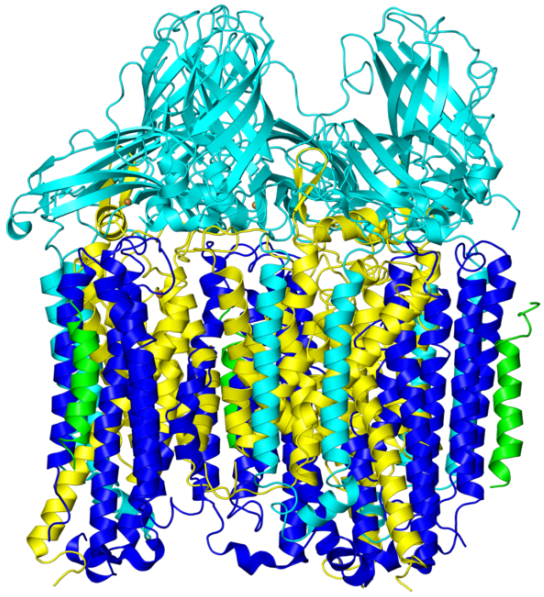

Figure 1.3. Structure of the hydroxylase component of pMMO from *Methylococcus capsulatus* Bath. The PmoB, PmoA, PmoC and some unknown helix polypeptides are depicted in light blue, dark blue, yellow, and green, respectively. Copper is depicted as brown spheres. (Sirajuddin et al., 2014)

I.2.1.2 Methanol dehydrogenase

Methanol is oxidized to formaldehyde by a periplasmic, pyrroloquinoline quinone (PQQ)-linked methanol dehydrogenase (MDH). Two types of MDH have been identified in methanotrophs, i.e., a Mxa-type and a Xox-type. Mxa-MDH is a heterotetramer ($\alpha_2ß_2$) composed of two large subunits (MxaF) and two small subunits (MxaI) with molecular weights of 67 kDa and 8.5 kDa, respectively (Anthony & Williams, 2003) (Figure 1.4). MxaF binds a Ca^{2+} ion and acts as the catalytic center. It also contains PQQ whose reduction to $PQQH_2$ is coupled to the oxidation of methanol. While crystal structures showed tight wrapping of MxaI against MxaF, the function of MxaI remains elusive (Xia et al., 1999, Xia et al., 2003, Choi et al., 2011). Electrons are transferred from $PQQH_2$ to the terminal oxidase via cytochrome c_{551} and cytochrome c_{550} (Anthony, 1992, Goodwin & Anthony, 1995).

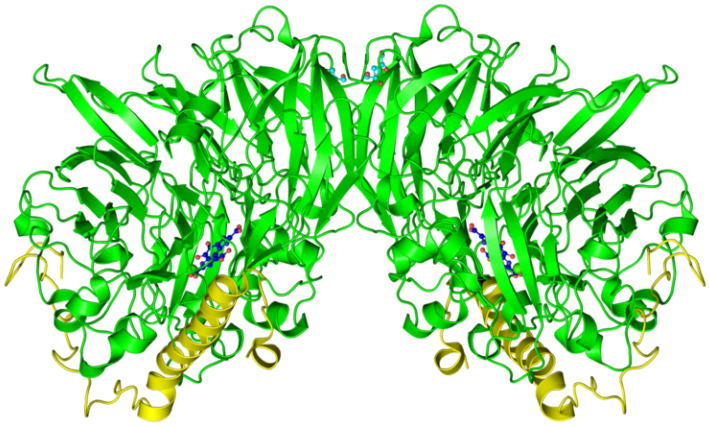

Figure 1.4. Structure of the methanol dehydrogenase from *Methylobacterium extorquens*. Two α subunits and two ß subunits are depicted in green and yellow, respectively. Two PQQ molecules and two calcium ions (green sphere) are bound in α subunits (Williams et al.,2004).

Xox-MDH was studied more recently as genomic studies found an *mxaF* (encoding for MxaF) homolog, named *xoxF* (Chistoserdova & Lidstrom, 1997, Chistoserdova, 2011). Comparatively, the sequence of *xoxF* displays less than 50% identity to *mxaF* and the

xoxF gene cluster lacks most of the genes coding for Ca^{2+} insertion and maturation as well as the gene coding for the small subunit (*mxaI*). However, the motifs for binding PQQ and Ca^{2+} are conserved in *xoxF* (Keltjens et al., 2014). Recent genome mining reveals that *xoxF* is more abundant than *mxaF* in environmental systems (Chistoserdova, 2011) (Table 1.1). Some methanotrophs contain only *xoxF* (Pol et al., 2007, Hou et al., 2008, Vekeman et al., 2016).

Early proof that *xoxF* encodes for a true MDH is provided by a study on the facultative formaldehyde-oxidizing bacterium *Rhodobacter sphaeroides*, in which a deletion mutant of *xoxF* lost the ability to use methanol (Wilson et al., 2008). Later studies in *Methylobacterium radiotolerans* and *Methylobacterium extorquens* AM1 showed that cerium and lanthanum both increased methanol oxidation by Xox-MeDH (Hibi et al., 2011; Nakagawa et al., 2012). Further, growth and overall MeDH activity of a *M. extorquens* AM1 mutant in which *mxaF* was knocked out was severely limited in the absence of lanthanum but growth recovered in its presence, regardless of whether calcium was simultaneously present or not (Nakagawa et al., 2012). Such results indicate that lanthanum was required for the activity of Xox-MeDH. Subsequent studies on methanotrophic strain *M. fumariolicum* SolV (that only has XoxF-MDH) found that its growth can be enhanced in the presence of rare earth elements (Pol, et al., 2014). Purification of the active MDH of *M. fumariolicum* SolV grown in the presence of praseodymium showed ~ 0.5 - 0.7 atoms of praseodymium per monomer, indicating praseodymium to be part of the active site. The XoxF-MDH is homodimeric proteins containing a large subunit only and has PQQ as the prosthetic group (Pol, et al., 2014).

Another interesting aspect of MDH is the formation of a super-complex between pMMO and MxaF-MDH (Myronova et al., 2006). Cryoelectron microscopy and single particle analysis showed that pMMO and MxaF-MDH form a "cap-body"-like complex that possibly contributes to protein stability and make electron transport more efficient. (Figure 2.5) (Leak et al., 1985). The source of electron donor to pMMO has yet to be elucidated. Direct electron transfer from MeDH has been proposed but has not been directly shown (Kalyuzhnaya et al., 2015). The co-localization of pMMO and MeDH, however, supports the hypothesis of direct coupling, i.e., methanol oxidation supplying electrons for methane oxidation (Fassel. et al., 1993; Myronova et al., 2006). Other theories include: formaldehyde and formate oxidation generate NAD(P)H, which could in turn be used to generate ubiquinol from ubiquinone (Choi et al., 2003; Vorholt 2002). Methanol oxidation could also partially support methane oxidation with the additional input from respiratory Complexes I/III (Torre et al., 2015). A recent study by Torre et al., (2015) constructed an *in silico* stoichiometric flux balance model of *Methylomicrobium buryatense* 5G(B1) and suggested that reverse electron transfer from MeDH is a better fit to experimental data.

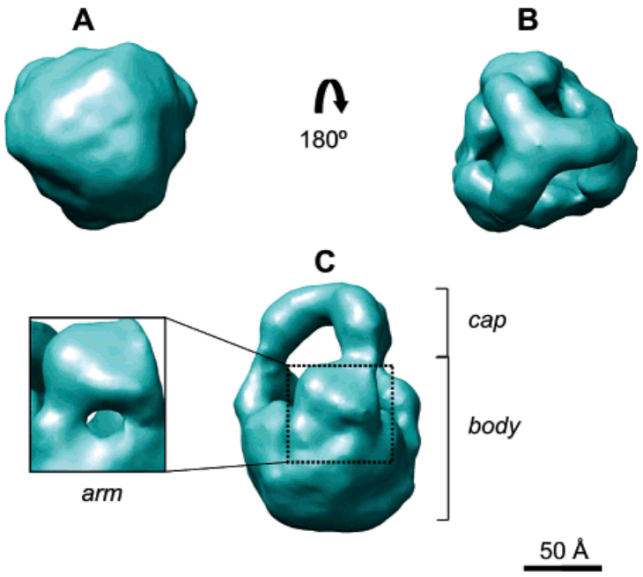

Figure 1.5. 3D structures of pMMO-MDH supercomplex (Myronova et al., 2006)
(A) Putative intracellular side of pMMO-MDH complex showing a relatively flat complex triangular in shape. (B) Putative periplasmic face of the complex revealing three protein densities joining in the center to form a three-pronged star arrangement. (C) Putative side view of the complex illustrating that the purified complex is composed of two densities termed the cap and body.

Despite the fact that *xoxF* clusters do not have the gene encoding for the small subunit of Mxa-MDH, a recent study by Wu et al. (2014) found that XoxF could bind MxaI in *Ca.* Methylomirabilis oxyfera. The concerted actions of different proteins from different gene clusters raised the possibility of a joint regulatory system between *mxa* and *xox* gene clusters and is discussed in later sections.

I.2.1.3 Oxidation of formaldehyde to carbon dioxide

Formaldehyde is either further oxidized to CO_2 or serves as the starting substrate for carbon assimilation. Formaldehyde can be oxidized to formate either via a single enzyme system of formaldehyde dehydrogenases (FDH) or multi-enzyme cofactor-linked C_1 transfer pathways, such as the tetrahydromethanopterin (H_4MPT) pathway or

tetrahydrofolate (H_4F) pathways. (Vorholt, 2002, Chistoserdova et al., 2009) (Figure 2.6) For the latter, the pathways generally follow the condensation of formaldehyde and the respective C_1 carrier, the oxidation of the cofactor-bound C_1 unit and its conversion to formate, and the oxidation of formate to CO_2 (Vorholt 2002). Formaldehyde is also oxidized via the cyclic ribulose monophosphate pathway (RuMP) (Anthony, 1982).

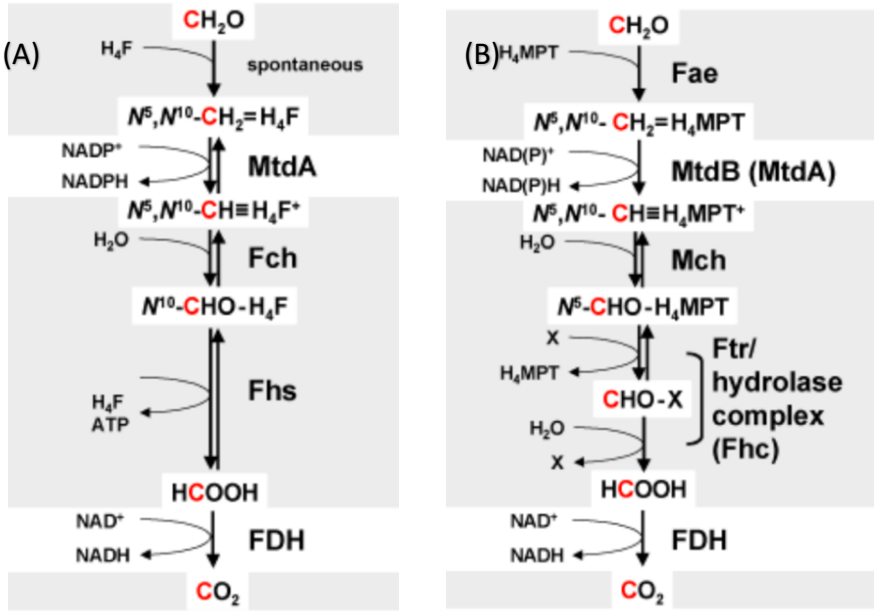

Figure 1.6. Comparison of different linear pathways for formaldehyde conversion in methylotrophic bacteria, as found in *Methylobacterium extorquens*.
(A) H_4F- dependent pathway, (B) H_4MPT-dependent pathway. MtdA NADP-dependent methylene-H_4MPT dehydrogenase, Fch methenyl-H_4F cyclohydrolase, Fhs formyl-H_4F synthetase, FDH formate dehydrogenase, Fae H_4MPT -dependent formaldehyde activating enzyme, MtdB NAD(P)-dependent methylene-H_4MPT dehydrogenase, Mch methenyl-H_4MPT cyclohydrolase, Ftr formyltransferase, Fhc Ftr/hydrolase complex, Gfa glutathione-dependent formaldehyde activating enzyme, GD-FALDH NAD+- and glutathione-dependent formaldehyde dehydrogenase, FGH formyl-glutathione hydrolase. X Unknown cofactor, which is assumed to be an analogue to methanofuran (MFR) from methanogenic archaea. (Vorholt, 2002)

The H_4MPT pathway is the most widespread pathway in methylotrophs (Chistoserdova et al., 2009). It involves four groups of enzymes- Fae catalyzes the condensation of formaldehyde with H_4MPT to form N^5, N^{10}-methylene-H_4MPT, which is the oxidized sequentially by MtdA, MtdB, and Mch to ultimately form N^{10}-formyl-H_4MPT. Formate is

then produced via oxidation of N^{10}-formyl-H_4MPT by FhcABCD. (Vorholt, 2002) The H_4F -pathway follows a similar route as does the H_4MPT pathway. It is more integrated with the serine pathway (discussed in the next section) as H_4F pathway helps maintain high concentration of N^5, N^{10}-methylene-THF as a formaldehyde acceptor for serine pathway (Vorholt, 2002, Ward et al., 2004).

Formate is oxidized to CO_2 by the formate dehydrogenase (FDH). NAD-linked (Yoch et al., 1990) and ferredoxin-linked (Chen & Yoch, 1988) FDH have been purified from *M. trichosporium* OB3b. Multiple copies of genes putatively encoding FDH has been found in *M. capsulatus* Bath (Ward et al., 2004) but their functions are not fully understood. Differential expression of FDHs has been observed in *M. extorquens* AM1 in response to molybdenum or tungsten, suggesting that a similar mechanism may exist in methanotrophs. (Chistoserdova et al., 2004, Trotsenko & Murrell, 2008) NAD(P)H is generated in MtdB/A- and FDH- mediated steps as a reductant for biosynthesis.

I.2.2 C_1 assimilation

The two major pathways employed by methanotrophs for C_1 assimilation are the ribulose-monophosphate (RuMP) pathway at the level of formaldehyde and serine pathway that happens at the level of methylene-H_4F and CO_2. (Quayle, 1980) In the RuMP cycle, formaldehyde is added to a C_5 sugar, ribulose-5-phosphate, and produces glucose 6-phosphate (G6P). G6P is then partially converted into phosphotrioses via either Entner-Doudoroff (EDD)-variant (Strom et al., 1974) or Embden-Meyerhof-Parnas (EMP)-variant (Leak & Dalton, 1986; Kalyuzhnaya et al.,2013) pathway, partially for

cell biosynthesis, and partially oxidized to regenerate ribulose-5-phosphate (Anthony, 1982). In the serine cycle, formaldehyde, after condensing with THF, reacts with glycine to produce serine. Serine is sequentially phosphorylated, carboxylated, and reduced to acetyl-CoA, which partially is converted to biomass, and partially oxidized to glyoxylate. Glyoxylate accepts the amino group from serine to regenerate glycine to complete the cycle. (Anthony, 1982; Chistoserdova *et al.*, 2009) (Figure 1.7)

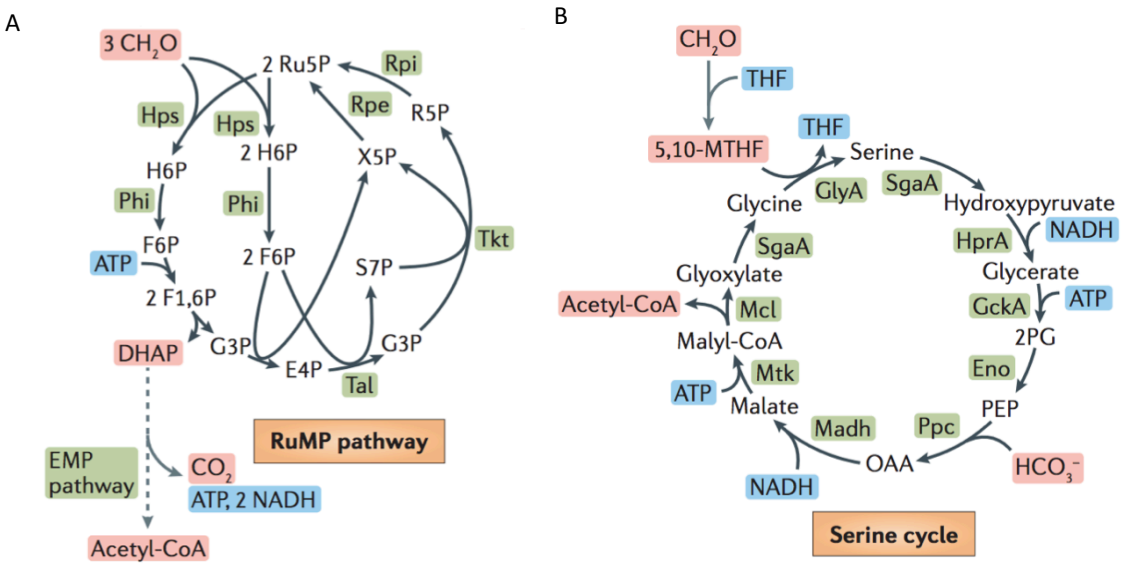

Figure 1.7. (A) RuMP pathway (B) Serine cycle (Liao et al., 2016)

Historically, the serine cycle was attributed to Alphaproteobacterial methanotrophs (Type II) and the RuMP cycle was attributed to Gammaproteobacterial methanotrophs (Type I). A subset of methanotrophs belonging to Type I, physiologically classified as Type X including *Methylococcus* and *Methylocaldum*, assimilate C_1 mainly by RuMP pathway while also possessing serine pathway and the Calvin-Benson-Bassham (CBB) cycle. (Taylor *et al.*, 1981, Stanley & Dalton, 1982) The contribution of CBB cycle remains poorly understood, although methanotrophic Verrucomicrobia *Methylacidiphilum infernorum* V4 (Op den Camp *et al*., 2009) and methanotrophs belonging to the NC10

phylum (Ettwig *et al.*, 2010) are known to assimilate carbon by using the CBB cycle to fix CO_2. (Figure 1.8)

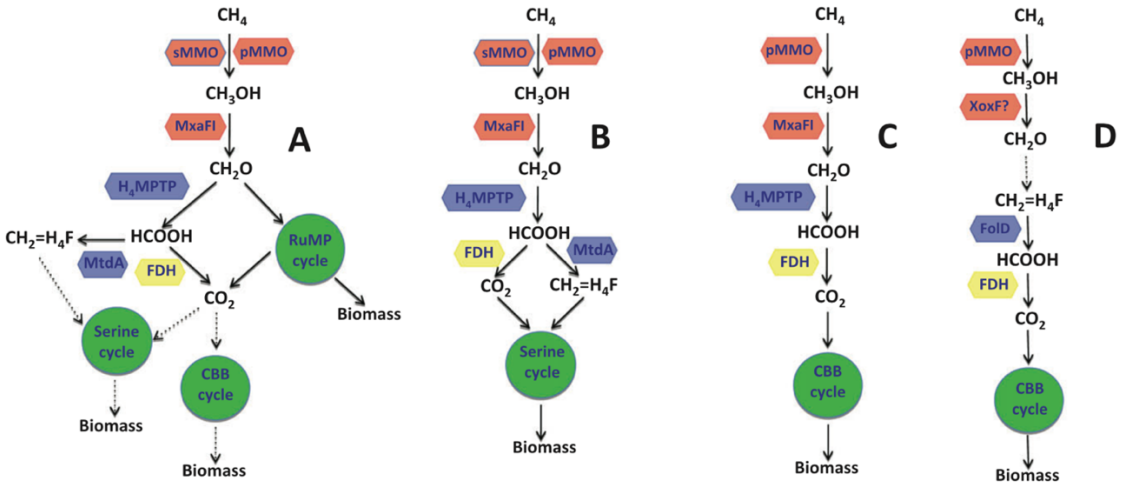

Figure 1.8. Examples of methanotrophy metabolic modules.
(A) *M. capsulatus*; (B) *M. trichosporium*; (C) Phylum NC10; (D) methanotrophic *Verrucomicrobia* (Chistoserdova, 2011)

Recent transcriptomic and isotopic labeling study by Kalyuzhnaya et al. (2014) found that methane assimilation can also coupled with a pyrophosphate-mediated glycolytic pathway in *Methylomicrobium alcaliphilum* strain 20Z. When grown under under oxygen limitation conditions, *M. alcaliphilum* 20Z undergoes a fermentation-based methanotrophy and excretes organic compounds and hydrogen. This finding has major implications for the environmental role of methanotrophic bacteria in O_2-limiting environments suggesting that methane oxidation occurs more broadly than initially assumed. Methanotrophs can serve as keystone species for the development of microbial communities *in situ*.

I.2.3 Facultative methanotrophy

Although some early studies showed that acetate and other multi-carbon compounds can be assimilated to a certain extent during growth on methane by some methanotrophs

(Eccleston & Kelly, 1973, Patel et al., 1978), the vast majority of methanotrophs are obligate, i.e., they grow only on methane or in some cases, other one-carbon compounds, such as methanol. Attempts to isolate and characterize facultative methanotrophs that can grow on multi-carbon compounds have been reported since 1970s. Most results, however, were inconclusive, due to either failure of repeating the initial findings or subsequent discovery of contamination (Patt et al., 1974, Patel et al., 1978, Lidstrom-Oconnor et al., 1983, Semrau et al., 2011). It was not until 2011 that unequivocal demonstration of facultative methanotrophy in genus *Methylocella* was collected with the help of improved and more comprehensive assays, including phase-contrast microscopy, whole-cell hybridization, and sequencing (Dedysh et al., 2005). Subsequently, species of other genera have been shown to be capable of growth on acetate or ethanol in addition to methane, including species of *Methylocapsa* and *Methylocystis* (Dunfield et al., 2010, Belova et al., 2011, Im et al., 2011).

Limited studies have looked into the metabolism of multi-carbon compounds in facultative methanotrophs. In a transcriptomic study of *Methylocystis* sp. SB2 grown on ethanol, it was found that ethanol is first converted to acetyl-coenzyme A, which then enters the TCA cycle for energy generation and the EMC pathway for conversion to biomass, while the expression of the central methane oxidation pathway and serine cycles were down-regulated. These findings reveal an effective coordination of different pathways that is likely based on complex regulatory network in methanotroph (Vorobev et al., 2014). Another study on *Methylocella silvestris* BL2 that has only soluble form of MMO and can grow on several organic acids and alcohols (Dedysh et al., 2005),

investigated the mechanism by which *M. silvestris* grows on propane. Genomic analysis revealed two copies of a soluble di-iron center monooxygenase of which the second copy was functionally identified as propane monooxygenase (PrMO) based on mutagenesis (Crombie & Murrell, 2014). Interestingly, both sMMO and PrMo are required for propane utilization by *M. silvestris*. The 2-propanol produced during propane oxidation by sMMO is needed to induce the expression of PrMO.

I.3 Regulation of gene expression by copper

I.3.1 *mmo* and *pmo* operons

sMMO is encoded by the *mmo* operon. sMMO is composed of a reductase encoded by *mmoC*, a protein B encoded by *mmoB*, and a hydroxylase component with $\alpha_2\beta_2\gamma_2$ structure encoded by *mmoX, mmoY*, and *mmoZ*, respectively. All these genes are co-transcribed from a six-gene operon (Stainthorpe et al., 1990, Cardy et al., 1991), together with another gene, *mmoD*, which participates in the genetic regulation of *mmo* and *pmo* operons. The arrangement of these genes in *M. trichosporium* OB3b is shown in Figure 2.9A. A σ^{54}/σ^{N}-like promoter is present 5' of *mmoX* (Nielsen et al., 1997, Barrios et al., 1999) and a σ^{70} promoter at 5' of *mmoY*. Upstream of *mmoX*, there is *mmoR,* encoding a σ^{N}-dependent transcriptional activator, and *mmoG,* encoding a chaperonin GroEL homologue (Figure 1.5 A). A regulatory system has been proposed to involve the σ^{N} promoter, *mmoR* and *mmoG*. It was shown by mutagenesis studies that the initiation of the σ^{N} promoter requires the σ^{N} encoded by *rpoN*, and the expression of *mmoR* and *mmoG*. (Csáki et al., 2003, Stafford et al., 2003). *mmoG* is transcribed in a σ^{N} and

MmoR-independent manner and regardless of copper availability (Stafford et al., 2003). Also, MmoG is required for MmoR binding to DNA, it is thus speculated to function as a co-regulator of *mmo* expression via interaction with MmoR, or a chaperone for MmoR. It also may be multi-functional and play a role in sMMO assembly (Scanlan et al., 2009). The inability to purify MmoG from heterologous expression systems, however, makes it difficult to draw any strong conclusion (Scanlan et al., 2009).

The gene arrangement of the *mmo* operon is identical in most sMMO-possessing methanotrophs. The position of *mmoR* and *mmoG*, however, can vary. In *M. capsulatus* Bath, *mmoR* and *mmoG* are downstream of *mmoC*. Moreover, they are in a cluster with *mmoQ* and *mmoS*. The latter two are transcribed in the opposite orientation under a putative σ^{70} promoter and correspond to a homologue sensor and regulator components of a two-component system. This kind of system in other bacteria can detect the environmental signal via sensor protein and transmit it to the regulator protein via transphosphorylation (West & Stock, 2001). It was suggested that MmoG and MmoQ can sense copper levels and transmit the signal to MmoR (Csáki et al., 2003, Ukaegbu & Rosenzweig, 2009).

Bioinformatic analysis indicates that most methanotrophs possessing sMMO have only one copy of *mmo* operon (data not shown). *Methylosinus sporium* strain 5 was recorded to have duplicate copies of *mmoX* (Ali et al., 2006). While both copies are transcribed, only one copy (*mmoX1*) was essential for sMMO activity.

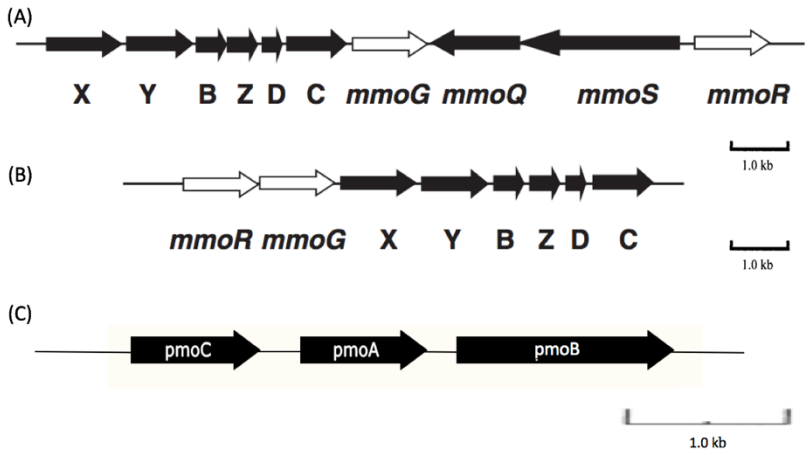

Figure 1.9. (A) *mmo* operon of *Methylococcus capsulatus* Bath, (B) *mmo* operon of *Methylosinus trichosporium* OB3b (Scanlan et al., 2009) and (C) *pmo* operon of *Methylosinus trichosporium* OB3b (Costello et al., 1995; Semrau, et al., 1995)

The structural genes for pMMO lie in a three-gene operon in the order of *pmoC-A-B* (Figure 1.9 B) encoding α, β, and γ subunits, respectively. The *pmo* operon is under the control of a σ^{70} promoter. (Ali & Murrell, 2009) There are typically two complete *pmo* operons and a third copy of *pmoC* in methanotrophs genome (Semrau et al., 1995, Gilbert et al., 2000, Stolyar et al., 2001). Chromosomal insertion mutations suggest that both copies of *pmoCAB* are functional. However, the relative expression and enzyme activity from the second copy of *pmoCAB* (*pmoCAB2*) are higher than that of *pmoCAB1* (Stolyar et al., 1999, Stolyar et al., 2001). The mutation of the third copy of *pmoC3* cannot be obtained suggesting it may play an essential role in growth on methane.

Methylocystis sp. strain SC2 contains two very different types of *pmoA*. The first type, *pmoA1* (i.e., conventional *pmoA*), has two copies in *Methylocystis sp.* SC2 and are identical with the *pmoA* identified in *M. trichosporium* OB3b and *M. capsulatus* Bath. The second type, *pmoA2*, exhibits 73% similarity at nucleotide level with *pmoA1*

(Dunfield et al., 2002). This novel *pmoA* was later found to be widely distributed in *Methylocystis* and *Methylosinus* genera (Yimga et al., 2003). *pmoA2* is also in a *pmoCAB* gene cluster (*pmoCAB2*) under the control of a σ^{70} promoter (Ricke et al., 2004). Mutagenesis analysis showed that both *pmoCAB1* and *pmoCAB2* are transcribed into functional pMMOs (pMMO1 and pMMO2). Very interestingly, they have distinct methane oxidation kinetics. pMMO1, was only expressed at CH_4 concentrations > 600 p.p.m.v., and had an apparent affinity of CH_4 of 9.3 μM The other isozyme, pMMO2, was constitutively expressed, had an apparent affinity of CH_4 of 0.11–0.12 μM and can oxidize CH_4 at atmospheric concentrations. Further studies also indicate that methanotrophs oxidizing CH_4 at atmospheric concentrations in acidic forest soils were expressing pMMO (Kolb et al., 2005, Baani & Liesack, 2008).

In most identified *pmo* operons, *pmo* genes cluster in a canonically *C-A-B* order. However, in 2011, a *pmo*-like gene cluster, substantially divergent from previously characterized *pmo* with ~53% identity in sequence, has a unique cluster order of *A-B-C*. These genes are named *pxmABC.* They are found in several Gammaproteobacteria methanotrophs, e.g., *Methylomonas* sp. Strain LW13, *Methylonomas methanica* strain S1, etc. (Tavormina et al., 2011) (Table 1.1). More divergent *pmo* genes are discovered in other methanotrophs such as Proteobacteria *Crenothrix polyspora* (Stoecker et al., 2006), acidophilic Verrucomicrobial *Methylacidiphilum* species (Vuilleumier et al., 2012), and *Candidatus* Methylomirabilis oxyfera (Wu et al., 2011). The relevance of these divergent *pmo* genes, however, is still unclear.

I.3.2 Copper uptake via methanobactin (mb)

Copper is an essential metal for methanotrophic activity and plays a regulatory role in methanotrophs, most notably on the expression of the sMMO and pMMO (Stanley et al., 1983, Nielsen et al., 1997). The general effect of copper on methanotrophic activity has been noted for more than 30 years (Dalton et al., 1984; Stanley et al., 1983). However, the copper sensing and uptake mechanisms by methanotrophs was only recently determined. Phelps et al., (1992) isolated an *M. trichosporium* OB3b mutant that constitutively expressed sMMO up to 10 μM Cu (mutant smmoC), suggesting possibly a specific Cu uptake system was disrupted. Later, a copper binding compound was identified in association with pMMO during its purification from *M. capsulatus* Bath and was thought to be a cofactor. (Zahn & DiSpirito, 1996). This small copper binding molecule, later named methanobactin (mb), turns out to be part of a novel metal-uptake system used by methanotrophs for copper sequestration.

I.3.2.1 Structure and properties of mb

Early studies on mb produced by *M. trichosporium* OB3b (mb-OB3b) showed that mb is a short, modified chromopeptide produced by methaontrophs under low-copper conditions (Kim et al., 2004). While the amino acid sequence was determined by MS-based sequencing, the modified residues had novel structures that were difficult to elucidate (Kim, 2003). Using NMR, two oxazolone rings were identified in mb-OB3b, which are formed by modified proteinogenic amino acids of the sequence X-Cys. (Behling et al., 2008, Krentz et al., 2010) (Figure 1.10A). Mb-OB3b has characteristic UV-Vis spectrum with two major peaks at 340nm and 394 nm assigned to the two

oxazolone rings (Figure 1.11). The molecule was proposed to fold with the two rings in proximity to each other and bind Cu (I) with coordination of N and S. Following the study of mb-OB3b, mbs from other methanotrophs have been isolated and characterized, which include *Methylocystis* strain SB2 (Krentz *et al.*, 2010), *Methylocystis* strain M, *Methylocystis hirsuta* CSC1, *Methylocystis rosea* (El Ghazouani *et al.*, 2012), and *Methylosinus* LW4 (Kenney et al., 2015).

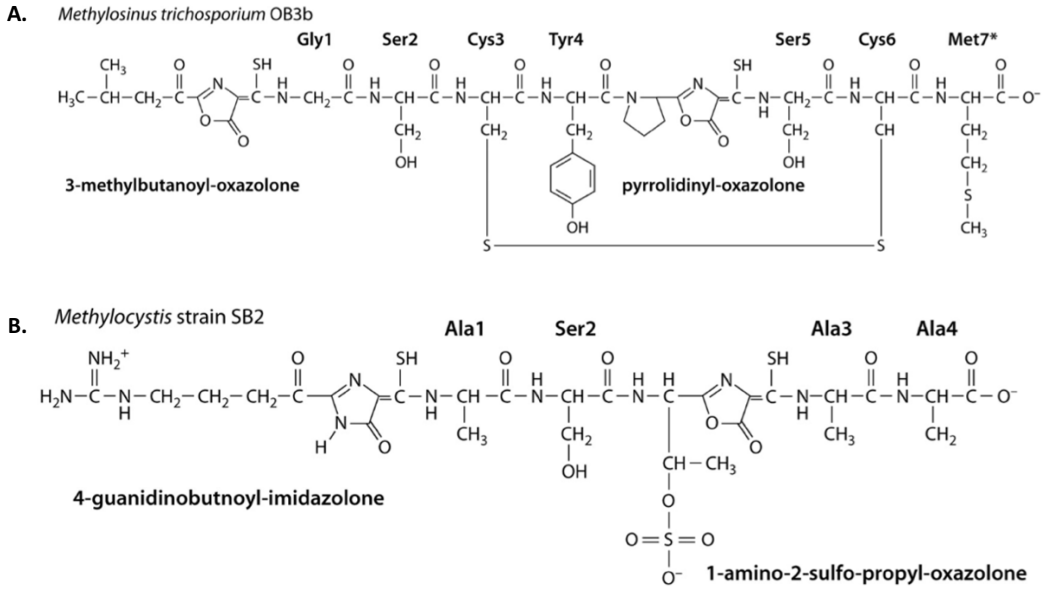

Figure 1.10. Chemical structure of (A) mb-OB3b and (B) mb-SB2 (Krentz et al., 2010)

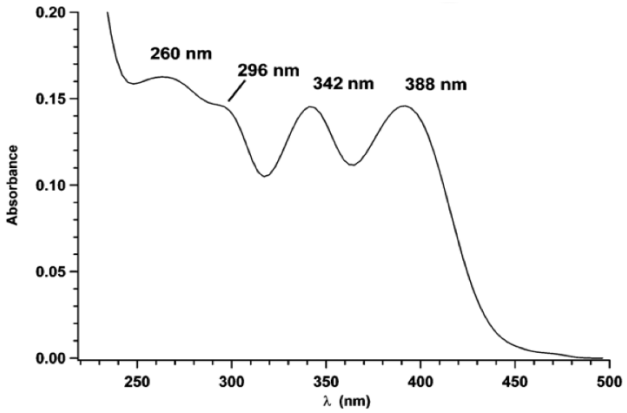

Figure 1.11. UV–visible absorption spectra of mb from *M. trichosporium OB3b* (Kim et al., 2005)

A review of the structurally identified mbs reveals a core structure featuring one oxazolone ring and a second of either oxazolone, imidazolone, or pyrazinedione ring with adjacent thioamide groups. (DiSpirito, et al., 2016) Based on their structural variation, mbs are divided into two groups. Group 1 mb, represented by mb-OB3b (Figure 1.6), contains Cys residues in the mature peptide, which are linked by an intramolecular disulfide bond. Group 2 mbs, represented by mb-SB2 (Figure 1.10B), lack the Cys residues in the mature peptide and thus no disulfide bond. Instead, the group 2-mbs have a sulfate group in front of the second oxazolone ring which aids the formation of bend in the molecule though in a less rigid way than group 1-mbs. Group 2-mbs are also smaller that group 1-mbs (DiSpirito, et al., 2016).

Mb can bind both Cu^{2+} and Cu^{1+} but appears to favor Cu^{1+} (Choi et al., 2006; El Ghazouani et al., 2011; Bandow et al., 2012). After binding to Cu^{2+}, it quickly reduces Cu^{2+} to Cu^{1+} (Ghazouani, et al., 2011; Bandow et al., 2012; Choi et al., 2006; Pesch. et al., 2012). The Cu^{1+} binding affinity of mb was calculated to be as high as ~$10^{21}M^{-1}$ (determined by competition studies). In addition to copper, mb-OB3b and mb-SB2 also bind to a number of transitional and near-transitional metals including Hg^{2+}, Au^{3+}, Zn^{2+}, Cd^{2+}, Co^{2+}, Fe^{3+}, Mn^{2+}, Ni^{2+} (listed in a descending order of binding preferences for mb-OB3b) (Choi et al., 2006; Bandow, 2014). This property of mb leads to several interesting phenomena, which will be discussed in more detail later.

Copper binding compounds from the Type I methanotroph *M. capsulatus* Bath have also been isolated (Choi et al., 2008, Choi et al., 2011) but their structures have not been determined. These compounds from Type I methanotrophs show distinct spectrum properties from mb indicating different structures and also are known to have weaker copper-binding constants (Choi et al., 2008, Choi et al., 2011). This difference may lead to different copper sequestering ability between Type I and II methanotrophs and help define the structure and composition of methanotrophic communities *in situ* (Semrau et al., 2010).

I.3.2.2 Mb genetic organization

In the study by Krentz et al. (2010) a short open reading frame (*mbnA*) was identified in the genome of *M. trichosporium* OB3b that matches the amino acid sequence of a hydrolyzed form of mb, providing evidence that mb is derived from a ribosomally produced peptide. Definitive proof was provided later by a mutagenesis study in which the ability of *M. trichosporium* OB3b to produce mb was lost after *mbnA* was knocked out (Semrau et al., 2013).

The genome sequence near *mbnA* in *M. trichosporium* OB3b has been analyzed bioinformatically (Semrau et al., 2013; Kenney & Rosenzweig, 2013). Several ORFs have been identified and speculated to involve in mb synthesis and transport (Figure 1.12A). *mbnA* is the precursor polypeptide for mb. Following *mbnA* are *mbnB* and *mbnC*, two putative genes with no significant homologues in the current database and are speculated to involve in mb biosynthesis. A putative multi-antimicrobial extrusion

protein (MATE) efflux pump gene (*mbnM*) follows *mbnC*, and is proposed to export mb out of cell. Downstream of *mbnM* is *mbnN*, putatively encoding for a transaminase, which may be involved in mb maturation. *mbnP* and *mbnH* are downstream to *mbnN*, and encodes for a di-heme cytochrome c peroxidase homologue and its partner, respectively. Similar pairs of proteins are found in *M. capsulatus* Bath (SACCP and MopE) and *M. album* BG8 (CorB and A) though with low similarity. MopE is involved in an alternative Cu sensing system in some methanotrophs (Fjellbirkeland et al., 2001). CorB, the same as MopE, is down-regulated in the presence of copper and a mutant with *corA* knocked out grew poorly indicating its important physiological role (Berson & Lidstrom, 1997). The function of MbnPH pair however, is not clear and may be involved in the oxidation steps required for ring formation (DiSpirito et al., 2016).

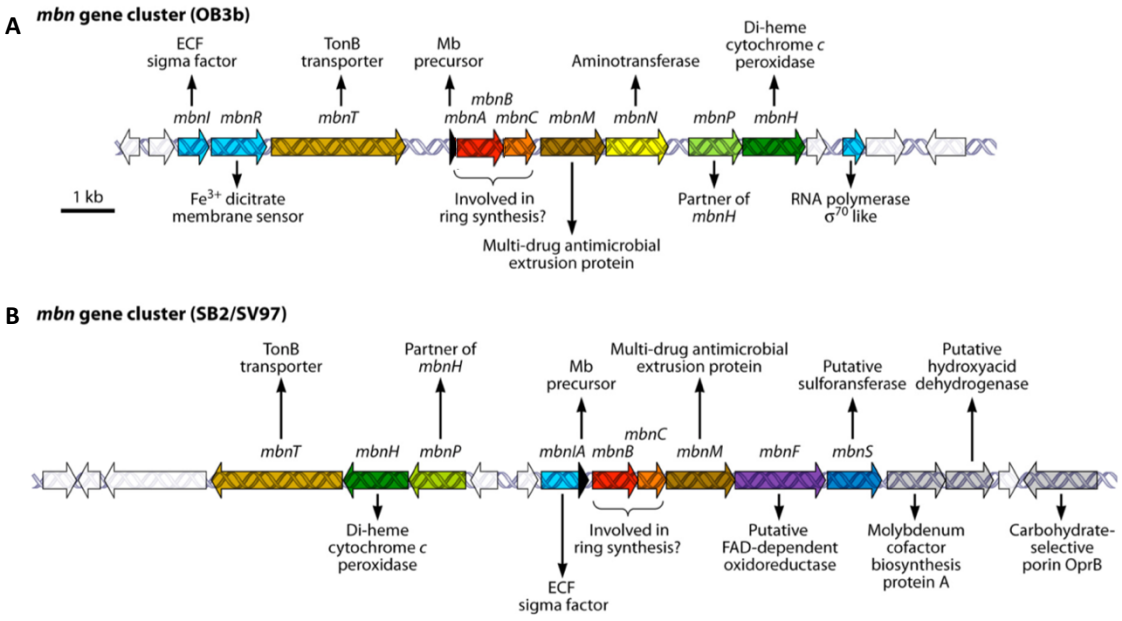

Figure 1.12. *mbn* gene cluster in (1) *Methylosinus trichosporium* OB3b and (2) *Methylocystis* sp. strain SB2. (Dispirito *et al.*, 2016)

Putative σ^{70} promoters upstream of *mbnA* and *mbnI* have been identified. Putative promoters are found inside *mbnM* and *mbnN,* as well as in intergenic region between *mbnN* and *mbnP*, but with lower scores (BPROM package, www.softberry.com). Polycistronic transcripts of the *mbn* operon have been found that include *mbnA* and at least *mbnB* and *mbnC* (Semrau et al., 2013).

Upstream of *mbnA*, there are *mbnI, mbnR*, and *mbnT*. MbnT is a homologue of TonB-dependent transportors (TBDTs). TBDTs act as importers for siderophores and it is speculated to have a similar role for mb import. MbnI/R are putative homologs of FecI/R pairs, which are often seen in siderophore systems. FecI is "Fe(III) dicitrate membrane sensor" and FecR is "ECF sigma factor". They work together with TBDT in siderophore systems in that upon binding a siderophore, TBDT may interact with FecR, which then may send a signal to FecI that regulates expression of siderophore biosynthesis and transport proteins (Koebnik, 2005, Postle & Larsen, 2007, Brooks & Buchanan, 2008). If similar functions apply here, *mbnIR* could regulate mb synthesis.

Interrogation of the genome of *Methylocystis* sp. strain SB2 also reveals a putative methanobactin gene cluster (Figure 1.12B). It has similar *mbnABCM* gene arrangement as the *M. trichosporium mbn* operon. By comparison, the aminotransferase MbnN is missing from the *mb*-SB2 gene cluster and instead there is *mbnF* and *mbnS*. MbnF (a FAD-dependent oxidoreductase homologue) may be involved in the oxidation steps required for ring formation, and MbnS (a sulfotransferase homologue) may catalyze the sulfonation of the threonine (DiSpirito et al., 2016). Also, the interesting observation that

mbnA of *Methylocystis* sp. strain SB2 is embedded at the 3' end of *mbnI* makes one wonder its implication in genetic regulation, i.e., MbnI is involved in regulating expression of mb (DiSpirito et al., 2016).

Interestingly, genome mining of mb gene cluster (not only queried by the short and diverse *mbnA*, but rather, also the adjacent *mbnB* and *mbnC*) (Table 1.1) against available databases returns several non-methanotrophic bacteria strains, suggesting that such gene clusters may encode peptide-derived products with more diverse functions (Krentz et al., 2010; DiSpirito. et al., 2016).

I.3.2.3 Regulation of gene expression by mb and MmoD

It has been long observed that there is a "copper-switch" in methanotrophs. That is, in cells grown under high copper-to-biomass ratios, the pMMO is expressed while under low copper-to-biomass ratio, the sMMO enzyme is highly expressed. (Stanley et al., 1983, Dalton et al., 1984)

A study by Semrau et al., (2013) shed light on the genetic bases of the "copper-switch". In this study, the expression of several key genes of a *M. trichosporium* OB3b SMDM mutant, (created by Borodina et al.,(2007) in which *mmoXYBZDC* were knocked-out) as well as a *mbnA*::Gm^r mutant (in which *mbnA* was knocked-out) grown at various copper conditions were quantified by quantitive reverse transcription (qRT)-PCR. Several observations were made: (1) *mbnA* expression is regulated by the availability of copper, i.e., its expression level dropped >3 orders of magnitudes when cells were growing at

1uM Cu compared to the absence of copper; (2) the copper switch between sMMO and pMMO still existed in the *mbnA*::Gm^r mutant but to a lesser degree; (3) the copper switch was inverted in the SMDM mutant, i.e., *pmoA* expression was greatest in the absence of copper and dropped by ~2 orders of magnitude at presence of copper, and *mbnA* expression was invariant with respect to copper at a low level. Since MmoX, Y, B, Z, C are known to encode for structural peptides of sMMO, it was thus proposed that MmoD is the switching factor, and mb acts as a "magnifier" to the copper-switch. More finding supporting this hypothesis includes that *mmoD*, while being partly co-regulated together with the rest of *mmo* operon, is constitutively expressed with respect to copper (DiSpirito, et al.,2016). Moreover, in a study on *Methylomicrobium buryatense* 5GB1C (Yan et al., 2016), a *mmoD*::Gm^r mutant was created where MmoD were knocked-out. The mutants showed lack of sMMO activity at absence of copper.

Starting from the above, a genetic regulation model was built (Semrau et al.,2014) and improved (DiSpirito et al., 2016) to include the earlier findings of MmoG/R as *mmo* regulaters as well as recent hypothesis on MbnIR, which have both been discussed in earlier sections. This revised model (Figure 1.13) hypothesized that MbnI induces expression of the *mbn* operon and *mmoRG* MbnI also binds to and induces the σ^{70} promoter upstream of *mmoY*. In turn, mb, MmoR, and MmoG interact to induce expression from the σ^N promoter upstream of *mmoX*. *mmoD* is constitutively expressed and can repress the *pmo* and *mbn* operon at low-copper condition. However, MmoD associates with copper when it is present and lift the repressions.

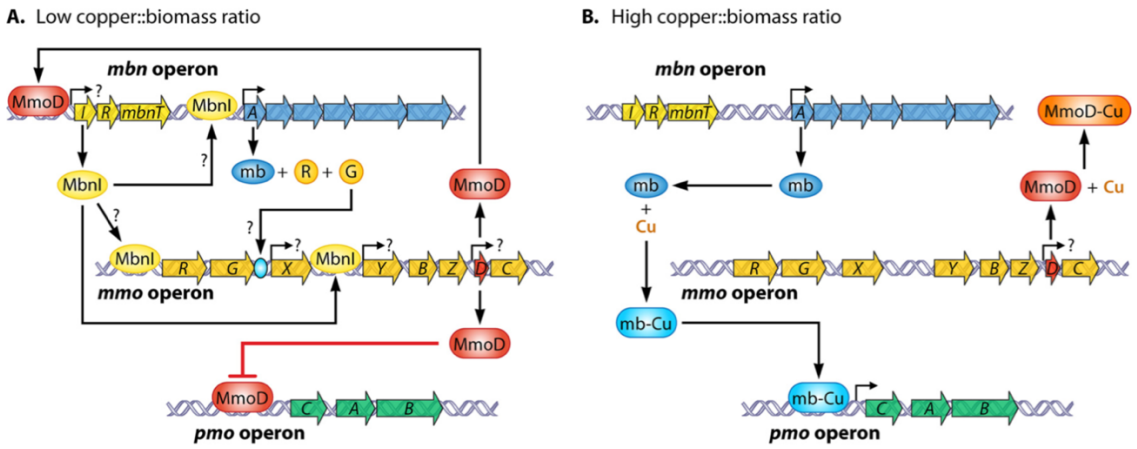

Figure 1.13. Proposed regulatory scheme of *mmo*, *pmo* and *mbn* operons by copper, methanobactin and MmoD. (A) low copper:biomass ratio; (B) high copper:biomass ratio. (DiSpirito, *et al.*, 2016)

I.3.2.4 Physiological roles of mb

Methanotrophs secrete mb under low-copper conditions to acquire copper. Under laboratory conditions where copper is provided in a soluble form, it was found that mb is not necessary for copper acquisition or induction of "copper-switch" (Semrau et al., 2013). The role of mb in acquiring mineral copper source was investigated and showed that mb facilitates copper uptake from mineral copper source but the degree (with respective to relative activities of sMMO and pMMO) largely varies between different forms of mineralogy. (Knapp et al., 2007; Fru et al., 2011) These studies can be very informative for application of *in situ* bioremediation where the estimation of methanotrophic activity in soil environments is needed.

After shuttling copper inside the cells, Cu-mb can provide copper to pMMO (Zahn & DiSpirito, 1996). The activity of pMMO has long been known to correlate with intracytoplasmic membrane formation. (Dalton et al., 1984; Green et al., 1985; Prior &

Dalton, 1985; Choi et al., 2003) As shown by DiSpirito et al., (2006), while the SMDM mutant had intracytoplasmic membrane development similar to wild type *M. trichosporium* OB3b, the *mbnA*::Gm^r mutant appears to have a clear defect in intracytoplasmic membrane development. (Figure 1.14) However, how the defect is caused by mb is not known. Whether mb is directly involved in the development of the intracytoplasmic membranes in methanotrophs could be very valuable for methanotrophic application of biolipid production.

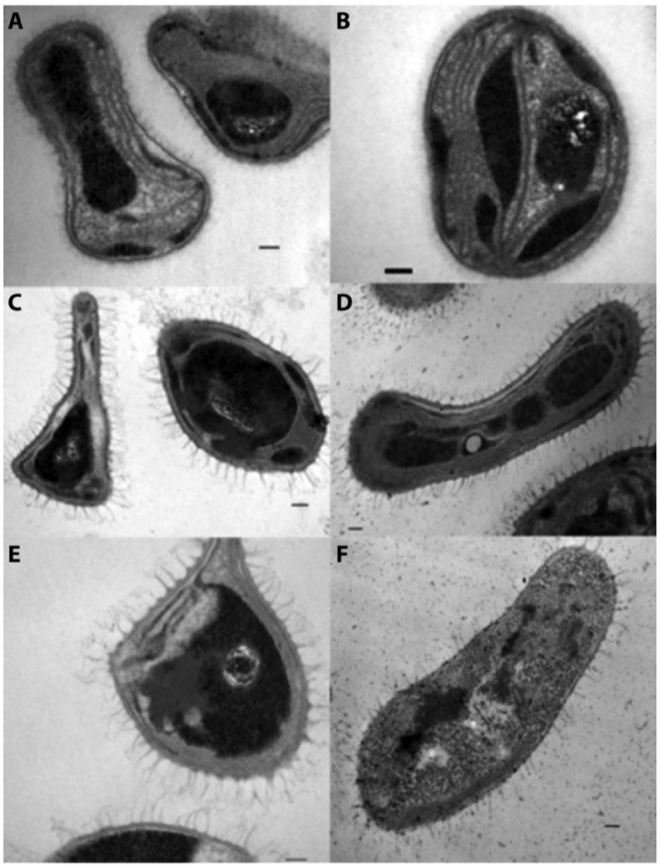

Figure 1.14. Transmission electron micrographs of *M. trichosporium* OB3b wild-type (A and B), SMDM mutant (C and D), and *mbnA* deletion mutant (E and F) cultured in nitrate mineral salts (NMS) medium (A, C, and E) or NMS medium amended with 5 M CuSO4 (B, D, and F).

As has been mentioned, mb can bind to a variety of metals other than copper with relatively high affinity. A study by Vorobev et al., (2013) found that after binding to

mercury, mb significantly alters the speciation and bioavailability of mercury and thereby reduced its toxicity. These results raised the possibility that mb could serve to protect the microbial community from mercury toxicity in the environment, which was shown as *Methylomicrobium album* Strain BG8 is also protected by mb-OB3b from mercury. Another study by Kalidass et al., (2015) looked at the interaction of mb with gold and their effect on methanotrophic activity. It was found that when copper, gold, and mb-OB3b are provided in the medium, gold can bind to mb more rapidly and block the binding and availability of copper to *M. trichosporium* OB3b leading to sMMO expression in the presence of copper. However, if mb was pre-incubated with copper and added exogenously together with gold to *M. trichosporium* OB3b, sMMO expression was repressed, suggesting that gold cannot displace copper bound to mb. These findings extend our understanding of *in situ* methanotrophic activity where complicated environments are present.

Other studies have shown that methanotroph can take up mb produced by another methanotrophic member. By doing so, the "copper-switch" could be induced (Ghazouani et al., 2011; Farhan UI Haque et al., 2015). It was also found that the addition of mb-SB2 can enhance the expression and activity of sMMO in *M. trichosporium* OB3b, a similar response as to the addition of its native mb (Semrau et al., 2013; Farhan UI Haque et al., 2015). This finding suggests that mb may serve as a signaling molecule to regulate genetic expression between methanotrophic strains. As mentioned earlier, copper binding compounds from the Type I methanotroph (i.e. *M. capsulatus* Bath) have different structures and a lower copper-binding constant compared to the mbs from Type II

methanotrophs. (Choi et al., 2008, 2011) There is also a difference in copper binding affinities between the mbs from Type II methanotophs, especially to Cu^{2+} (Ghazouani et al., 2011). It will be interesting to see if there is interaction between Type I and II methanotrophs (and even with other groups of bacteria) based on mbs and to see how the difference in mb properties affect the structure and composition of methanotrophic communities (Semrau et al., 2010).

I.3.2.5 Applications of mb

Mb has several properties that make it industrially and medically valuable. Both mb-OB3b and mb-SB2 have been shown to reduce Au^{3+} to Au^{0} and form gold nanoparticles with high uniformity (Bandow, 2014; Choi et al., 2006). Gold nanoparticles have applications in catalysis, biosensing, drug delivery, and photonics. However, obtaining mono-dispersed gold nanoparticles with a narrow size distribution remains challenging (Daniel et al., 2004). Microbial-mediated production of gold nanoparticles has been considered (Korbekandi et al., 2009). Mb stands out as a strong candidate in that they produce gold nanoparticles of well-defined sizes of 2.0+/-0.7mm (Bandow, 2014; Choi et al., 2006).

Other research has shown that mb is an effective chelator for copper in a rat model for Wilson disease. Wilson disease is an autosomal recessive disorder where the body is unable to correctly assimilate copper, with copper accumulating in the liver and brain, and can result in severe and irreversible damage (Ala et al. 2007, Roberts, 2011). Current treatment therapies include prescription of chelating agents such as penicillamine and

trientine, but it is not uncommon for serious side effects to occur, and in any case copper is excreted when using these compounds through the urine and not the bile, which is the preferred or normal physiological route. Mb, however, was found to bind copper very strongly in a rat model of Wilson disease. Copper was then quickly removed via the bile and animals treated with mb had sustained clinical recovery (Lichtmannegger et al., 2016). Such findings indicate that mb has the potential to be an alternative treatment for Wilson disease, particularly for those patients with acute liver failure (Kaler, 2016).

The application of mb for different purposes is held back currently by the lack of knowledge of its synthesis pathways and the slow growth of methanotrophs, which leads to low yield of mb (~50 mg/L culture). The latter is an obstruction faced by many methanotroph-based applications. There is a great deal of interest in enhancing methanotrophic activity and in up-scaling the production of mb.

I.3.3 Alternative copper uptake mechanism(s)

The finding that *mbnA*::Gm^r mutant is able to take up copper and respond to copper indicates that an alternative copper uptake pathway(s) exist in methanotrophs (Semrau et al., 2014). Several candidates have been suggested. For example, Balasubramanian et al., (2011) argue a porin-dependent passive transport mechanism exists besides the active uptake of Cu-mb in *M. trichosporium* OB3b based on uptake-inhibition studies. Another possible candidate is a CopC encoding gene which was found to respond to copper levels in a transcriptomic study on *M. capsulatus* Bath (Larsen & Karlsen, 2015). CopC family proteins are located to the periplasm where they have been shown to function as copper

chaperones (Djoko et al. 2007). Moreover, as discussed previously, the MbnP (a putative di-heme cytochrome c peroxidase) and MbnH (the partner protein) are homologues of SACCP/MopE in *M. capsulatus* Bath and CorB/CorA in *M. album* BG8. These have been indicated to be involved in copper sensing system (Berson & Lidstrom, 1997, Fjellbirkeland et al., 2001) in Type I methanotrophs. Specifically, MopE was found to have a copper binding site and its C-terminal region can be secreted for copper sensing (Kalsen et al., 2005; 2008; 2010). Expression of *corAB* responds to copper and are downregulated in the presence of copper in *M. album* BG8 (Berson & Lidstrom, 1997). MbnPH could be an alternative copper sensing mechanism if these proteins function like MopE. However, MbnP has low similarity to either MopE or CorA.

I.4 Regulation of gene expression by rare earth elements

The complexity of genetic regulation in methanotrophs is not only shown in MMOs. It is now known that MDH expression also involves a complicated regulatory network. A mutagenesis study on *Methylobacterium extorquens* AM1 identified five genes required for the transcription of MxaF-MDH. These five genes consist of two and a half pairs of sensor kinase/response regulators (Springer et al., 1997). These two-component regulatory systems are commonly used by bacteria as a mechanism to respond to rapid environmental changes (Krell et al., 2010). The first pair is *mxbDM*, located upstream of *pqq* operon *pqqABCED,* genes required for the synthesis of PQQ. This pair responds to one-carbon substrate as compared to growth on succinate. Hierarchically above *mxbDM*, there is a second pair of genes, *mxcQE*, which are required for expression of *mxbDM* and indirectly control expression of the *mxa* operon (Springer et al., 1997). A third regulator

named *mxaB* also exists and is required for the transcription of *mxa* operon as well. It is an orphan response regulator without a sensor kinase (Springer et al., 1998).

With the identification and characterization of XoxF-MDH, it was found that *xox* genes are also co-regulated with the *mxa* operon. Skovran et al. (2011) found that (1) with the two copies of *xoxF* in *M. extorquens* AM1 (*xox1* and *xox2*), at least one copy of *xoxF* is required for the expression of *mxa*-promoter; (2) MxbM is require for the repression of *xox1* operon; and (3) *xoxF12* are required for inducing *mxcQE* and *mxbDM* expression.

However, early observation regarding the expression of *xoxF* itself was controversial. While *xoxF* is hardly expressed in typical laboratory culturing conditions, it was found to have at a high level of expression in several proteomics studies on environmental samples (Delmotte et al., 2009, Ettwig et al., 2010, Sowell et al., 2011). These inconsistent observations were attributed to the availability of rare-earth elements (REE) like lanthanum (III), since lanthanum was found to increase the activity of XoxF-MDH (Nakagawa et al., 2012, Wu et al., 2014). The effect of cerium on the expression of *xox* operon was then investigated in methanotrophs (Farhan UI Haque et al., 2015, 2016). Cerium was found to induce the expression of *xox* operon and represses the *mxa* operon. Consistent observations were made later in *M. extorquens* AM1 by Vu et al., (2016). In the same study, a regulatory model of *xox* and *mxa* operons was proposed in *M. extorquens* AM1 (Figure 2.15). The accuracy of the model, however, is yet to be tested as the existence of an apo-form of XoxF, the interaction of XoxF with MxcQ, and the direct binding of MxcE, MxbM with different promoter regions have not been demonstrated.

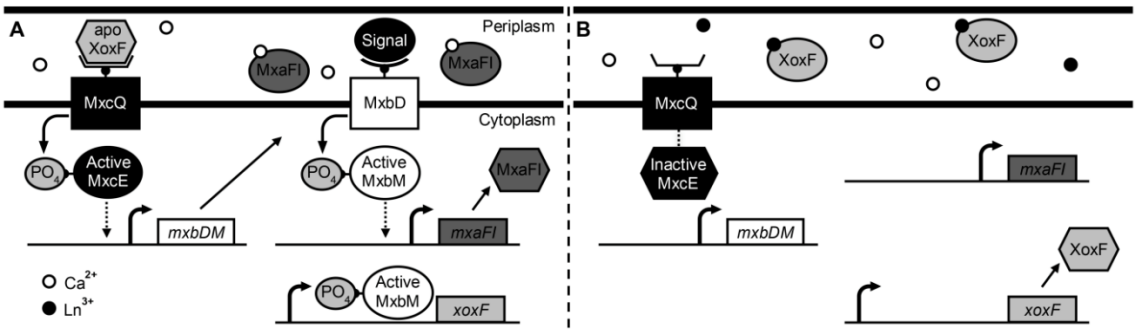

Figure 1.15. Hypothesis for how XoxF and lanthanides (Ln) differentially regulate expression of the *mxa* and *xox1* genes in the absence (A) and presence (B) of lanthanides. (Vu et al., 2016)

As mentioned above, the genetic regulation by REE in methanotrophs was initiated by Farhan UI Haque et al., (2015), in which the expression levels of Mxa-MeDH and Xox-MeDH in *M. trichosporium* OB3b under different cerium and copper conditions were investigated. It was found that Mxa-MeDH and Xox-MeDH significantly decreased and increased, respectively, when grown in the presence of cerium compared to the absence of cerium. In the presence of copper, however, the repression of cerium on *mxaF* was less significant, while the induction on *xoxF* was at similar level as compared to the absence of copper. This indicates a cross-regulation of gene expression by copper and cerium methanotrophs.

These findings broaden our understanding of the complicated regulation system in methanotrophs and can be instructive for better manipulation of methanotrophic activities. Many new topics should be investigated, for example, the sensing and uptake mechanism of the sparingly soluble REEs by methanotrophs; the effect on electron transport to pMMO, and the relative regulation of MDHs by REEs.

I.5 Applications of methanotrophs

Methanotrophs grow on methane as their sole carbon and energy source. Methane is renewable if produced by methanogenic activity. Methane has become an attractive choice for liquid fuel and chemical production. Nearly $3x10^{13}$ ft^3 of natural gas was produced in the US in 2012, representing a 30% increase since 2002 (US Energy Information Administration, 2015). The production of natural gas is estimated to keep increasing with 25% of global energy derived from natural gas by 2035 (International Energy Agency, 2015). Due to the development of shale gas production, the cost of natural gas (80-95% v/v methane mixed with other heavier alkanes) has dropped significantly, from \$10.79 per 1000 ft^3 in July 2008 to \$3.38 per 1000 ft^3 in 2012 (US Energy Information Administration, 2015). Nevertheless, about 5% of the annual production of natural gas is currently flared or vented around the globe, contributing to greenhouse gas emissions. This waste is largely caused by the lack of economic incentive to capture the unwanted natural gas. Therefore, alternative processes to produce value-added products from methane is currently of great interest. Current technologies of the conversion of natural gas into liquid products (e.g. the Fischer-Tropsch process) are usually energy intensive and have low carbon conversion efficiency (25-50%).

Due to their unique physiology as the biological methane sink and versatile metabolic abilities, methanotrophs have drawn substantial attention for bioconversion of methane. Applying methanotrophs for methane conversion has the following advantages: (1) methanotrophs are able to convert methane into value-added products under ambient

conditions; (2) bioconversion of methane does not require pipelines facilities and can be realized in scattered, remote areas; (3) using methane as a starter material for chemical production can relieve the dependence on other substrates (e.g., sugar) with high costs; and (4) bioconversion of methane by methanotrophs is inexpensive and efficient (in carbon conversion) compared to many other traditional chemical processes. Many potential applications of methanotrophs in the bioconversion of methane have been proposed and thoroughly reviewed (Semrau et al., 2010; Jiang et al., 2010; Fei et al., 2014; Kalyuzhnaya et al., 2015; Khmelenina et al., 2015). A few aspects are discussed below.

I.5.1 Mitigation of methane emission

CH_4 is approximately 34 times as efficient as carbon dioxide at absorbing infrared radiation as a greenhouse gas. Processes like landfill and mining activities are significant sources of CH_4 emission (IPCC, 2013), in particular, globally landfills release 799 metric tons of CO_2 equivalent of the methane entering the atmosphere (US EPA, 2011). Reduction of fugitive methane emissions from these sources is required. Much attention has been put into stimulatory methanotrophic activity in landfill cover soils or other engineered systems (e.g., biocover and biofilter) to reduce fugitive emissions of CH_4 (Park et al., 2008; Scheutz et al., 2009; Nikiema et al., 2007; Huber-Humer et al., 2008). These systems use supporting materials with sufficient porosity and a high moisture holding capacity to increase gas transfer to better establish methanotrophic growth. Field trials and experimental studies have shown that methanotrophic biofilters can remove appreciable amounts of methane at concentrations ranging from 700 to 1500 p.p.m.v.

(Melse & Van Der Werf, 2005; Nikiema et al., 2009; Barlaz et al., 2004).

I.5.2 Bioremediation

Both forms of MMO can bind and oxidize a range of hydrocarbons and some halogenated derivatives (Colby et al., 1977, Grosse et al., 1999). Methanotrophs have been investigated for bioremediation of halogenated compounds (Westrick et al., 1984, Wilson & Wilson, 1985, Semprini, 1997, DiSpirito et al.,1992), aromatic hydrocarbons (Rockne et al., 1998), and chlorinated biphenyls (Lindner et al., 2000). Methanotrophs biodegrade organic pollutants oxidatively, which produce less toxic intermediates as compared to reductive biodegradation. Also, methanotrophs are ubiquitous and are easily stimulated with the provision of methane.

There is some controversy as whether sMMO- or pMMO-expressing cells are more useful for bioremediation. The sMMO has a wider substrate range, being able to oxidize alkanes up to C-8, as well as ethers, cyclic alkanes, and aromatic hydrocarbons (Colby et al., 1977; Burrows et al., 1984). pMMO has a narrower substrate range being able to oxidize alkanes up to C_5 but not aromatic compound (Burrows et al., 1984). However, pMMO has a higher affinity for CH_4 (Lontoh & Semrau, 1998) and gives methanotrophs a higher efficiency of CH_4 conversion into biomass (Leak et al., 1985). As a result, methanotrophs expressing pMMO appear to have a competitive advantage over cells expressing sMMO for degrading mixtures of substrates over the long term. This is because pMMO has greater specificity for methane and cells are more effective at turning over the growth substrate (methane) in the presence of non-growth substrates. Further the

accumulation of toxic degradation products is slower. (Lee et al.,2006; Yoon & Semrau, 2008).

Methanotrophs have also been considered for immobilizing heavy metals. Methanotrophs influence the speciation and bioavailability of metals in the environment (Choi 2006, Jenkins et al.,1994, Knapp et al.,2007). Hasin et al. (2010) reported the reductive transformation of soluble and more toxic Cr (VI) into a less toxic Cr (III) species by *M. capsulatus* Bath. This strain was also found to reduce mercury using reducing equivalents obtained from the dissmililation of methane (Boden and Murrell, 2011). As discussed in the previous section, methanotrophs can interact with metals via mb. The expanding knowledge of mb will thus likely expand the application of methanotrophs in bioremediation of heavy metals.

I.5.3 Single cell protein production

There has been interest in the use of microorganisms as an alternative source of protein for animal consumption since the early 1980s (Kuhad et al., 1997). The use of cheap, non-agricultural products as a starting material, i.e., CH_4, for single-cell protein production by methanotrophs has been put into use at a commercial scale (e.g., UniBio, Denmark, 2011). Although bacteria typically possess a high protein content (50-60%), they also possess high nucleic acid content (8-12%) which can cause significant immunological effects (NCSF, 2006). As a result, bacterial protein is best suited as a feed ingredient for animals with a short life span. UniProtein produced by UniBio has been tested as feed for salmon, calves, pigs and chickens with positive results in terms of

acceptance and growth.

I.5.4 Poly (3-hydoxybutyrate) (PHB) production

Biopolymers like poly(3-hydoxybutyrate) (PHB) are biodegradable, biocompatible, and thermoplastic polyesters that are of interest for the production of plastics. PHB can be accumulated by bacteria by exposing an active culture to excess carbon while under some nutrient limitation. Many studies have explored the potential of utilizing methanotrophs for PHB production, most of which tried to increase PHB production by manipulating the growth conditions of methanotrophs, e. g., C:N ratios (Lee et al., 1994; Kim et al., 1998; Zhang et al., 2008), and also limiting potassium (Kim et al., 1998; Helm et al., 2008). It was found that pMMO-expressing cells displayed greater and more rapid PHB accumulation as well as greater biomass (Shah et al., 1996). A maximum PHB content of 70% (w/w) could be obtained in a culture of *Methylocystis parvus* OBBP (Asenjo and Suk, 1986). However, the production cost of microbial PHB is relatively high compared to traditional petrochemical-based plastics (Lee et al., 2005). It has been suggested that higher-value polymers used in biomedical applications could be the target to bridge initial commercialization of biopolymers from methanotrophy (Strong et al., 2015). Indeed, methanotrophic production of PHB has been commercialized (Newlight Technology, Costa Mesa, CA; Mango Materials, CA, USA) by using biogas produced from anaerobic digestion of organic material.

I.5.5 Biofuel production

The use of methanotrophs to produce biofuels from methane has also been recently evaluated (Conrado & Gonzalez, 2014; Fei et al., 2014). Because of the formation of extensive intracytoplasmic membranes (ICM) under pMMO-expressing conditions, methanotrophs have a relatively high lipid content compared to most other bacteria. As a result, they have metabolic potential for the production of biodiesel from these lipids. The ICM consists of phosphatidyl-glycerol (PG) and phosphatidyl methyl ethanolamine (PE)-type phospholipid, e.g., phosphatidyl methyl ethanol-amine (PME) and phosphatidyl dimethyl ethanolamine (PDME) (Lechevalier and Moss, 1977; Weaver et al., 1975). The composition is different from typical biodiesels rich in triglycerides (Fang et al., 2000). Methanotrophic lipids are thus proposed to produce renewable dieseal via hydroprocessing (Fei et al., 2014). The lipid fraction in the biomass can be more than 20% on a dry cell weight basis in methanotrophs under pMMO-expression conditions (Collins et al., 1991; Kaluzhnaya et al., 2001). However, this yield is not yet competitive over the utilization efficiency of glucose for production of other biofuels. An increase to approximately 35% lipid content could justify methane to biodiesel conversion (Khmelenina et al.,2015) but would likely require a synthetic biology approach to achieve.

I.5.6 Challenges in applications of methanotrophs

Many other potential applications of bio-conversion of methane by methanotrophs have been proposed and evaluated including cell-free catalysis, production of primary and secondary metabolites, biosensors for methane detection amongst others. (Semrau et al., 2010; Jiang et al., 2010; Fei et al., 2014; Kalyuzhnaya et al., 2015; Khmelenina et al.,

2015). However, there are still obstacles in realizing any of these applications in pilot- or commercial scales. These include: (1) incomplete understanding of metabolic shifts/gene regulation in response to different growth/nutrient conditions, (2) lack of high-efficiency tools and approaches to genetically manipulate methanotrophs, (3) inability to obtain active enzymes either *in vitro* or via heterologous expression, and (4) slow and limited growth of methanotrophs, mostly due to limited gas-liquid phase transfer of methane and oxygen.

I.6 Project aims

There is great need for a better understanding of how methanotrophs regulate their metabolism and also to develop better genetic manipulation systems to enhance the utility of methanotrophs for various applications. The aims of the work described here are thus to:

1. investigate mb-mediated copper uptake in *M. trichosporium* OB3b;
2. develop systems to facilitate the genetic manipulation in *M. trichosporium* OB3b, especially to characterize mb synthesis;
3. identify other systems possibly involved in copper uptake and/or sensing in *M. trichosporium* OB3b;
4. determine how REEs affect gene expression in *M. trichosporium* OB3b, and;
5. investigate the cross-regulation of gene expression by copper and REE in *M. trichosporium* OB3b through transcriptomic analyses.

CHAPTER II MATERIALS AND METHODS

II.1 Materials

Chemicals were purchased through Sigma-Aldrich Corporation (St Louis, MO, USA) or Fisher Scientific (Fair Lawn, NJ) as analytical-grate or higher. Methane used for growth of cultures was 99.999% purity grade obtained from Airgas Company (Ann Arbor, MI). Custom oligonucleotide primers were obtained from Integrated DNA Technologies (Coralville, IA). Enzymes are purchased through New England Biolab (Ipswich, MA), Invitrogen (Carlsbad, CA), and Bio-Rad (Hercules, CA).

II.2 Cultivation, maintenance, and storage of bacterial strains

All solutions and growth media were prepared with Milli-Q water (>18.2 MΩ·cm at 25 °C) and sterilized either by autoclaving or filtering using 0.22 μm SFCA or PVDC filters purchased from EMD-Millipore (Billerica, MA) before use. Solid media were prepared by the addition of 1.5 % to 1.8% (w/v) agar and sterilized via autoclaving. A summary of bacterial strains used is shown in Table 2.1. Frozen stocks of strains were stored at -80°C in the presence of 15 % (v/v) glycerol sterilized via autoclaving.

II.2.1 Antibiotics

Antibiotics were filter sterilized and added aseptically to cooled, sterilized growth medium. Where appropriate, antibiotics were added to the following concentrations: ampicillin 100 $\mu g \cdot ml^{-1}$; kanamycin, 25 to 50 $\mu g \cdot ml^{-1}$; gentamicin 5 $\mu g \cdot ml^{-1}$; nalidixic acid 15 $\mu g \cdot ml^{-1}$ for *E. coli* strains, kanamycin, 10 $\mu g \cdot ml^{-1}$, gentamicin 2.5 $\mu g \cdot ml^{-1}$, and specitnomycin 20 $\mu g \cdot ml^{-1}$. Cycloheximide (30 $\mu g \cdot ml^{-1}$) was used to prevent fungi contamination when necessary.

II.2.2 Preparation of chemically competent *Escherichia coli* cells

Chemically competent *E. coli* were prepared via $CaCl_2$ (Mandel & Higa, 1970, Cohen *et al.*, 1972). A single colony from a fresh plate of *E. coli* Top10 cells was transferred to 10 ml of Luria-Bertani (LB) medium and incubated at 37 °C with shaking at 220 rpm overnight. 1mL of the overnight culture was then used to inoculate 500 ml flasks containing 100 ml LB medium, and incubated at 37 °C with shaking for 2-3 hours until OD_{600} reached 0.20-0.30. Cells were then cooled on ice, harvested by centrifugation (2,000 × g, 15 mins, 4 °C), and resuspended in 40 ml ice-cold 0.1M $MgCl_2$. The cells were then centrifuged again, resuspended in 20 ml ice-cold 0.1M $CaCl_2$, and treated for at least 20 min on ice. The cells were harvested for the third time and resuspended in 2ml of ice-cold 85mM $CaCl_2$, 15% glycerol and incubate for 10 min followed by distributing 200 µl aliquots into cooled microcentrifuge tubes, and stored at -80 °C.

Table 2.1. Bacterial strains and plasmids used in this study.
Abbreviations, Gm^r, gentamicin resistance; Km^r, kanamycin resistance; Ap^r, ampicillin resistance; Na^r, nalidixic acid resistance.

Strains/Plasmids	Description	Reference/Source
Escherichia coli		
TOP10	F– *mcrA* Δ(*mrr-hsdRMS-mcrBC*) Φ80*lacZ*ΔM15 Δ*lacX74 recA1 araD139* Δ(*ara leu*) *7697 galU galK rpsL* (StrR) *endA1 nupG*	Invitrogen
S17.1 *λpir*	*recA1 thi pro hsdR*- RP4-2Tc::Mu Km::Tn*7* λ*pir*	(Simon, 1984)
Methylosinus trichosporium		
OB3b	Wild-type strain	
Δ*mbnAN*	*mbnABCMN* deleted	this study
Δ*mbnAN* + pWG101	Δ*mbnAN* back-complemented by pWG101	this study
Δ*mbnN*	Δ*mbnAN* carrying pWG102	this study
Δ*mbnM*	Δ*mbnAN* carrying pWG105	this study
Δ*mbnB*	Δ*mbnAN* carrying pWG103	this study
Δ*mbnC*	Δ*mbnAN* carrying pWG104	this study
Δ*mbnT*::Gm^r	*mbnT* deleted with insertion of Gm cassette	this study
Δ*copCD*::Gm^r	*copCD* deleted with insertion of Gm cassette	this study
Δ*mbnAH*	*mbnABCMNPH* deleted	this study
Δ*mbnPH*	Δ*mbnAH* carrying pWG101	this study
Plasmids		
pK18mobsacB	Km^r, RP4-mob, mobilizable cloning vector containing *sacB* from *B.subtilis*	(Schäfer et al., 1994)

Table 2.1 Continued

Strains/Plasmids	Description	Reference/Source
pTJS140	Sp^r, Sm^r cloning vector	(Smith et al., 2002)
p34S-Gm	Source of Gm^r cassette	(Dennis & Zylstra, 1998)
pWG011	pK18mob*sacB* carrying 2 ligated arms with a Gm cassette used to knock out *mbnT*	this study
pWG012	pK18mob*sacB* carrying 2 ligated arms used to knockout *mbnABCMN*	this study
pWG013	pK18mob*sacB* carrying 2 ligated arms used to knockout *mbnABCMNPH*	this study
pWG014	pK18mob*sacB* carrying 2 ligated arms with a Gm cassette used to knockout *copCD*	this study
pWG101	pTJS140 carrying *mbnABCMN* with its native promoter	this study
pWG102	pTJS140 carrying *mbnABCM* with its native promoter	this study
pWG103	pTJS140 carrying *mbnACMN* with its native promoter	this study
pWG104	pTJS140 carrying *mbnABMN* with its native promoter	this study
pWG105	pTJS140 carrying *mbnABCN* with its native promoter	this study

For transformation, cells were thawed on ice and less than 50 ng of plasmid DNA or ligation mix was added to 50 – 100 µl competent cell suspensions and gently mixed. Cells were subjected to heat shock at 42 °C for 45 s, and cooled on ice for at least 3 min. Warm SOC medium (Corning, Manassas, VA) was added and cells recovered at 37 °C with shaking for one hour. Aliquots of different amount were spread on selective LB plates and incubated at 37 °C for 24 - 48 h before colony screening.

II.2.3 Methanotrophs

M. trichosporium strains were grown on nitrate mineral salt (NMS) medium (Whittenbury et al., 1970) with addition of antibiotics if necessary at 30 °C in 250 ml side-arm Erlenmeyer flasks shaken at 200 rpm. CH_4 was added at a methane-to-air ratio of 1:2. The optical density at 600 nm (OD_{600}) was measured with a Genesys 20 Visible spectrophotometer (Spectronic Unicam, Waltham, MA) at 12-h intervals. For growth on solid media, agar plates were incubated in a gas-tight container under a methane/air (1:2) atmosphere.

II.2.4 Biparental mating of methanotrophs and *E coli*

The transfer of plasmid DNA from *E. coli* to methanotrophic strains was done following the method by Martin and Murrell (1995). A 10 ml *E. coli* S17.1 culture grown overnight containing the plasmid of interest, and a 50 ml culture of *M. trichosporium* OB3b in early exponential phase (OD_{600} 0.2-0.3) were separately centrifuged (4,000 × g, 15 min, room temperature), both were washed once in NMS medium, resuspended and mixed together in 10 ml NMS medium, filtered through a 0.2 µm pore-size nitrocellulose filter (Millipore, Billerica, MA). The filter holding cells was placed on a NMS agar plate supplemented with 0.02 % (w/v) proteose peptone and

incubated for 24-48 hours at 30 °C. Following incubation, the cells were resuspended with 10 ml NMS medium, pelleted and resuspended finally in 2 ml NMS medium. Aliquots of 100 -200 µl were spread on NMS plates containing selective antibiotics and incubated in the presence of methane/air at 30 °C. Colonies appeared on plates after 10-20 days.

II.3 Nucleic acid manipulation techniques

II.3.1 Nucleic acid extraction and quantifications

DNA and RNA were isolated using the method modified from Griffiths *et al.* (2000). For extraction of genomic DNA, cells were harvested by centrifuging at 4,000 g for 10 minutes at 4 °C. The cell pellets were resuspended in 0.75 mL of extraction buffer [100 mM Tris-HCl (pH 8.0), 1.5 M NaCl, 1% (w/v) hexadecyltrimethylammonium bromide (CTAB)].

Total RNA was extracted from the cells grown in exponential phase, collected from 5 or 10 mL of culture mixed with 0.6 or 1.2 mL of stop solution [5 % buffer equilibrated phenol (pH 7.3) in ethanol] to stop any new mRNA synthesis. Cells was then resuspended in 0.75 mL of the extraction buffer as described above and subsequent steps were as described by Semrau et al. (2013). DNA was removed by Qiagen RNase-free DNase through at least two treatments (one in solution and one on column), followed by purification using a Zymo RNA Clean & Concentrator kit (Zymo Research, Irvine, CA) following the manufacturer's instructions. Removal of all traces of DNA was confirmed by the absence of a 16S rRNA PCR product in reactions using 1 µl to 2 µl of RNA template and > 30 PCR cycles.

Plasmid preparations were carried out on 5 -10 ml overnight *E. coli* cultures using the Qiaprep Miniprep Kit (Qiagen) according to the manufacturer's instructions.

DNA and RNA concentrations were estimated using an ND-1000 spectrophotometer (NanoDrop Technologies Inc., Wilmington, DE).

II.3.2 Polymerase chain reaction (PCR)

Polymerase chain reactions (PCR) were conducted using a C1000 Touch (Bio-Rad, Hercules, CA) or T-48 Personal (Biometra) thermal cycler, using recombinant GoTaq Green polymerase (Promega, Madison, WI) or, for high fidelity applications like cloning, iProof (BioRad) polymerase. A typical 25 µl reaction contained 1 × MasterMix and 0.5 µM forward and reverse primer. Cycling conditions followed the manufacturer' suggestions. Annealing temperature was calculated using OligoAnalyzer 3.1 (https://www.idtdna.com/calc/analyzer).

For PCR directly from colonies, a colony was picked aseptically using autoclaved pipet tips and suspended in 10 µl sterilized water. 5 µl of the suspension was mixed with 5 µl 0.5M NaOH solution and heated at 95 °C for 10 min for quick breaking of cells. 0.2 µl of the cell lysis solution was used in a 15-25 µl PCR reaction as DNA template. Negative (with water as template) and positive controls (with constructed plasmid or extracted genome as template) were included in all cases. PCR primers used are listed in Table 3.2.

II.3.3 Agarose gel electrophoresis

DNA fragments were separated in 0.8 – 1.0 % (w/v) agarose gels in 1 × TAE buffer (Invitrogen, Carlsbad, CA). 100 bp or 1 kb DNA ladders (New England Biolab, Ipswich, MA) were used to estimate the sizes of DNA fragments. Ethidium bromide (10 μg ml^{-1}) was added to gels prior to casting. Gels were visualized on a Gel Logic 100 (Kodak, Rochester, NY) imaging system.

II.3.4 DNA purification from PCR reaction

DNA fragments from PCR reactions were checked on agarose gels. Those with a clear, specific band were purified using QIAquick (Qiagen) purification kits. Otherwise DNA fragments were excised from TAE agarose gels and purified using QIAquick (Qiagen) gel extraction kits following the manufacturers' instructions.

II.3.5 DNA restriction digests

Restriction digestion of DNA was typically carried out with enzymes purchased from New England BioLabs (Ipswich, MA) overnight at 37°C. The reactions were set up according to the manufacturers' recommendations. DNA fragments after restriction digestions were routinely purified from gel to remove undesired digested fragments.

II.3.6 DNA ligations

Ligations were carried out using T4 DNA ligase (New England BioLabs, Ipswich, MA) in a volume of 20 μl comprising vector and insert fragments in 1:3-1:4 molar ratios or two PCR products in 1:1 molar ratio. The simpler ligation reactions (e.g., ligation of two short DNA

fragments) were performed at room temperature for > 3 hours. For ligation of large inserts into plasmids, reactions were typically carried out at 16°C overnight to increase efficiency.

II.3.7 Cloning of PCR products

For DNA fragments that were subject to cloning, PCR primers were typically designed with an added restriction site and a 6 nt-overhang for enzyme binding at 5' (Table 2.2). iProof high-fidelity polymerase was used for PCR amplification, followed by purification of PCR product, restriction digestion, gel purification of digested fragment, and ligation into vectors. The ligation mix was then used to chemically transform *E. coli* TOP10 for selection and maintenance. Inserts were confirmed by colony PCR using vector specific primers and sequencing.

II.3.8 RT-quantitative PCR (RT-qPCR)

Differential expression of genes was tested by RT-qPCR. A list of primers used for RT-qPCR are listed in Table 3.2. qPCR reactions were performed in 96-well reaction PCR plates in a volume of 20 µl containing 0.8 µl cDNA or DNA, 1 × iTaq Universal SYBR Green Supermix (Bio-Rad, Hercules, CA), 0.5 µM of each of forward and reverse primers and nuclease-free sterile water (Fisher Scientific, Pittsburgh, PA). CFX Connect Real Time PCR Detection System (Bio-Rad, Hercules, CA) was used to run a three step qPCR program consisting of an initial denaturation at 95 °C for 3 min and 40 cycles of denaturation (95°C for 20 s), annealing (58°C for 20 s) and extension (68°C for 30 s). To confirm specificity, qPCR products were subjected to melting curve analysis with temperature ranging from 65°C to 95°C after the completion of amplication cycles. The threshold amplication cycle (C_T) values were then imported from CFX Manager Software (Bio-Rad, Hercules, CA) into Microsoft Excel to quantify the expression of different genes.

Table 2.2. Primers for PCR and sequencing.

Name qRT-PCR primers are underlined.	**Sequence (5'-3')** Restriction sites are noted with lower case letters. Added overhangs for binding by restriction enzyme are underlined.	**Reference**
27F	AGAGTTTGATCMTGGCTCAG*	(Lane, 1991)
1492R	TACGGYTACCTTGTTACGACTT*	(Lane, 1991)
M13F	GTAAAACGACGGCCAG	Invitrogen
M13R	CAGGAAACAGCTATGAC	Invitrogen
pmoA-F	GGNGACTGGGACTTCTGG*	(Holmes et al., 1995)
pmoA-R	CCGGMGCAACGTCYTTAC*	(Costello & Lidstrom, 1999)
mmoX-F	ATCGCBAARGAATAYGCSCG*	(Hutchens et al., 2004)
mmoX-R	ACCCANGGCTCGACYTTGAA*	(Hutchens et al., 2004)
mbnA-F	TGGAAACTCCCTTAGGAGGAA	(Semrau et al., 2013)
mbnA-R	CTGCACGGATAGCACGAAC	(Semrau et al., 2013)
Ton41	ATTTTTgaattcCCAGAAATATGAGATTCCGC	this study
Ton42	ATTTTTggatccCACGACCAGATCGATGATAC	this study
Ton43	ATTTTTggatccTTCGGTTCGATCAACGAGG	this study
Ton44	ATTTTTaagcttGCCAATCAGCGTGGAGAACC	this study
dmbnaF (mbn56)	ATTTTTggatccCGAAGGACAATAACAAGGCG	this study
dmbnaR (mbn57)	ATTTTAggtaccACTCCAAACAgcatgcGATA	this study
dmbnbF (mbn60)	ATTTTAggtaccATCCTTCTATGTCTGCAGCC	this study
dmbnbR (mbn61)	ATTTTTaagcttGATCCTCCTCGAATTCCCTC	this study
dmbnAHbF	ATTTTTctagaGTTTCTCTGATCCCTGGAGA	this study
dmbnAHbR	ATTTTTaagcttGAAAGAGAGATCACAGCCAC	this study
pK18-bb-F	CTCTGGTAAGGTTGGGAAGC	this study
pK18-bb-R	GCAATACACGGGTAGCCAA	this study
mbnANf (wgu21)	ATTTTTggtaccGACGTTCGGGTCTTCTTCGC	this study
mbnANr (wgu22)	ATTTTTggtaccCGCCTCTAGATCATTCCGAC	this study
mbnAMr (mbn64)	ATTTTTggtaccTTCGTTTCACATGGGATCGC	this study

Table 2.2 Continued.

Name	Sequence (5'-3')	Reference
qRT-PCR primers are underlined.	Restriction sites are noted with lower case letters. Added overhangs for binding by restriction enzyme are underlined.	
copCDaF	ATTTTTaagcttCCGTTATCGCTATGTCGGGT	this study
copCDaR	ATTTTAggatccAATCTCTCATCGCTGAAAGC	this study
copCDbF	ATTTTTggatccCAGCTTCATTCTTCGGCTCC	this study
copCDbR	ATTTTTgaattcCCGTTCCTCTCGCTGTTTTGC	this study
pmxa-F (wgu51)	ATTTTTgcatgcGAACTTCCTCGTCTGCTTC	this study
pmxa-F (wgu52)	ATTTTTtctagaCCTCGTGGCGCTTTCGTCGA	this study
mbn1_SB2	TAAAAAtctagaCAGACGAAATCAAAACAGGAGG	this study
mbn2_SB2	TAAAAAggtaccGTTGATCCCATGCGCTTT	this study
mbn3_SB2	TAAAATggtaccTCGACCACTCTCCTTTGCGA	this study
mbn4_SB2	TAAAAAggtaccCAGAGCAAGGAGAGGTCG	this study
mbn5_SB2	ATTTTTgaattcCGTCGCTGTTTTCTTGCTCT	this study
mbn63	ATTTTTggtaccCTCGAACGTTTGCCCAGAG	this study
mbn64	ATTTTTggtaccTTCGTTTCACATGGGATCGC	this study
mbn65	ATTTTTggtaccCTAGGCGCATCATCATCACA	this study
mbn66	ATTTTTggtaccCGAACAATGTGTGCCAGTAG	this study
mbn67	ATTTTTggtaccTGGAATACGGCCAGAATCG	this study
mbn65	ATTTTTggatccCTAGGCGCATCATCATCACA	this study
mbn66	ATTTTTggatccCGAACAATGTGTGCCAGTAG	this study
mbn67	ATTTTTggatccTGGAATACGGCCAGAATCG	this study
mbn68	ATTTTTggatccGCTCGGAATTCTCGCTTTCC	this study
mbn69	ATTTTTggatccCGATATTTTCCCCTGCGTCG	this study
mbn70	ATTTTTggatccGTTCGGCTATTTCCTGACGC	this study
qpmoA_FO	TTCTGGGGCTGGACCTAYTTC	(Knapp et al., 2007)
qpmoA_RO	CCGACAGCAGCAGGATGATG	(Knapp et al.,2007)

Table 2.2 Continued.

Name qRT-PCR primers are underlined.	Sequence (5'-3') Restriction sites are noted with lower case letters. Added overhangs for binding by restriction enzyme are underlined.	Reference
qmmoX_FO	TCAACACCGATCTSAACAACG	(Knapp et al.,2007)
qmmoX_RO	TCCAGATTCCRCCCCAATCC	(Knapp et al.,2007)
q16SrRNA_FO	GCAGAACCTTACCAGCTTTTGAC	(Knapp et al.,2007)
q16SrRNA_RO	CCCTTGCGGGAAGGAAGTC	(Knapp et al.,2007)
qmbnA_FO	TGGAAACTCCCTTAGGAGGAA	(Semrau et al.,2013)
qmbnA_RO	CTGCACGGATAGCACGAAC	(Semrau et al.,2013)
qmxaF_FO	CTACATGACCGCCTATGACG	(UI Haque et al.,2016)
qmxaF_RO	ATTGGCCTTGTTGAAGTCGT	(UI Haque et al.,2016)
qXoxF_F1	TCATTTCCGTGATGTGCTGC	(UI Haque et al.,2016)
qXoxF_R1	CTTTCCAGACGATCTTGCCG	(UI Haque et al.,2016)
qcopC2_FO	GATCCTCGACTCGACTGGC	this study
qcopC2_RO	TTTCACGACATAGCTCCCGA	this study
qcopD_FO	CCTATCTCACGAGCCATCCC	this study
qcopD_FO	GAGCGGTCGATCAGGAAATG	this study
nifH-f-o	CTATGCCGATCCGTGAGAAC	this study
nifH-r-o	TCAGAATGCCCTTGGAGATG	this study
pvdF-f-o	CGAAGATGGCGAAGACGAAG	this study
pvdF-r-o	CTCCTTTGTAGTCGATGTACCG	this study
yjgP-f-o	ATGCCTCGCCTCTTGTTC	this study
yjgP-r-o	AGCGTGTAGAGCAGATAGGA	this study
clpX-f-o	CCACTATAAGCGGCTCAATCA	this study
clpX-r-o	GTGAAGGGCACATCGAGAAT	this study
*copCD*_f	GCCGTATCGCCCTTGTTATG	this study
*copCD*_r	GGAGCCGAAGAATGAAGCTG	this study

* Symbols for mixed bases are R: A,G; Y: C,T; M: A,C; K: G,T; S: C,G; W: A,T; H: A,C,T; B: C,G,T; V: A,C,G; D: A,G,T; N: A,C,G,T.

The levels of expressed genes were measured by either absolute or relative quantification methods. In absolute quantification, calibration curves based on plasmid preparations with known copy numbers for each gene were used to calculate the gene transcripts per ng RNA and copy numbers per ng of DNA. The average ratios of transcript number to copy number determined from the RNA and DNA extracted from the same culture at the same growth point, were represented as a measure of expression levels. When using relative quantification, the relative gene expression levels were calculated by using a comparative C_T method (Schmittgen et al., 2008) with 16S rRNA, *yjgP*, or *clpX* as the housekeeping gene.

II.4 Construction of mutants

II.4.1 Markerless mutagenesis of *mbnABCMN* and *mbnABCMPH*

To study the function of the genes in the mb-gene cluster and for manipulation of mb structure, *M. trichosporium* Δ*mbnAN* and Δ*mbnAH* mutants were constructed, in which *mbnABCMN* and *mbnABCMNPH* were deleted via counter-selection techniques.

A suicide vector pK18*mobsacB* (Schäfer et al., 1994) was used to introduce inactivated genes of interest into the chromosome of *M. trichosporium* OB3b, thereby allowing homologous recombination. pK18*mobsacB* includes the broad host range transfer elements allowing for mobilization from *E. coli* donor strain S17.1 into methanotrophs. It contains the counter-selecting gene *sacB*. It is based on the narrow host range plasmid pBR322 and is only maintained by *E. coli*. (Schäfer et al., 1994)

Specifically, for the construction of Δ*mbnAN***,** a 1.1-kb DNA fragment upstream of *mbnA*

("armA", amplified using dmbnaF/dmbnaR primers, Table 2.2, Figure 2.1), and a 1-kb fragment spanning 3' *mbnN* and its downstream regions ("armB", amplified using dmbnbF/dmbnbR primers, Table 2.2, Figure 2.1) were ligated together using a *KpnI* site and then cloned into pK18mob*sacB* at *BamHI* and *HindIII* sites to create pWG012 plasmid. For the construction of Δ*mbnAH,* armB was replaced by a 1.2-b fragment spanning 3' *mbnH* and downstream regions amplified by dmbnAHbF/dmbnAHbR primers (Table 2.2) which created pWG013 plasmid. The constructed plasmids for mutation was then conjugated into *M. trichosporium* OB3b wild type strain.

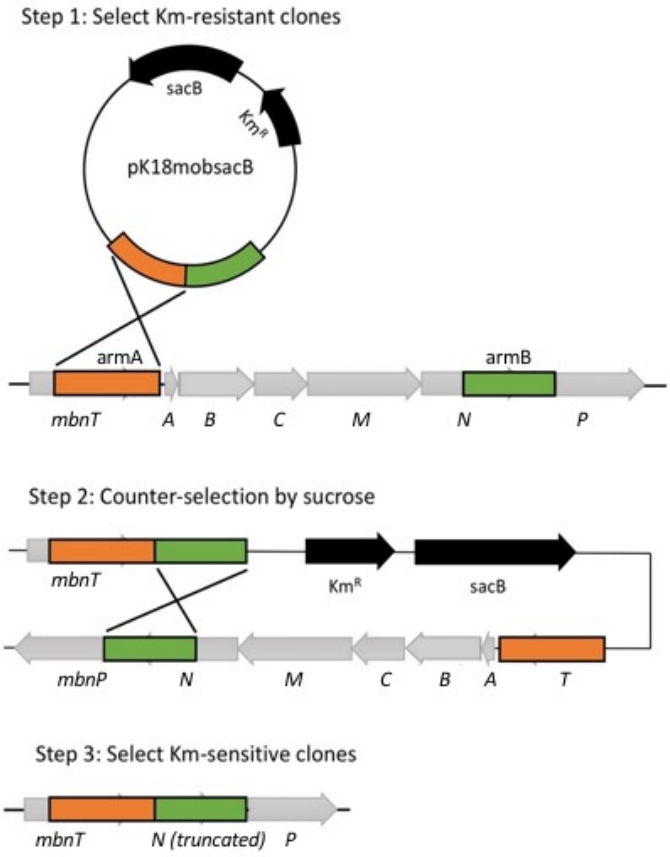

Figure 2.1. Mutagenesis of *M. trichosporium* OB3b Δ*mbnAN* via counterselection technique.

For counterselection, transconjugants were first selected by resistance to kanamycin for successful single homologous recombination and nalidixic acid to remove donor *E. coli*.

Secondly, selected transconjugants were grown on NMS containing 2.5% (mass/vol) sucrose for counterselection of double homologous recombination events (Figure 2.1). Resulting colonies were then checked for kanamycin sensitivity and genotype determined via sequencing. A 3.5-kb region containing complete *mbnABCM* and 490 bp of 5' *mbnN* (>40%) was knocked out in Δ*mbnAN* (Figure 2.1), and a 6.6-kb region containing complete *mbnABCMNPH* was knocked out in Δ*mbnAH* (Figure 2.2).

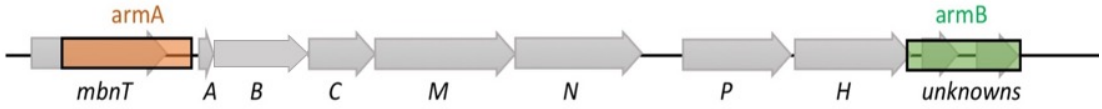

Figure 2.2. Location of arms used to create *M. trichosporium* OB3b Δ*mbnAH* via counterselection technique.

II.4.2 Marker exchange mutagenesis of *mbnT* and *copCD*

Marker exchange mutagenesis has been successfully applied to create mutants in *M. trichosporium OB3b* using the pK18*mobsacB* vector (Semrau et al., 2013). In counterselection mutagenesis, the second recombination step counter-selected by sucrose can lead to either a mutation event or to a recovery of wild type genotype. For difficult genetic regions, the odds of recombination can be quite low. In comparison, marker-exchange mutagenesis inserts an antibiotic marker into regions of mutation. The inserted marker can increase the probability of selecting knocke-outs.

To create the *mbnT* mutant, two sets of primers, Ton41/42 and Ton43/44 (Table 2.2), were used to amplify two 700-bp DNA fragments internal to *mbnT* flanking a 500-bp knock-out region. These two arms were ligated together at *BamHI* site, and cloned into pK18*mobsacB* at *EcoRI* and *HindIII* sites. A gentamicin (Gm) cassette from pS34-Gm was later inserted in between of the

two arms at *BamHI* site (Figure 2.3) to create the plasmid pWG011. To knock-out *copCD*, primers, copCDaF/R and copCDbF/R (Table 2.2), were used to amplify two 1-kp DNA fragments flanking a 2.4-kb region of *copCD* (Figure 2.4). These two arms were used to create pWG014 following the same cloning process as described above. The constructed pWG011 and pWG014 were conjugated into *M. trichosporium* OB3b with help of *E. coli* S17, separately, to created *ΔmbnT*::Gm^r and *ΔcopCD*::Gm^r.

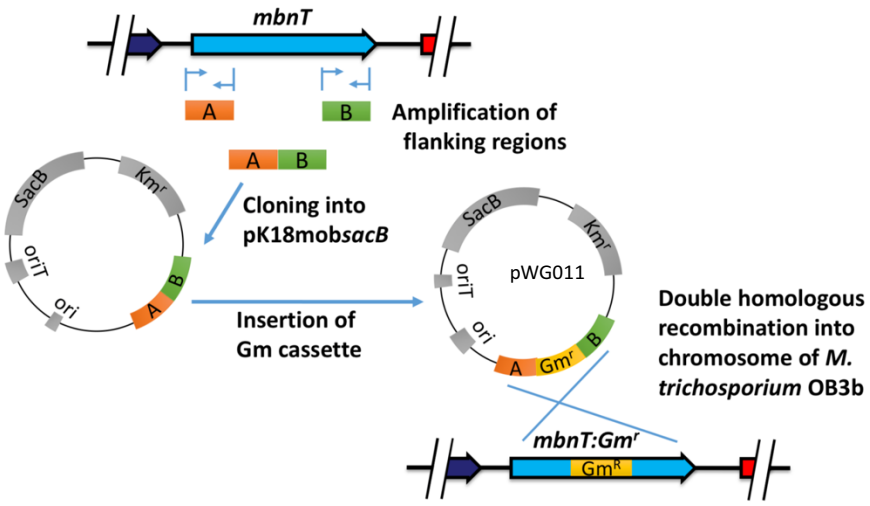

Figure 2.3. Construction of *M. trichosporium ΔmbnT*::Gm^r via marker exchange mutagenesis.

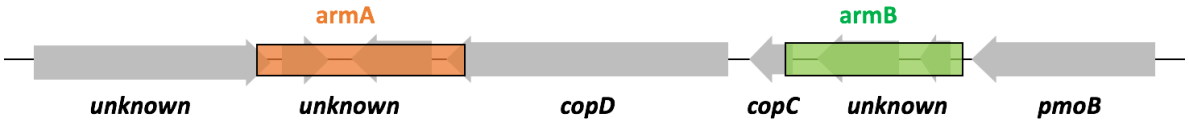

Figure 2.4. Location of arms used to knock-out *copCD* in *M. trichosporium* OB3b wild type and Δ*mbnAN*.

Conjugation colonies became visible on selective NMS plates containing Gm after about 10 days of incubation. Colonies were transferred twice onto fresh NMS plates supplemented with nalidixic acid, to remove *E. coli*, and Gm, to select for recombinants. The recombinants were screened directly for successful double homologous recombination by checking for pheynotypes of Kanamycin-sensitive and sucrose-resistance (10% w/v sucrose), which indicate loss of

plasmid backbone. Alternatively, Gm-resistant recombinants were plated on NMS containing a lower concentration of sucrose (2.5% w/v) and gentamycin for counterselection. Resulting colonies were again checked for kanamycin sensitivity and genotype via sequencing.

II.4.3 Construction of various mb mutants

In order to study the function of different genes in the *mbn* gene cluster, Δ*mbnAN* was used as a host for expression of various recombinant mb-synthesizing genes. The suitability of Δ*mbnAN* as a host for expression was established by first introducing pWG101, an expression vector containing wild-type *M. trichosporium* OB3b mb-gene cluster (*mbnABCMN*) with its native promoter, into Δ*mbnAN* for back complementation. Further, to characterize the function of various genes in the *mbn* operon from both *M. trichosporium* OB3b, different fragments of mb-synthesizing genes were amplified, assembled by ligation, and inserted to pTJS140 at the *KpnI* site. The details of construction of different plasmids are listed and described in Table 2.3. Figure 2.4 graphically illustrates the composition of various mb mutants.

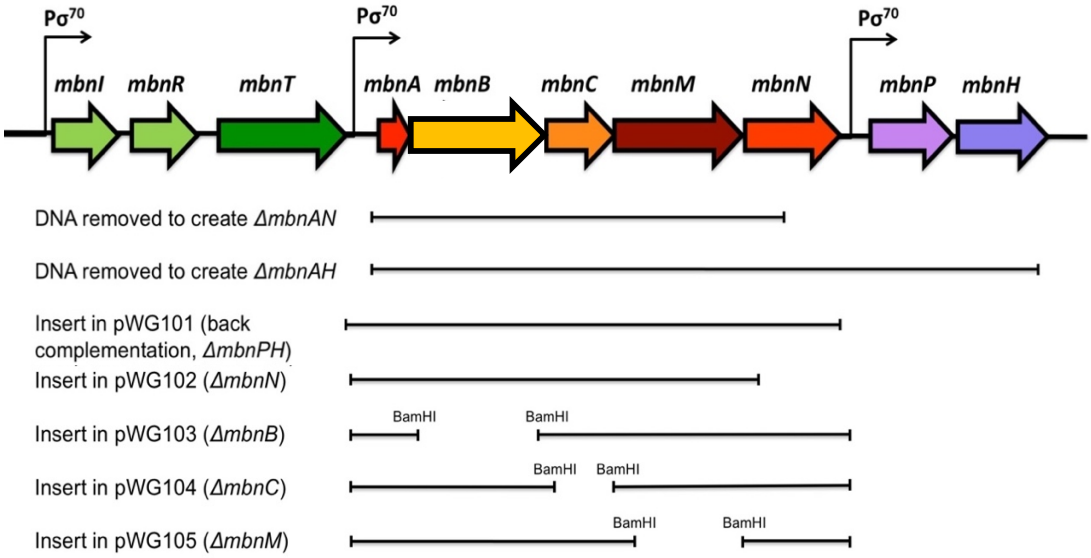

Figure 2.5. DNA removed to construct *M. trichosporium* OB3b Δ*mbnAN*, Δ*mbnAH* mutants and inserts used to construct various single mutants.

Table 2.3. Construction of various methanobactin mutants.

M. trichosporium construct	Host + Plasmid	Construction of insert to pTJS140
Δ*mbnAN* + pWG101	Δ*mbnAN* + pWG101	amplified by wgu21/22 (mbnABCMN with promoter) insert into KpnI
Δ*mbnN*	Δ*mbnAN* + pWG102	wgu21+mbn64 (P+mbnA)
Δ*mbnB*	Δ*mbnAN* + pWG103	wgu21+mbn67 (P+mbnA)-BamHI-mbn69+wgu22(mbnCMN)
Δ*mbnC*	Δ*mbnAN* + pWG104	wgu21+mbn66 (P+mbnAB)-BamHI-mbn70+wgu22(mbnMN)
Δ*mbnM*	Δ*mbnAN* + pWG105	wgu21+mbn65 (P+mbnA)-BamHI-mbn68+wgu22(mbnCMN)
Δ*mbnPH*	Δ*mbnAH* + pWG101	amplified by wgu21/22 (mbnABCMN with promoter) insert into KpnI

II.5 Naphthalene assay

The assay of Brusseau et al. (1990) was used to detect sMMO activity. 1.6 ml of cells in exponential phase was incubated with a few crystals of naphthalene for 1 h at 30 °C with shaking. Cells were pelleted by centrifuging. 130 µL of 4.21 mM tetrazotized o-dianisidine was added to 1.3 mL of supernatant and tranfered to cuvettes for measurement of absorbance at 528 um. Immediate development of a pink/purple color was taken as evidence of naphthalene oxidation by sMMO.

II.6 Mb production assay

Screening of mb production was based on the plate chrome azurol S (CAS) assay developed by Yoon et al., (2010). Screening of mb production by methanotrophic strains used split NMS/50

mM Cu–CAS plates. Culture was streaked on NMS half plates and incubated at appropriate growth conditions.

Alternatively, production of mb was determined by collecting the spent medium of cultures after overnight induction, and the UV-Vis spectrum was obtained by Varian Cary 3 UV-Vis spectrophotometer (Agilent, Santa Clara, CA) to identify the characteristic peaks of mb-OB3b at 340 and 394 nm.

II.7 Metal analysis

Copper associated with the methanotrophic biomass was determined using an inductively coupled plasma mass spectrometer (ICP-MS, Agilent Technologies, Santa Clara, CA). After growing to the late exponential phase, cultures (20 ml) were harvested by centrifugation at 4,300 *g* for 15 min. The cell pellets then were resuspended in 1 ml fresh NMS. 1 ml of 70% nitric acid (vol/vol) was added to the cell suspension. The mixtures were incubated for 2 h at 95°C with inversion every 20 min. Digested cell suspensions were subsequently diluted with fresh NMS medium and nitric acid to achieve a final concentration of 2% nitric acid and analyzed using ICP-MS. The ICP standards of metals were purchased as 1, 000 ppm stocks. The stocks were serially diluted to create standard curves with measured correlation coefficients of >0.99. Protein concentrations were converted from cell densities (as OD_{600}) measured by Genesys 20 Visible spectrophotometer (Spectronic Unicam, Waltham, MA). The correlation was obtained using the Bradford assay (Bio-Rad, Hercules, CA) as descried previously (Semrau et al. 2013). For each condition, at least duplicate biological samples were analyzed.

II.8 Sequencing and bioinformatic analysis

II.8.1 Mining selected genes in available methanotrophic genomes

Select genes as discussed in the introduction were searched in all the methanotroph genomes that were available in NCBI, including "NCBI genomes" and "whole-genome shotgun" databases. The results are presented in Table 1.1. *pmoA*, *mbnB/C* from *M. trichosporium* OB3b, *mxaF, xoxF* from *M. extorquens* AM1, *pxmA* from *Methylomonas* sp. M5 were used as the seeds to query the genomic sequences by blastn. Alignment length of 60% and identity of 60% were generally used as standard to evaluate the results. For *xoxF* and *pxmA*, it was manually inspected in the neighboring sequences for the absence of *mxaI*-like genes and a *pxmA-B-C* clustering order, respectively, to avoid any mixed identification with *mxaF* or *pmoA*. The results were checked with literature when possible.

II.8.2 Sanger Sequencing

Purified DNA was submitted for Sanger sequencing together with 1 μM primer to the University of Michigan Sequencing Core (https://seqcore.brcf.med.umich.edu/).

II.8.3 RNA-Seq sample preparation and analysis

To study how copper and cerium (co-)regulate gene expression in *M. trichosporium* OB3b and to identify potential genes involved in copper/cerium uptake and homeostasis, whole-cell transcriptomic differential expression of *M. trichosporium* OB3b was investigated using RNA-seq analysis. 10 μM copper (as $CuCl_2$) and 25 μM cerium (as $CeCl_3$) were prepared as stock solution and were suplemented to NMS media where neceassary. *M. trichosporium* OB3b was grown in four conditions: Cu-Ce (uM): 0-0, 10-0, 0-25, and 10-25 in triplicate. RNA was

extracted and purified as described in Section III.3.1. The quality of total RNA from the samples were checked by BioAnalyzer with results of RNA integration number (RIN) all higher than 9. Total RNAs were sent to University of Michigan DNA Sequencing Core. rRNA removal was performed by the Sequencing Core using the RiboZero kit for Gram- bacteria (Illumina, San Diego, CA). 12 non-stranded mRNA-seq libraries were prepared and sequenced in one lane using Illumina HiSeq4000 (San Diego, CA) SE 50 (Haas, et al., 2012; Chhangawala, et al., 2015).

The raw reads obtained from the sequencing facility were trimmed using Sickle (Joshi & Fass, 2011) with default parameters and then aligned to the *M. trichosporium* OB3b genome downloaded from genoscope (WGS ADVE02) using the Burrows-Wheeler alignment tool (BWA) backpack 0.7.12 (Li & Durbin, 2010). The resulting Sequence alignment/map (SAM) files were sorted using SAMtools-1.3.1 (Li et al., 2009). Reads counts were obtained from HTSeq 0.6.1 with intersection-nonempty mode (Anders et al., 2015) and analyzed by DESeq2 1.12.4 (Anders et al. 2013). Genes were considered to be differential expressed with a 2-fold change of higher than 1.5 and adjusted p-value of less than 0.01.

CHAPTER III FUNCTION OF GENES IN METHANOBACTIN (MB) GENE CLUSTER

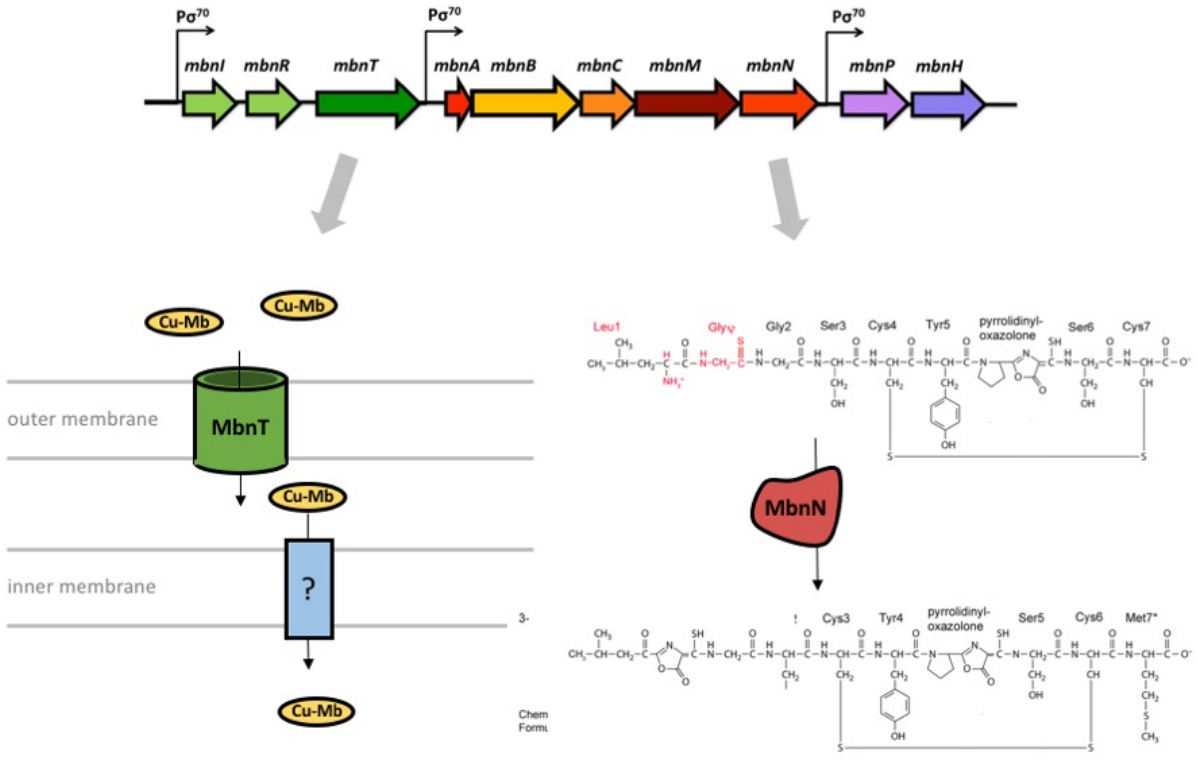

Figure 3.0 Elucidation of functions of mb gene cluster of *M. trichosporium* OB3b

Published:

A TonB-Dependent Transporter Is Responsible for Methanobactin Uptake by *Methylosinus trichosporium* OB3b. Applied and Environmental Microbiology, 82(6), 1917-1923.

An Aminotransferase is Responsible for the Deamination of the N-terminal Leucine and Required for Formation of Oxazolone Ring A in Methanobactin of *Methylosinus trichosporium* OB3b. Applied and Environmental Microbiology, 83(1): e02619-16.

III.1 TonB-dependent uptake of mb

III.1.1 Introduction

Bioinformatic studies of the genome of *M. trichosporium* OB3b revealed a putative TonB-dependent transporter (TBDT), i.e., *mbnT*, upstream of *mbnA*. *mbnT* is in a putative operon with *mbnI* and *mbnR*, i.e., a putative "Fe(III) dicitrate membrane sensor" and "ECF sigma factor", respectively (Figure 3.1). (Kenney & Rosenzweig, 2013) This pairing resembles the FecIRA-like systems found in *E. coli* and *Pseudomonas aeruginosa* for siderophore-mediated iron uptake, e.g., Fpv/PvdS-FpvR-FpvA, PupI-R-B (Lamont et al., 2002, Visca et al., 2002). In these systems, genes encoding for transporters and proteins involved in siderophore biosynthesis are regulated at multiple levels. When iron is available, siderophores are loaded and bind to TBDTs. The TBDTs transduce the signal across the outer membrane to a regulator "R". This regulator is typically an inner membrane protein that transmits the signal to an inducer "I", which enhances RNA polymerase to binding to specific promoter regions. Usually, there is another layer of regulation from a transcriptional repressor, e.g., Fur (Ferric Uptake Regulator). At high iron concentrations, Fur binds DNA sequences using Fe^{2+} as a cofactor and represses the expression of the regulators I, R, as well as genes encoding TBDT and proteins for siderophore synthesizing, thus controlling intercellular iron levels. When iron is limiting, Fur cannot bind DNA, leading to de-repression of the target genes. An example of this system is shown in Figure 4.2.

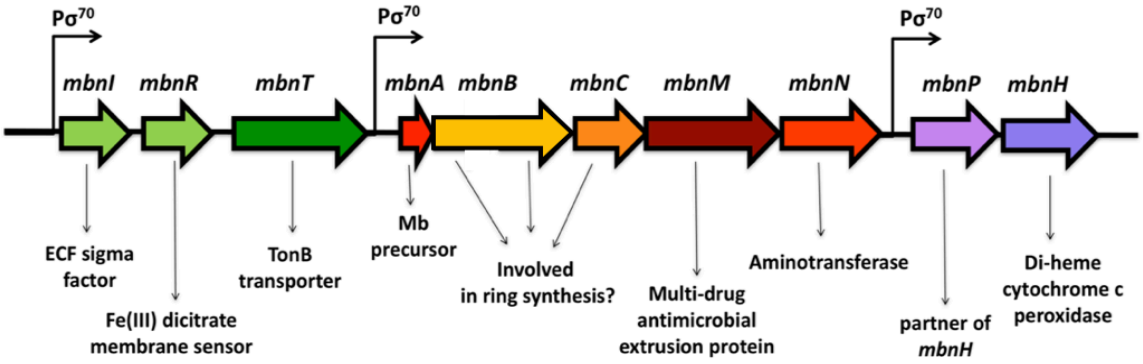

Figure 3.1. Methanobactin gene cluster of *M. trichosporium* OB3b

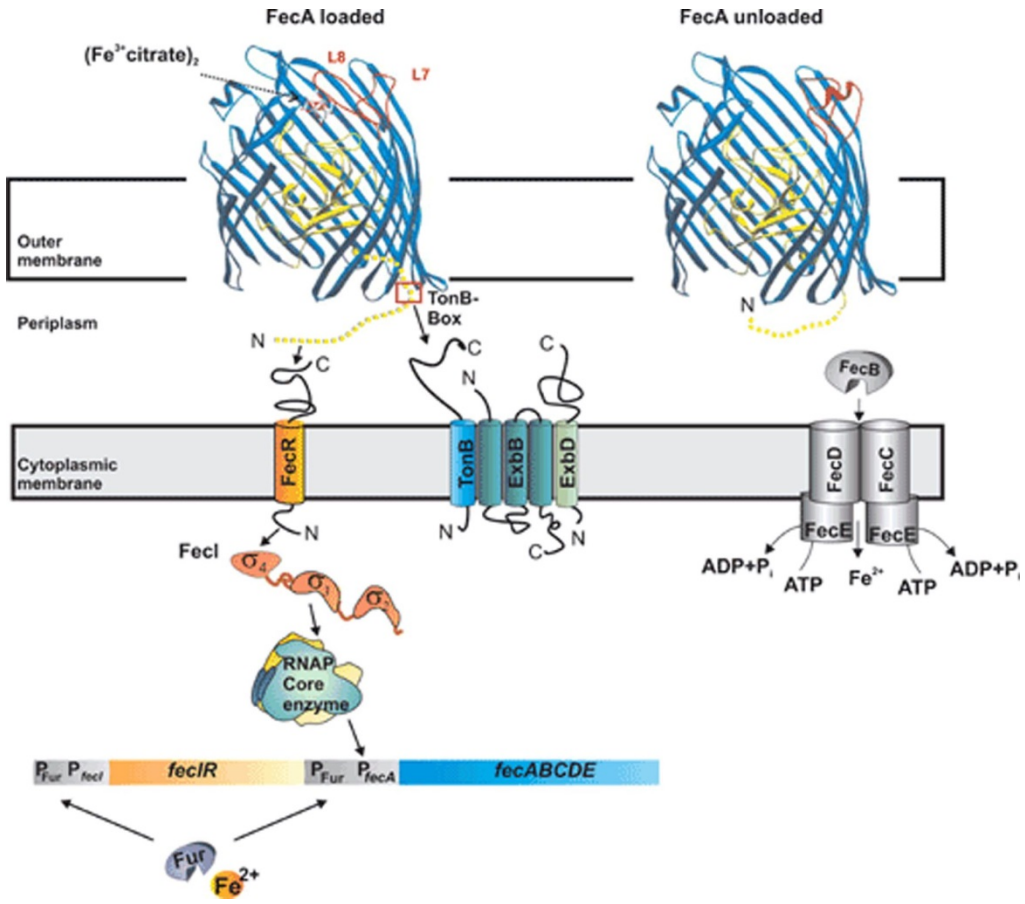

Figure 3.2. The ferric citrate transport and regulatory system.
The signaling pathway from FecA to FecI; TonB-ExbB-ExbD complex is involved in signaling and transport; the periplasmic FecB protein and the ABC transporter FecCDE proteins are involved in iron transport. Fe^{2+}-loaded Fur repressor binds to the promoter upstream of *fecI* and *fecA* and dissociates from the promoter under low iron conditions. There are interactions between the FecA TonB box and TonB and between the FecA signaling domain and FecR. N indicates the N-terminal end, C the C-terminal end of the proteins. σ^2 and σ^4 indicate FecI domains involved in binding to FecR and DNA, respectively. (Braun & Mahren, 2005)

A similar regulatory system may exist in *M. trichosporium* OB3b for copper uptake mediated by mb (Kenney & Rosenzweig, 2013). It has been hypothesized that MbnT functions as the transporter for Cu-mb and sends signals to MbnR. MbnR then activates MbnI, which thereby regulates the expression of *mbn* operon, *mbnIRT*, and possibly *mmo* and *pmo* operons. If this is true, it will be a new level of regulation involved in the "copper-switch" between sMMO and pMMO. It would be interesting to see how *mbnIRT* fit into the regulatory model based on MmoD and mb (Semrau et al., 2013, DiSpirito et al., 2016). In this model, it was hypothesized that MmoD up-regulates the expression of *mbn* operon at low copper-biomass condition, which explains the observation that the highest production of mb was found to occur at copper concentration between 0.1 and 0.7 μM while cells express sMMO. The induced *mbn* operon encodes MbnI, which in turn induces the expression of *mmo* operon.

It is also reasonable to speculate that a negative regulator like "Fur" exists in methanotrophs to control intercellular copper levels. Interestingly, two copies of "Fe^{2+}/Zn^{2+} uptake regulation protein, Fur like protein" was identified in *M. trichosporium* OB3b genome (ADVE02_v2_13735, ADVE02_v2_13735) with highest similarity of 55% at amino acid level with Fur family protein in *Nitratireductor indicus* C115. However, these two genes are not near *mbn* operon or other identifiable copper-related proteins. It is also possible that there is a novel copper-binding protein that acts as a negative regulator. As iron is vital for the growth of bacteria like *E. coli* and *P. aeruginosa*, complicated regulatory networks have been found involving in iron homeostasis in these microbes with different regulators. It will not be surprising to see a similar picture in methanotrophs regarding to copper considering its important role in methanotrophic activity.

III.1.2 Knocking out *mbnT* in *M. trichosporium* OB3b

To elucidate the role of *mbnT* in mb uptake, a mutant of *M. trichosporium* OB3b was created in which *mbnT* was selectively knocked out via marker exchange mutagenesis as described in Chapter 3. The mutation of *mbnT* was confirmed by phenotype of Gm-resistance, Km-sensitive, and sucrose-resistance, as well as by PCR for *mbnT* and the pK18*mobsacB* plasmid backbone, and by sequencing. PCR product of mutated *mbnT* is 400 bp larger than that of WT *mbnT* amplified by TonB27/44, and no product was observed from PCR of plasmid backbone in the mutant (Figure 3.3)

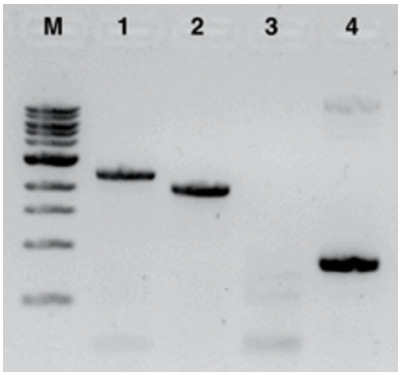

Figure 3.3. Verification of knockout of *mbnT* in *M. trichosporium* by PCR.
M, molecular weight markers; lane 1, PCR of *mbnT* from the *M. trichosporium* OB3b *mbnT*::Gm^r mutant; lane 2, PCR of *mbnT* from wild-type *M. trichospo- rium* OB3b; lane 3, PCR of pK18*mobsacB* backbone in *M. trichosporium* OB3b *mbnT*::Gm^r; lane 4, PCR of pK18*mobsacB* backbone in pWG011.

III.1.3 Characterization of *mbnT*::Gm^r mutant

III.1.3.1 Metal uptake and regulation of gene expression by copper

Our initial hypothesis was that if MbnT was truly involved in Cu-mb uptake, knocking out *mbnT* would lead to the cell being unable to sense and incorporate copper, thus sMMO would be expressed and active at a wider range of copper concentrations. To test these hypotheses, the phenotype of the *mbnT*::Gm^r mutant was further examined and compared to that of *M.*

trichosporium wildtype. When grown in varying copper concentrations (0, 0.5, and 1 μM), both *mbnT*::Gm^r mutant and wildtype had increasing amounts of copper associated with biomass (Figure 3.4 A). Further, gene expression in both mutant and wildtype showed clear evidence of the "copper-switch". i.e., as copper increased, expression of *mmoX* decreased by several orders of magnitude, while *pmoA* expression increased over an order of magnitude (Figure 3.4 B, C). Finally, expression of *mbnA*, encoding for the precursor polypeptide of mb, decreased substantially in both in *M. trichosporium* OB3b wildtype and *mbnT*::Gm^r mutant as copper increased, indicating that the knock-out of *mbnT* did not affect mb expression (Figure 3.4 D).

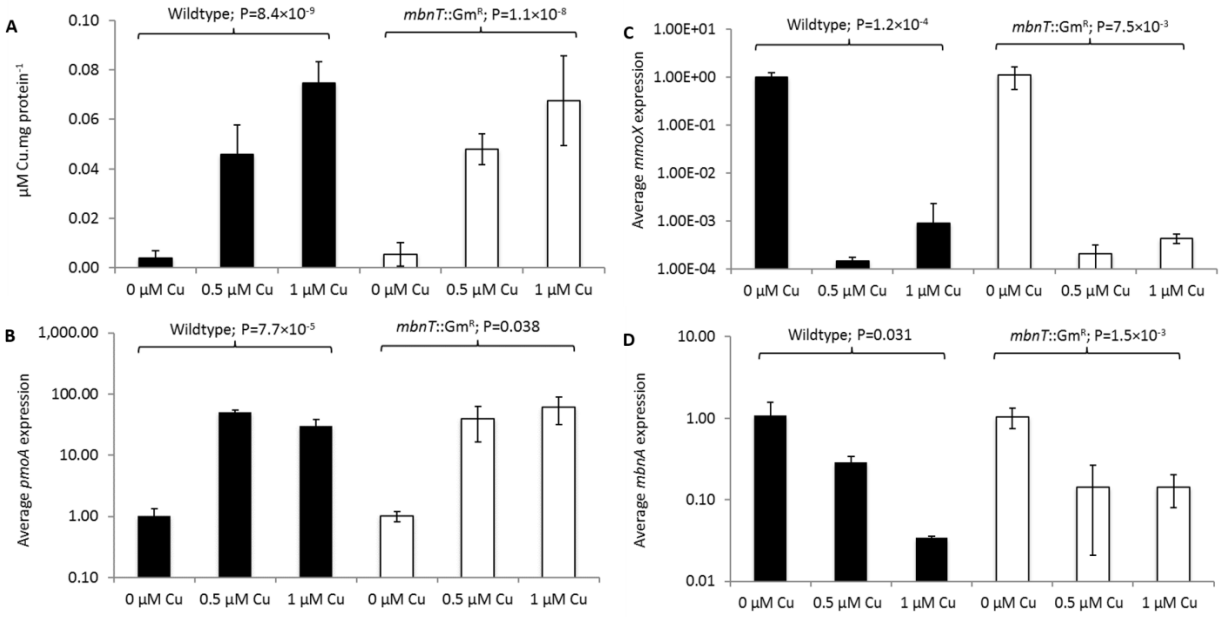

Figure 3.4. Characterization of wild-type *M. trichosporium* OB3b (black bars) and the *mbnT*::Gm^r mutant (white bars) grown in the presence of various amounts of copper.
(A) Copper associated with biomass; (B) RT-qPCR of *pmoA*; (C) RT-qPCR of *mmoX*; (D) RT-qPCR of *mbnA*. Error bars indicate standard deviations from at least duplicate biological replicates. Indicated *P* values are from one-way analysis of variance (ANOVA).

III.1.3.2 Mb uptake

These findings suggest that either *mbnT* is either not involved in copper uptake (i.e., binding of copper-mb complexes) or there are multiple mechanisms for copper uptake in *M. trichosporium*

OB3b, such that the copper-switch is still operative. To differentiate between these possibilities, mb in the spent medium and cell extracts of the *mbnT*::Gm^r mutant and wildtype strain of *M. trichosporium* OB3b was assayed for a wide range of copper concentrations using immuno-blotting assays. As shown in Figure 3.5, as the growth concentration of copper increased, the amount of mb in the spent medium decreased in *M. trichosporium* OB3b wildtype, but was readily apparent in the spent medium of the *mbnT*::Gm^r mutant at all tested copper concentrations. Conversely, mb was found in the cell extract of *M. trichosporium* OB3b wild type under all conditions, indicating that mb was taken up after secretion. No mb was ever observed in the cell extract of the *mbnT*::Gm^r mutant, indicating that the mutant produced and secreted mb, but was unable to subsequently take it up.

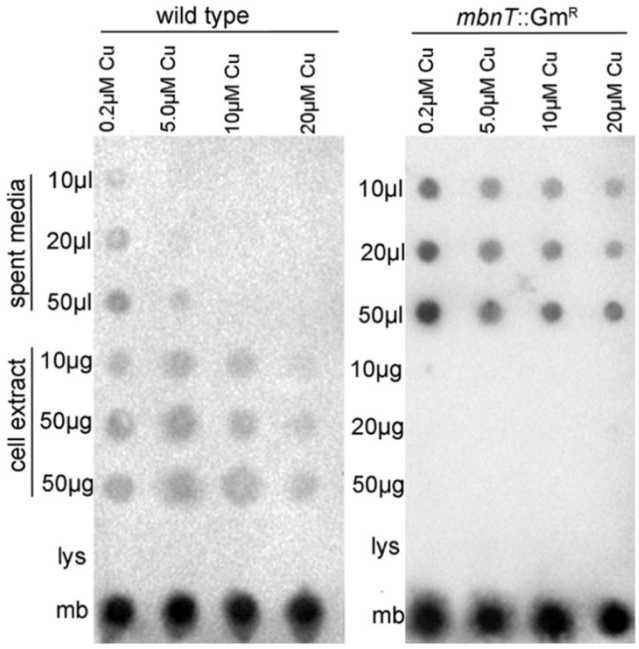

Figure 3.5. Immuno-blotting assays for location of methanobactin in wild-type *M. trichosporium* OB3b and in the *mbnT*::Gm^r mutant as a function of the concentration of copper in the growth medium (0.2, 5, 10, or 20 μM copper).
Fifty nmol lysozyme (lys) and 50 nmol methanobactin (mb) were used as negative and positive controls, respectively.

III.1.3.3 Metal uptake and regulation of gene expression with addition of mb

The *mbnT*::Gm^r mutant and wildtype strain of *M. trichosporium* OB3b were then grown in the presence of 1 μM copper and varying amounts of copper-free mb. As shown in Figure 3.6 A, in the presence of either 5 or 50 μM mb, copper associated with biomass of the *mbnT*::Gm^r mutant decreased over three-fold, while no significant change in copper levels of *M. trichosporium* OB3b wildtype was observed. Further, expression of *mmoX* increased over three orders of magnitude in the *mbnT*::Gm^r mutant while *pmoA* expression dropped by approximately eight-fold. No significant change in expression of either *mmoX* or *pmoA* was observed, however, in *M. trichosporium* OB3b wildtype (Figure 3.6 B, C). Collectively, these data show that in the presence of molar excess of mb, copper was still bioavailable to *M. trichosporium* OB3b wildtype, but was not for the *mbnT*::Gm^r mutant. Additionally, it was assayed if the addition of exogenous mb affected *mbnA* expression in *M. trichosporium* OB3b wildtype and *mbnT*::Gm^r mutant. As shown in Figure 3.6, as increasing amounts of mb were added, *mbnA* expression increased in both wildtype and mutant strains.

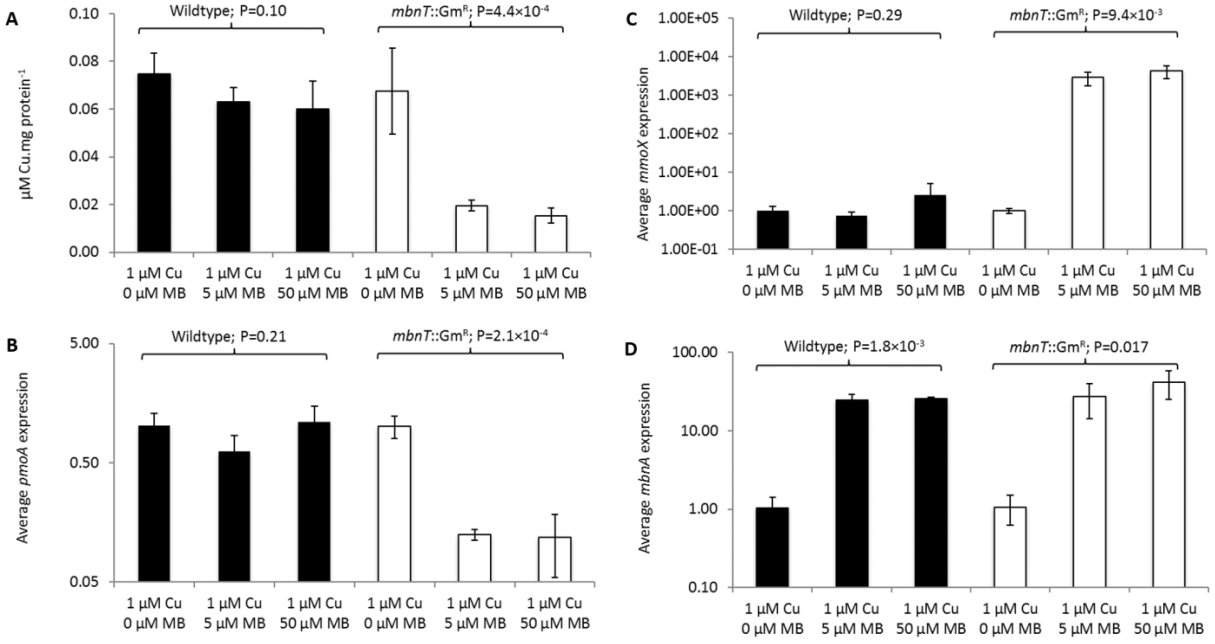

Figure 3.6. Characterization of wild-type *M. trichosporium* OB3b (black) and the *mbnT*::Gm^r mutant (white) grown in the presence of 1 M copper and various amounts of mb.
(A) Copper associated with bio- mass; (B) RT-qPCR of *pmoA*; (C) RT-qPCR of *mmoX*; (D) RT-qPCR of *mbnA*. Error bars indicate standard deviations from at least duplicate biological replicates. Indicated *P* values are from one-way analysis of variance (ANOVA).

III.1.4 Discussion

Since the discovery of the mb gene cluster, it has been speculated that a TonB-dependent transporter encoded by *mbnT* is responsible for mb uptake (Semrau, et al., 2013). Here it is shown that mb uptake is indeed mediated by *mbnT*, as: (1) mb could be taken up by *M. trichosporium* OB3b wildtype but not the *mbnT*::Gm^r mutant, and; (2) the *mbnT*::Gm^r mutant of *M. trichosporium* OB3b was not able to take up copper if mb was exogenously added to bind copper, but *M. trichosporium* OB3b wildtype was.

The data also show, however, *M. trichosporium* OB3b has an alternative mechanism(s) for copper uptake, i.e., in the absence of any exogenous mb, the amount of copper in the wildtype

and *mbnT*::Gm^r strains of *M. trichosporium* OB3b was indistinguishable. The conclusion of multiple copper uptake systems, however, is not novel, as it was reported earlier that at least two pathways for copper uptake exist in *M. trichosporium* OB3b (Balasubramanian, et al., 2010). Such redundancy in copper uptake systems in methanotrophs, although unusual when compared to other microbes, can be explained when one considers the importance of copper in methanotrophic metabolism. That is, methanotrophs expressing pMMO have a strong need for copper as it occupies at least two of three metal centers found in purified pMMO (Martinho et al., 2007; Hakemian et al., 2008).

An interesting issue is that, as found earlier in a mutant of *M. trichosporium* OB3b where *mbnA* encoding for the precursor polypeptide of mb was knocked out, the "copper-switch" still existed in the *mbnT*::Gm^r mutant (Semrau et al., 2013). Given the similarity in genetic arrangement of *mbnIRT* and *fecIRA*-like system in other bacteria, as mentioned earlier, it has been speculated that after MbnT binds copper-mb, a signal cascade results whereby mb synthesis, and possibly expression of *mmo* and *pmo* operons is controlled (Kenney, et al., 2013). The findings presented here, however, suggest that although such a signal cascade may exist after MbnT binds copper-mb, such a regulatory scheme does not include the "copper-switch" between sMMO and pMMO. It is also difficult to conclude from these data that this signal cascade affects expression of *mbnA*. That is, *mbnA* expression in both *M. trichosporium* OB3b wildtype and the *mbnT*::Gm^r mutant decreased significantly with increasing copper, but the magnitude of the drop in expression was greater in wildtype (Figure 3.6D). Further, in the presence of 1 μM copper and varying amounts of exogenous mb, *mbnA* expression in *M. trichosporium* OB3b wildtype and *mbnT*::Gm^r mutant responded with the same pattern (Figure 3.6D). It appears that another regulatory circuit is

involved in controlling expression of *mbnA*, but the possibility that such expression is also controlled to some extent by *mbnI*, which is indirectly activated by MbnT binding copper-mb, cannot be excluded at this time.

III.1.5 Conclusions and future perspectives

In conclusion, here we report the successful knock-out of *mbnT*, and show that this is responsible for mb uptake. The phenotype of the *mbnT*::Gm^r mutant, however, indicates that *M. trichosporium* OB3b has multiple systems for copper uptake. It is tempting to speculate that mb may serve as a high affinity system to collect copper, but when copper is not limiting, an alternative lower affinity system is used. Such a hypothesis is supported by the finding that expression of *mbnA* decreases with increasing copper both in *M. trichosporium* OB3b wildtype and the *mbnT*::Gm^r mutant.

The nature of this imputed low affinity copper uptake mechanism is still elusive, but clues from other methanotrophs, e.g., *Methylomicrobium album* BG8 and *Methylococcus capsulatus* Bath may provide some suggestions. That is, it has been shown that in *M. album* BG8, an outer membrane protein, CorA, exists that is copper-repressible and may serve to bind copper (Berson et al., 1997). Further, it has been found that *M. capsulatus* Bath synthesizes a similar outer membrane protein, MopE, as well as a secreted truncated form, MopE* that both bind Cu(II) (Karlsen et al., 2013; Helland et al., 2008; Ve et al., 2012). A gene encoding for a protein similar to CorA and MopE, *mbnP*, is adjacent to the mb gene cluster in *M. trichosporium* OB3b, and it may be that this serves as an alternative copper uptake mechanism in *M. trichosporium* OB3b.

III.2 Synthesis pathway of mb

III.2.1 Introduction

As the first example of a chalkophore, or copper-specific chelating agent, mbs are characterized as being small (< 1300 Da) polypeptides with two heterocyclic rings each with an adjacent thioamide group. The N-terminal ring is an oxazolone, while the other is either another oxazolone or an imidazolone or pyrazinedione group (DiSpirito, et al., 2016). Specifically, mb from *M. trichosporium* OB3b (Figure 3.7), has two oxazolone rings and its N-terminal leucine is de-aminated (Krentz, et al., 2010).

The genetics underlying mb synthesis are slowly being unraveled. Given the unique structure of mb-OB3b, it was initially speculated that it was synthesized via a non-ribosomal peptide synthase (Kim et al., 2004). Subsequent investigation, however, suggested that it may be a ribosomally synthesized and post-translationally modified peptide (RiPP), with a gene -*mbnA* - possibly encoding for the polypeptide precursor of mb identified that includes a 19 amino acid leader sequence and a 10 amino acid core sequence (Krentz et al., 2010). When *mbnA* was knocked out in *M. trichosporium* OB3b, this microbe was unable to synthesize mb, providing evidence that mb is a RiPP (Semrau et al., 2013). With these data, the core polypeptide sequence of mb-OB3b was shown to be **Leu-Cys**-Gly-Ser-Cys-Tyr-**Pro-Cys**-Ser-Met, where the heterocyclic rings shown in Figure 3.7 are formed from the two X-Cys dipeptide sequences highlighted in bold (DiSpirito et al., 2016).

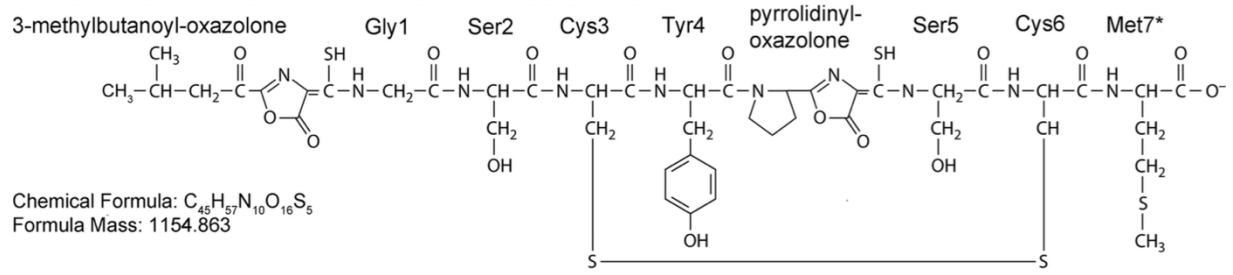

Figure 3.7. Molecular structure of methanobactin from *M. trichosporium* OB3b (Krentz et al., 2010).

Further bioinformatic analysis revealed that *mbnA* is part of a gene cluster in *M. trichosporium* OB3b as shown in Figure 3.1. As discussed in Section 1.3.2.2, downstream of *mbnA* are several genes, some of which have unknown function, but are likely involved in mb biosynthesis (*mbnB* and *mbnC*), as well as several genes annotated as either an extrusion protein that may be responsible for mb secretion (*mbnM*) or an aminotransferase that may play a role in mb biosynthesis (*mbnN*). These genes appear to be part of an operon under the control of a σ^{70}-dependent promoter as predicted using BPROM. Two additional genes, *mbnP* and *mbnH* that encode for a putative di-haem cytochrome *c* peroxidase and its partner are adjacent to *mbnN*, but look to be under the control of a separate σ^{70}-dependent promoter (again predicted using BPROM). The function of *mbnP* and *mbnH* is unclear, although they may be involved in ring formation in mb, or possibly part of a secondary copper uptake system (DiSpirito et al., 2016).

The formation of the heterocyclic rings in mbs are not clear and needs to be addressed experimentally. DiSpirito et al. (2016) provided a hypothesis as shown in Figure 3.8. In the proposed scheme, the oxazolone rings in mb-OB3b are synthesized via a tandem two-step sequence of peroxidation and dehydration reactions.

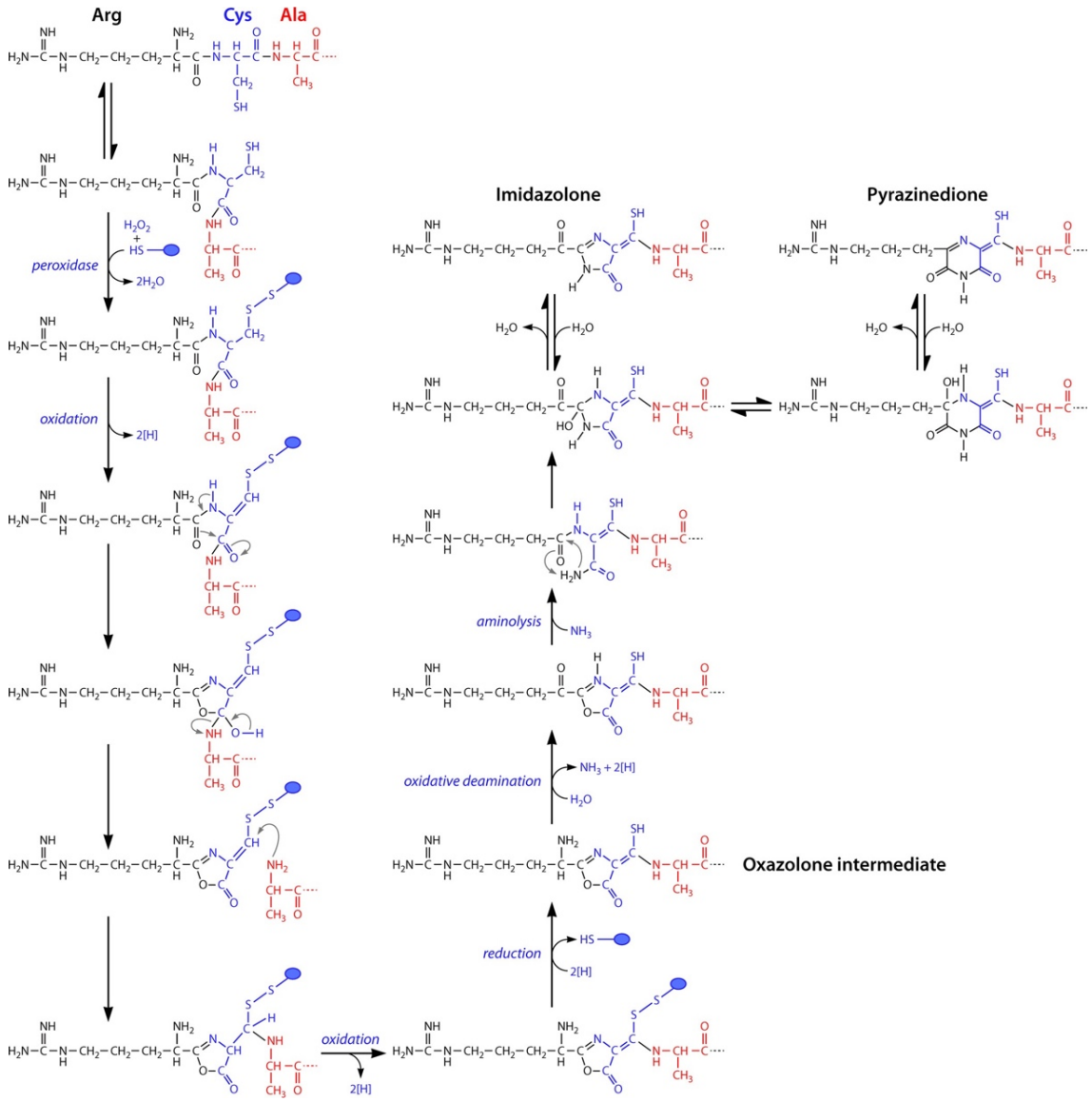

Figure 3.8. Proposed reaction schemes for biosynthesis of the oxazoline rings with associated thioamide groups via a tandem two-step sequence of peroxidation and dehydration reactions. Cysteine thiols are likely protected against oxidation, possibly as disulfides involving one of the proteins of the mb gene cluster (blue circles). For imidazolone and pyrazinedione ring formation, oxazolone rings are modified via a transamination/deamination step followed by an aminolysis step to open the oxazolone ring followed by ring formation and dehydration.

There is increasing interest to understand the biosynthetic pathway of mb, e.g., it has been recently shown that mb from *M. trichosporium* OB3b has the potential to treat individuals afflicted with Wilson disease (Summer et al., 2011, Zischka et al., 2011, Lichtmannegger et al., 2016).

III.2.2 Confirmation of mutants and gene expression

Previously a *M. trichosporium mbnA*::Gm^r mutant was constructed where *mbnA* was knocked out via marker-exchange mutagenesis (Semrau et al., 2013). While this mutant was unable to synthesize mb, it does not allow easy mutation of other genes in the *mbn* operon. We therefore constructed a new *M. trichosporium* Δ*mbnAN* mutant, in which *mbnABCMN* was deleted as described in Section 2.4.1. The successful knockout was confirmed by PCR amplification of *mbnA* through *mbnN* for Δ*mbnAN* mutant, as well as verification of the loss of plasmid backbone (Figure 3.9). This was further confirmed by sequencing as well as finding that the Δ*mbnAN* strains were kanamycin sensitive and sucrose resistant.

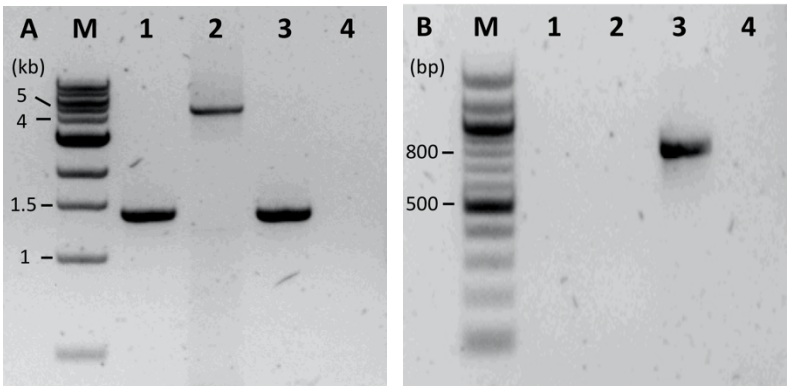

Figure 3.9. Confirmation of construction of *M. trichosporium* OB3b Δ*mbnAN* mutant. A: PCR of *mbnABCMN* using primers mbn21/22. Lanes 1 – 4 are PCR of *mbnABCMN* from: 1 - *M. trichosporium* OB3b *mbnAN* mutant; 2 - *M. trichosporium* OB3b wildtype; 3 - pWG012 plasmid (positive control); 4 - water (negative control). B: PCR of pK18mob*sacB* plasmid backbone using primers pK18-bb-F/R. Lanes 1 – 4 are PCR of pK18mob*sacB* plasmid backbone from: 1 - *M. trichosporium* OB3b *mbnAN* mutant; 2 - *M. trichosporium* OB3b wildtype; 3 - pWG012 plasmid (positive control); 4 - water (negative control).

For the Δ*mbnAN* mutant, the deletion of *mbnABCMN* had no effect on expression of *mbnPH* as confirmed by RT-PCR (Figure 3.10). Interestingly, expression of *mbnPH* was dependent on copper as found earlier for *mbnA* (Semrau et al., 2013), suggesting that expression of *mbnA,*

mbnP and *mbnH* utilizes a shared regulatory element.

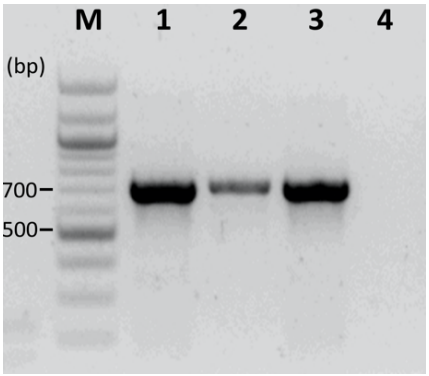

Figure 3.10. Confirmation of expression of *mbnPH* in Δ*mbnAN* mutant using primers *mbnPH*-F/R. Lanes 1 - 4 are RT-PCR of *mbnPH* from: 1 - *M. trichosporium* OB3b Δ*mbnAN* grown in the absence of copper; 2 - *M. trichosporium* OB3b Δ*mbnAN* mutant grown in the presence of 1 μM copper; 3 - *M. trichosporium* OB3b wild type grown in the absence of copper (positive control); 4- water (negative control).

The suitability of mutant Δ*mbnAN* as a host for expression of recombinant mb-synthesizing genes was established by introducing pWG101 (Table 2.3, Figure 2.4), an expression vector containing the wild-type *mbn* operon (*mbnABCMN*) with its native promoter, into Δ*mbnAN* for back complementation.

Expression of these back added genes was confirmed via RT-PCR (Figure 3.11). The native σ^{70}-dependent promoter upstream of *mbnA* was also incorporated into pWG101, and based on earlier findings showing that *mbnA* expression decreased with increasing copper in *M. trichosporium* OB3b wildtype (Semrau et al., 2014), similar results were expected in Δ*mbnAN* + pWG101. Indeed, in the presence of copper, expression of *mbnA* and *mbnN* was visibly reduced in Δ*mbnAN* + pWG101 as compared to when no copper was provided in the growth medium (Figure 3.11).

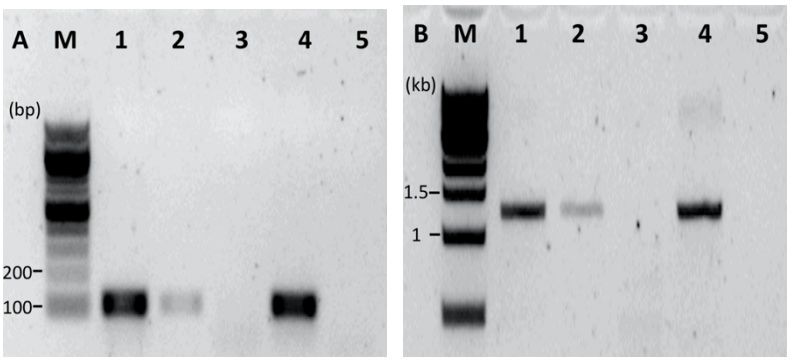

Figure 3.11. Expression of *mbnA* and *mbnN* in Δ*mbnAN* + pWG101.
A: RT-PCR of *mbnA* using primers qmbnA_FO/RO. Lanes 1 -5 are RT-PCR of *mbnA* from: 1 - *M. trichosporium* OB3b Δ*mbnAN* + pWG101 grown in the absence of copper; 2 - *M. trichosporium* OB3b Δ*mbnAN* + pWG101 grown with 1 μM copper; 3 - *M. trichosporium* OB3b Δ*mbnAN* grown in the absence of copper (negative control); 4 - *M. trichosporium* OB3b wild type grown in the absence of copper (positive control); 5 - water (negative control). B: RT-PCR of *mbnN* using primers mbnN-F/R. Lanes 1 – 5 are RT-PCR of *mbnN* from: 1 - *M. trichosporium* OB3b Δ*mbnAN* + pWG101 grown in the absence of copper; 2 - *M. trichosporium* OB3b Δ*mbnAN* + pWG101 grown in the presence of 1 μM copper; 3 - *M. trichosporium* OB3b Δ*mbnAN* grown in the absence of copper (negative control); 4 - *M. trichosporium* OB3b wild type grown in the absence of copper (positive control); 5 - water (negative control).

To characterize the function of each gene in mb gene cluster, a series of mutants were constructed by introducing different expression vectors (Table 2.1, Table 2.3) into Δ*mbnAN* mutant. We here first discuss the characterization of strain *ΔmbnAN + pWG102,* in which *mbnABCM* were cloned and expressed in Δ*mbnAN* mutant without *mbnN*. First, the expression of the insert *mbnABCM* from the plasmid in *ΔmbnAN + pWG102* was confirmed by RT-PCR as shown below.

III.2.3 Characterization of mb

The analysis on mb produced by various mutants was done by our collaborator Dr. Alan DiSpirito at Iowa State University. Currently, the characterization of Δ*mbnAN,* back-complemented Δ*mbnAN,* and Δ*mbnN* (*ΔmbnAN + pWG102*) are complete and the results are presented below.

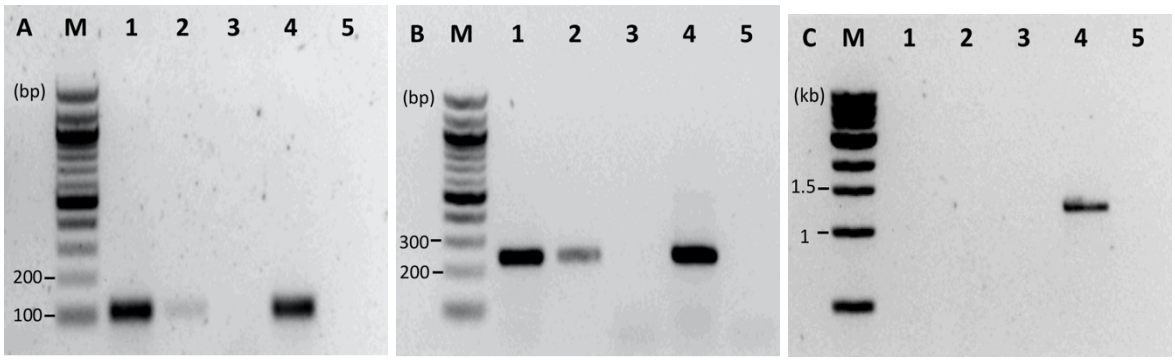

Figure 3.12. Expression of *mbnA*, *mbnM* and *mbnN* in Δ*mbnN*.
A: RT-PCR of *mbnA* using primers qmbnA_FO/RO. Lanes 1 -5 are RT-PCR of *mbnA* from: 1 - *M. trichosporium* OB3b Δ*mbnAN* + pWG102 grown in the absence of copper; 2 - *M. trichosporium* OB3b Δ*mbnAN* + pWG102 grown with 1 μM copper; 3 - *M. trichosporium* OB3b Δ*mbnAN* grown in the absence of copper (negative control); (4) *M. trichosporium* OB3b wild type grown in the absence of copper (positive control); (5) water (negative control). B: RT-PCR of *mbnM* using primers mbnM-F/R. Lanes 1 -5 are RT-PCR of *mbnM* from: 1 - *M. trichosporium* OB3b Δ*mbnAN* + pWG102 grown in the absence of copper; 2 - *M. trichosporium* OB3b Δ*mbnAN* + pWG102 grown with 1 μM copper; 3 - *M. trichosporium* OB3b Δ*mbnAN* grown in the absence of copper (negative control); (4) *M. trichosporium* OB3b wild type grown in the absence of copper (positive control); (5) water (negative control). C: RT-PCR of *mbnN* using primers mbnN-F/R. Lanes 1 - 5 are RT-PCR of *mbnN* from: 1 - *M. trichosporium* OB3b Δ*mbnAN* + pWG102 grown in the absence of copper; 2 - *M. trichosporium* OB3b Δ*mbnAN* + pWG102 grown with 1 μM copper; 3 - *M. trichosporium* OB3b Δ*mbnAN* grown in the absence of copper (negative control); 4 - *M. trichosporium* OB3b wild type grown in the absence of copper (positive control); 5 - water (negative control).

After verification of the deletion of *mbnA* through *mbnN* from the chromosome, mb production was examined in this mutant. The absence of color in the culture medium suggested no mb was being produced by this mutant even when it was cultured in low copper conditions (Figure 3.13). The lack of mb production in the Δ*mbnAN* was confirmed via UV/visible absorption spectral analyses of the spent medium (Figure 3.14). After back complementation, mb production was restored in Δ*mbnAN* + pWG101 (Figure 3.13, Figure 3.14). The mass of mb from this back-complemented mutant was found to be 1154.27 Da by both LC-MS/MS and FT-ICR-MS as determined by collaborators at Iowa State University, identical to the mass of mb from wildtype *M. trichosporium* OB3b, indicating that Δ*mbnAN* + pWG101 produced the same form of mb.

Also consistent with gene expression, mb production was markedly reduced when Δ*mbnAN* + pWG101 was grown in the presence of copper.

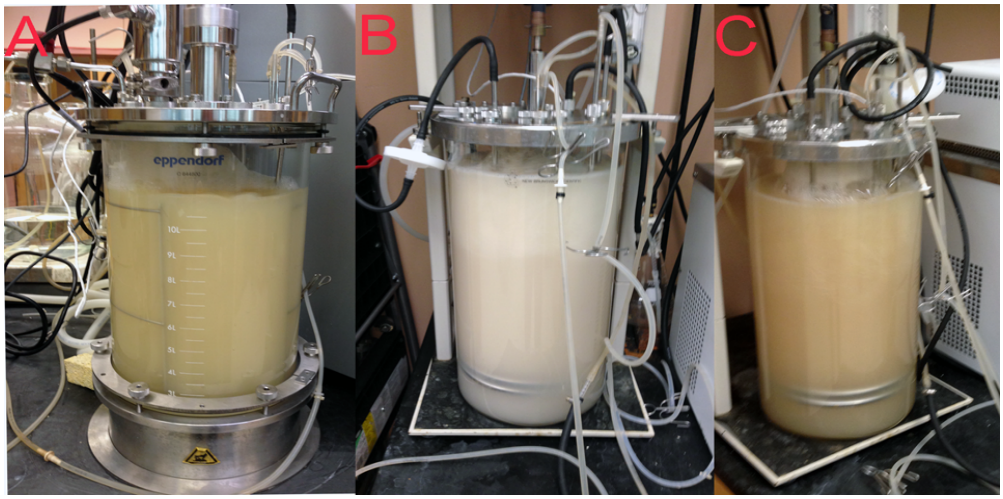

Figure 3.13. Fermenters of (A) wild-type *M. trichosporium* OB3b, (B) Δ*mbnAN*, and (C) Δ*mbnAN* + pWG101 cultured in NMS media amended with 0.2 µM $CuCl_2$.

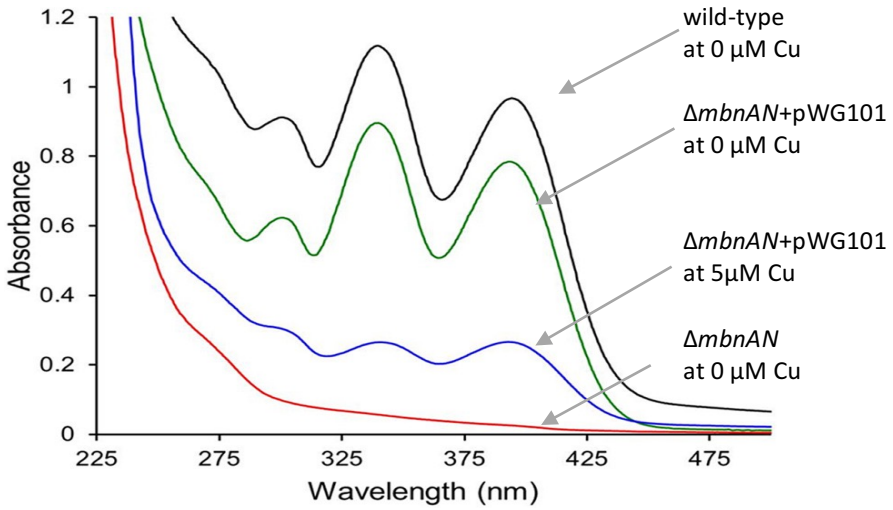

Figure 3.14. UV-visible light absorption spectra of the spent media from wild-type *M. trichosporium* OB3b (black trace), the Δ*mbnAN* mutant (red trace), and the Δ*mbnAN*+pWG101 mutant (green trace). Cells were cultured on NMS medium amended with 0.2 M $CuCl_2$ (black and red traces) or on NMS medium amended with 0.2 M $CuCl_2$ and 20 g · ml^{-1} spectinomycin (green trace). The blue trace shows methanobactin production in mutant Δ*mbnAN*+pWG101 grown on NMS medium amended with 5.0 M $CuCl_2$ and 20 g·ml^{-1} spectinomycin.

The molecular mass of mb produced by *ΔmbnAN* + pWG102 was found to be 999.47 Da by LC-MS/MS and 999.46 Da by FT-ICR MS, 154.7 Da smaller than mb isolated from *M.*

trichosporium OB3b wildtype. The difference suggests that one or both heterocyclic rings are not formed and an amino acid residue is missing. Subsequently mb from *ΔmbnAN* + pWG102 was subjected to Edman degradation and was found to have a polypeptide backbone with a sequence of Leu-?-Gly-Ser-?-Tyr-Pro-?-Ser-? (question marks suggest moieties with sulfhydryl groups, e.g., cysteines or non-amino acid moieties). It should be noted that the C-terminal methionine is missing from mb- *ΔmbnAN* + pWG102, and this can explain 131.2 Da of the difference in mass when comparing wildtype mb to that from *ΔmbnAN* + pWG102. More importantly, successful amino acid sequencing of mb from *ΔmbnAN* + pWG102 was surprising as previous attempts to sequence wildtype OB3b-mb via Edman degradation resulted in the non-mb sequence of Ser-Met-Tyr-Pro-? Ser-?-Met. The modification of the N-terminal leucine and the presence of the adjacent oxazolone ring A alters/disrupts N-terminal amino acid sequencing in wildtype mb. The successful collection of sequence data of mb from *ΔmbnAN* + pWG102 indicates that the N-terminal leucine has not been modified, and raises the possibility that oxazolone ring A may also be missing.

To help identify the unknown residues found in the initial amino acid sequence of mb from *ΔmbnAN* + pWG102, the composition of acid-digested mb from Δ*mbnAN*+pWG101 and Δ*mbnAN* + pWG102 was determined and compared. Mb from *ΔmbnAN* + pWG102 was found to have 0 leucine, 1.9 serine, 2.1 glycine, 0.8 proline, 1.8 cysteine, and 0.8 methionine per tyrosine. The presence of proline and one additional glycine than expected from the structure of wildtype mb (Figure 3.7) indicates that under these conditions, oxazolone ring B underwent hydrolysis and decarboxylation to form proline and a glycine (likely containing thioamide or Gly-Ψ), but oxazolone ring A was not degraded. Such a result is not unprecedented as earlier it was shown

that when mb from *M. trichosporium* OB3b is subjected to acid digestion, oxazolone ring B was hydrolyzed and decarboxylated to proline and a thioamide-containing glycine before ring A was converted to an α–oxo-leucine and a thioamide-containing glycine (Krentz, et al., 2010).

Mb from Δ*mbnAN* + pWG102 was found to have a different composition, i.e., 1.0 leucine, 1.8 serine, 3.3 glycine, 0.7 proline, and 1.6 cysteine per tyrosine. The absence of a Met was consistent with the N-terminal sequencing results. The presence of leucine and a third glycine is remarkable, and is unlikely to be the result of the degradation of oxazolone ring A as mb from Δ*mbnAN* + pWG102 was prepared in the same fashion as that from Δ*mbnAN* + pWG101. Rather, the finding of these residues supports the possibility that oxazolone ring A was not present in mb from Δ*mbnAN* + pWG102 mb.

To consider this further, UV/visible absorption spectral analyses of *ΔmbnAN* + pWG102 mb were performed and compared to that of mb produced by Δ*mbnAN* + pWG101 (Figure 3.15). The presence of only one major absorption peak at 337 nm indicates that *ΔmbnAN* + pWG102 mb has only oxazolone ring B, and not oxazolone ring A as a second major absorption peak would be expected at 394 nm. Further, copper titration of *ΔmbnAN* + pWG102 mb demonstrated copper binding, but the sample saturated at a copper:mb molar ratio of ~0.5, as compared to 1.0 for wildtype mb (Choi et al., 2006) and for mb from Δ*mbnAN* + pWG101 (Figure 3.15). The impaired copper binding by mb from *ΔmbnAN* + pWG102 again suggests that oxazolone ring A is missing. Finally, acid digestion of mb produced by Δ*mbnAN* + pWG102 followed the hydrolysis pattern observed for oxazolone B from both wild-type (Krentz et al., 2010) and Δ*mbnAN* + pWG101. In wild-type and Δ*mbnAN* + pWG101 mb, oxazolone ring B is hydrolyzed

before oxazolone ring A as evidenced by the decrease in absorption at 340 nm but little change at 394 nm (Figure 3.16). The mass changes for mb from Δ*mbnAN* + pWG101 (24.98 Da) and *ΔmbnAN* + pWG102 (25.99, 27 and 28 Da) after acid digestion were consistent with the predicted 25.98 Da change following hydrolysis of the oxazolone ring B (Krentz et al., 2010).

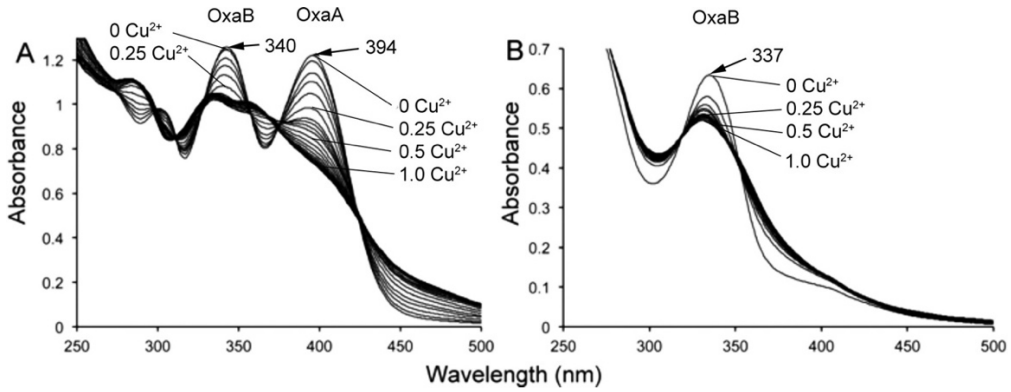

Figure 3.15. Comparison of the UV/visible light absorption spectra of methanobactin from (A) *M. trichosporium* OB3b *ΔmbnAN*+pWG101 and (B) *M. trichosporium* OB3b *ΔmbnAN* + pWG102 with the addition of 0.0 to 1.0 Cu(II) per methanobactin in 0.05 increments.

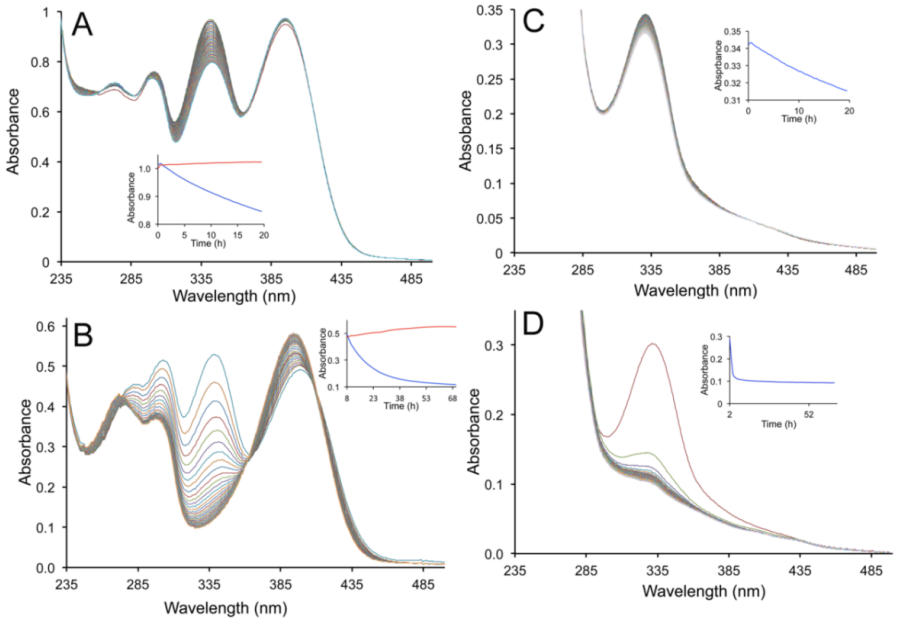

sFigure 3.16. UV/visible absorption spectra of methanobactin from Δ*mbnAN* + pWG101 (A and B) and Δ*mbnN* (C and D) of samples incubated in either 10 mM HCl (A and C) or 100 mM HCl (B and D). Spectra were taken either at 20 min (A and C) or at 120 min (B and C) intervals. Insets A and B, absorbance changes at 340 nm (blue trace) and 394 nm (red trace). Inserts C and D, absorbance changes at 337 nm (blue trace).

When we consider the mass spectral, amino acid sequence, composition, and UV/visible absorption data *in toto*, we propose that the metal-free form of mb from *ΔmbnAN* + pWG102 has the molecular structure shown in Figure 3.17. This structure, with a mass of 999.26 Da, agrees well with that measured via mass spectrometry. In particular, we predict that leucine is adjacent to a thioamide-containing glycine (Gly-Ψ), and that oxazolone ring B is also present. To verify the presence of this modified glycine in mb, our collaborators at Iowa State University assayed for the presence of thiol groups before and after reduction with tris (2-carboxyethyl) phosphine (TCEP). Before reduction, no thiol groups were measured in methanobactin from *M. trichosporium* OB3b wildtype, Δ*mbnAN* + pWG101 and *ΔmbnAN* + pWG102 strains, suggesting that the thioamide groups associated with the oxazolone rings are not detectable using this methodology and the cysteine thiol groups were oxidized. After reduction, however, mb from *M. trichosporium* OB3b wildtype and Δ*mbnAN* + pWG101 strain had 1.7 ± 0.3 and 2.0 ± 0.2 thiols per mb, respectively, and were likely created from the reduction of the disulfide bond connecting Cys 3 and Cys 6. Mb from *ΔmbnAN* + pWG102 had 3.1 ± 0.3 thiols per mb after reduction with TCEP. The finding of an additional thiol after reduction indicates that despite the lack of oxazolone ring A, the sulfur group remains, and as such supports the conclusion that a thioamide-containing glycine exists in place of oxazolone ring A.

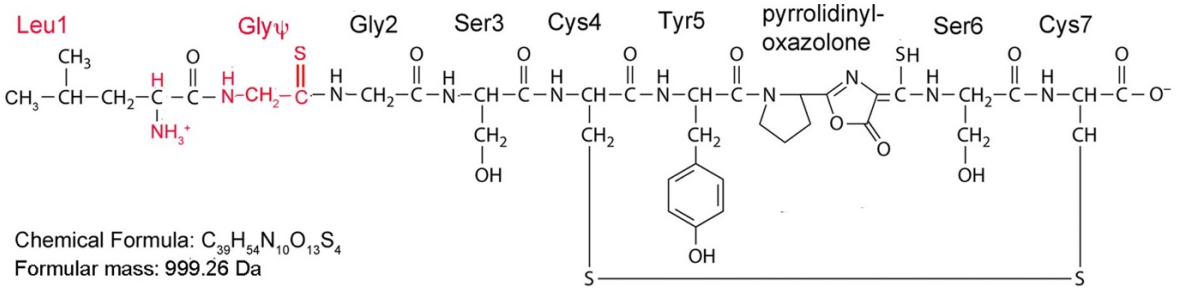

Figure 3.17. Proposed structure of methanobactin from *M. trichosporium ΔmbnAN* + pWG102. Major differences from wild-type methanobactin are shown in red.

IV.2.4 Discussion

Here, through the construction of markerless deletion of *mbnABCMN* and expression of *mbnABCM* off a plasmid, we show that the product of *mbnN* is necessary for the deamination of the N-terminal leucine. Further, *ΔmbnAN* + pWG102 is unable to construct oxazolone ring A in mb, but oxazolone ring B is formed, indicating that these two rings are made independently. It is unclear, however, if oxazolone rings A and B are formed via the same or different modifying enzyme(s), but from the data collected, it appears that the modifying enzyme(s) responsible for formation of oxazolone ring A can only bind and/or modify the N-terminal cysteine after the deamination of the adjacent leucine.

In the earlier hypothesized pathway for mb biosynthesis (Figure 3.8), it was speculated that ring closure occurred before changes in connectivity of the peptide backbone. Based on the findings reported here, however, it appears that deaminaton of the N-terminal acid must occur before formation of oxazolone ring A in *M. trichosporium* OB3b, and an alternative scheme for formation of mb is presented in Figure 3.18. It should be noted that we do not know if, in wildtype mb, re-arrangement of the peptide backbone occurs before leucine deamination (or vice-versa), only that both are required for formation of oxazolone ring A.

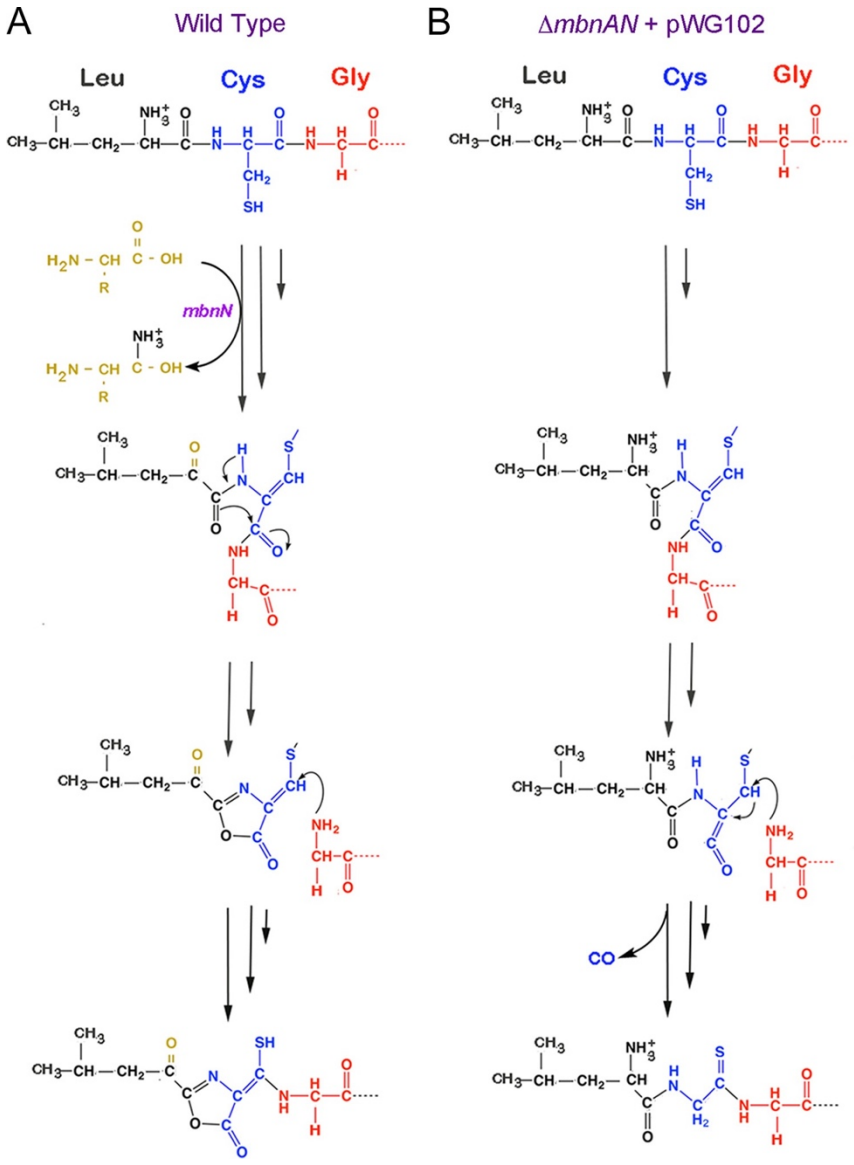

Figure 3.18. Proposed pathway of formation of (A) the N-terminal oxazolone group with associated thioamide group in wild-type methanobactin from *M. trichosporium* OB3b and (B) the resulting altered pathway in *M. trichosporium ΔmbnAN* + pWG102.

All mbs characterized to date have an oxazolone ring near the C-terminus, but the N-terminal heterocyclic ring is either an oxazolone, pyrazinedione or imidazolone ring. In the earlier hypothesized pathway for mb biosynthesis (Figure 3.8), it was speculated that pyrazinedione and imidazolone rings are formed from modification of an oxazolone ring, but further consideration of available bioinformatic data juxtaposed with the findings reported here suggests that

pyrazinedione and imidazolone rings can be created without an oxazolone ring platform. That is, in the original model of ring formation, deamination of the amino acid residue adjacent to the cysteine converted to an oxazolone ring was not necessary for ring formation. The data presented here, however, show such deamination is required for the formation of oxazolone ring A. For example, mb of *Methylocystis* strain SB2 has an N-terminal imidazolone ring, but its mb gene clusters does not show any clear evidence of an encoded aminotransferase (DiSpirito et al., 2016) (Figure 1.11, Figure 1.12). Given that the N-terminal oxazolone ring in mb of *M. trichosporium* OB3b is only formed when *mbnN* is expressed, it is possible that the creation of alternative rings found in other forms of mb do not require that an oxazolone ring be first formed. Rather, the formation of a pyrazinedione and imidazolone ring may be due to the concerted activity of a suite of modifying enzymes, including a putative FAD-dependent oxidoreductase found in the mb gene clusters of *Methylocystis* strain SB2 but not in *M. trichosporium* OB3b (DiSpirito et al., 2016). As noted earlier, however, formation of imidazolone or pyrazinedione rings without an oxazolone intermediate would likely necessitate multiple changes in the connectivity of the peptide backbone (DiSpirito et al., 2016).

IV.2.5 Conclusions and future perspectives

In conclusion, through the construction and back complementation of a deletion mutant defective in mb production, the function of *mbnN* is elucidated. With such information of synthesis pathway of mb, we can develop a better mechanistic understanding of the biosynthetic pathway of mb. With a better grasp on how mb is synthesized, we can then develop strategies to modify methanobactin to enhance its efficacy for the treatment of copper-related diseases such as Wilson disease.

It appears that different strategies have been developed by different methanotrophs for the formation of mb, and clearly creation and characterization of more mutants is required to fully re-construct these different biosynthetic pathways. A challenge, however, is *M. trichosporium* OB3b is the only methanotroph known to produce mb with a validated system for generation of mutants. Similar approaches may be possible in other methanotrophs that produce mb, but in the event that working genetic systems are difficult to construct in these strains, it may be useful to pursue efforts whereby mb genes from other strains are heterologously expressed in either *E. coli* or mb-defective mutants of *M. trichosporium* OB3b.

CHAPTER IV GENETIC REGULATION BY RARE EARTH ELEMENTS (REEs) AND COPPER

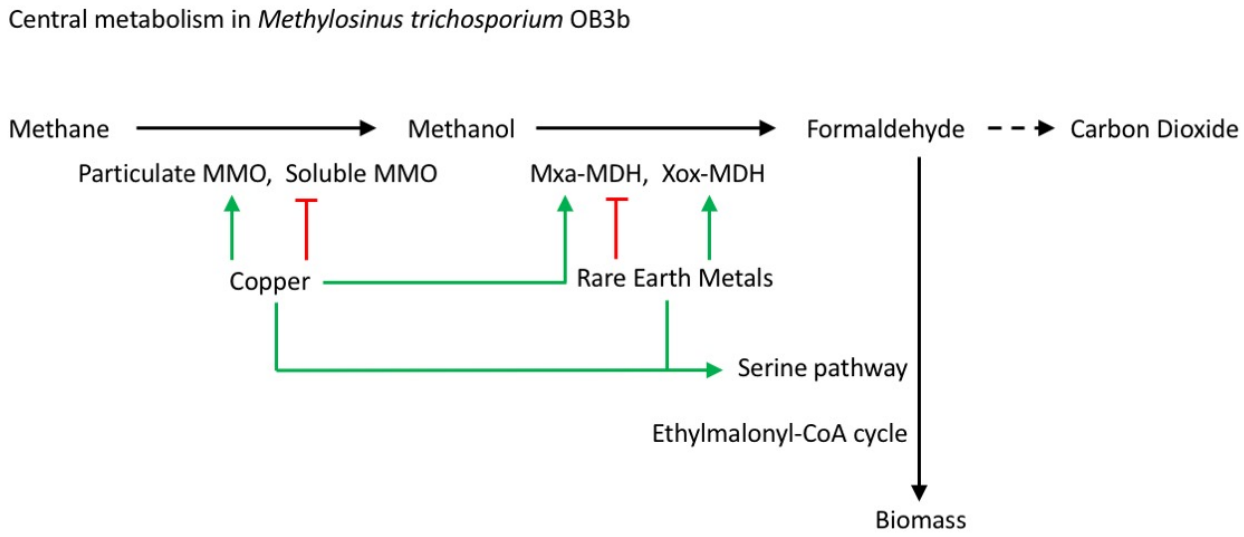

Figure 4.0 Effect of copper and REEs on gene expression in *M. trichosporium* OB3b

Published:

Uptake and effect of rare earth elements on gene expression in *Methylosinus trichosporium* OB3b. FEMS Microbiology Letters, 363(13), fnw129.

In preparation:

The Effect of Copper and Cerium on the Transcriptome of *Methylosinus trichosporium* OB3b.

IV.1 Genetic regulation by REEs

IV.1.1 Introduction

In methanotrophs and methylotrophs, microbes that utilize methane and/or methanol for growth, it was initially assumed that methanol oxidation was performed in these microbes by a calcium-containing pyrroquinolone quinone (PQQ)-linked methanol dehydrogenase (MeDH), or Mxa-

MeDH (Williams, et al. 2005). Recent genomic and biochemical evidence indicate, however, an alternative PQQ-MeDH that contains a rare earth element in its active site also exists (Xox-MeDH), and this form may actually be catalytically superior to Mxa-MeDH (Hibi, et al., 2011; Wu, et al., 2015; Keltjens, et al., 2014; Pol, et al., 2014). Early data suggested that expression of the alternative forms MeDH was not regulated by the (un)availability of rare earth elements (Nakagawa, et al., 2012), but it has been shown that in the presence of cerium, expression of *xoxF*, encoding for the single subunit of Xox-MeDH increased in the α-Proteobacterium, *Methylosinus trichosporium* OB3b, while expression of *mxaF* and *mxaI*, encoding for the large and small subunits of Mxa-MeDH, respectively, goes down (Farhan Ul Haque, et al., 2015). Subsequently, it was shown that cerium and other rare earth elements (lanthanum, praseodymium, and neodymium) exhibited a similar effect on MeDH expression in the methylotroph, *Methylobacterium extorquens* AM1 (Vu, et al., 2016). It was also later shown that cerium and lanthanum upregulate expression of *xox* genes, while repressing *mxa* genes in the γ-Proteobacterium, *Methylomicrobium buryatense* (Chu and Lidstrom, 2016).

One interesting finding was that although cerium controlled expression of alternative forms of MeDH in methanotrophs and methylotrophs, such regulation appears to be over-ridden by the "copper-switch" in methanotrophs (Farhan Ul Haque, et al., 2015). That is, in *M. trichosporium* OB3b, expression of *xoxF* increased in the presence of cerium regardless of the concentration of copper. In the absence of copper, expression of *mxaF* and *mxaI*, decreased, but cerium had little effect on expression of these genes in the presence of copper. Here we extend these initial findings to determine if other rare earth elements also serve to regulate expression of alternative forms of the MeDH, and if so, if such regulation is also over-ridden by copper.

IV.1.2 Metal analysis

M. trichosporium OB3b wildtype was grown in the presence of every tested rare earth element (lanthanum, praseodymium, neodymium and samarium) both in the presence and absence of copper. Metals associated with biomass was measured by ICP-MS. We found that more than 90% of the added rare earth element was associated with biomass (Table 4.1), indicating that methanotrophs appear to have a mechanism (as yet uncharacterized) for the uptake of these metals.

A *mxaF*::Gm^r mutant of *M. trichosporium* OB3b able only to express Xox-MeDH had been constructed in a previous study by Farhan HI-Haque et al. (2015). This mutant was also investigated in this study. It was found to be able to grow in the presence of lanthanum, praseodymium, neodymium, but not samarium (data not shown), and again, most of the added rare earth element was cell-associated (Table 4.1).

IV.1.3 Gene expression

Quantitative PCR was then used to determine if the "copper-switch" was still operative under these conditions, and if, as found earlier for cerium, expression of *mxaF* and *mxaI* was not affected by the presence of other rare earth elements in the presence of copper. The levels of expressed genes were measured by absolute quantification method as described in Session 2.3.9.

Table 4.1. Rare earth element (REE) and copper associated with biomass of *M. trichosporium* OB3b wild type and *mxaF*:Gm^r mutant as a function of the growth concentration of copper and REE. Values presented are mean ± standard deviation of triplicate cultures.

Strains	Growth conditions		nmol REE/mg protein	nmol Cu/mg protein	% REE uptake	% Cu uptake
Wild type	0 μM Cu	25 μM La	80.9±4.7	$2.6x10^{-2}±9.5x10^{-3}$	96.1±1.4	NA
		25 μM Ce	73.9±8.9	$9.0x10^{-3}±7.7x10^{-3}$	93.2±4.4	NA
		25 μM Pr	94.6±10.3	$1.4x10^{-2}±2.5x10^{-3}$	95.6±1.7	NA
		25 μM Nd	94.2±16.3	$3.5x10^{-2}±1.5x10^{-2}$	98.4±0.4	NA
		25 μM Sm	92.3±14.8	$5.1x10^{-2}±1.9x10^{-2}$	93.0±3.6	NA
		0 μM REE	0.2±0.3*	$3.1x10^{-2}±8.2x10^{-3}$	NA	NA
	10 μM Cu	25 μM La	60.6±6.5	7.3±0.6	91.9±0.7	23.2±1.4
		25 μM Ce	65.2±3.2	6.6±0.7	98.0±0.4	22.8±1.7
		25 μM Pr	78.3±9.4	7.9±1.4	94.6±6.4	27.5±3.1
		25 μM Nd	87.4±5.9	7.6±0.8	98.3±1.4	23.3±1.8
		25 μM Sm	84.6±16.1	6.2±1.4	97.6±0.9	20.1±0.8
		0 μM REE	$0.1±2.1x10^{-2}$*	4.3±0.3	NA	12.3±0.9
mxaF::Gm	0 μM Cu	25 μM La	76.4±3.8	$3.9x10^{-2}±1.7x10^{-2}$	91.8±0.2	NA
		25 μM Ce	63.1±17.3	$8.8x10^{-2}±1.3x10^{-2}$	83.9±1.9	NA
		25 μM Pr	78.0±5.7	$4.8x10^{-2}±2.4x10^{-2}$	89.0±1.4	NA
		25 μM Nd	89.7±9.7	$8.7x10^{-2}±7.8x10^{-2}$	96.5±1.6	NA
	10 μM Cu	25 μM La	51.9±1.4	5.4±0.5	64.7±0.7	14.6±1.7
		25 μM Ce	33.0±4.9	5.8±0.5	51.8±9.3	13.0±1.9
		25 μM Pr	59.4±3.0	5.9±0.7	81.2±1.0	18.4±0.3
		25 μM Nd	67.0±9.3	4.5±0.5	84.8±1.2	14.8±0.7

NA: No growth.
* measured as the sum of La, Ce, Pr, Nd, Sm.
Note: The background level of copper and lanthanides in the media were determined as follows: copper 0.52 ± 0.04 μg/L, lanthanum 0.56 ± 0.28 μg/L, praseodymium 0.32 ± 0.01 μg/L, neodymium 0.34 ± 0.03 μg/L, samarium 0.35 ± 0.01 μg/L.

As can be seen in Figure 4.1, expression of *pmoA* and *mmoX* in *M. trichosporium* OB3b wildtype was not affected by the presence of any rare earth element either in the absence or presence of copper, but the "copper-switch" was readily apparent, i.e., *pmoA* expression increased in the presence of copper while *mmoX* expression decreased. Expression of *mxaF* and *mxaI*, however, was significantly reduced ($p < 0.05$) in the absence of copper when a rare earth element was also

present (Figure 4.2). In the presence of copper, expression of *mxaF* and *mxaI* was not affected by the presence of any rare earth element. Finally, expression of *xoxF1* and *xoxF2* increased in the presence of most rare earth elements regardless of the presence or absence of copper; the only exception was expression of *xoxF2* in the presence of samarium (Figure 4.3).

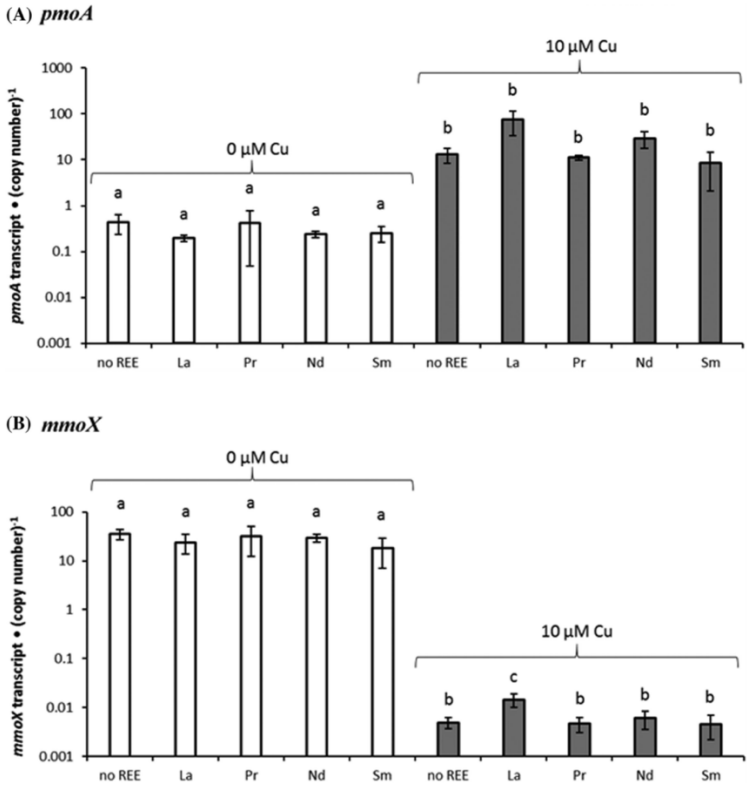

Figure 4.1. Expression analyses of *pmoA* (A) and *mmoX* (B) in *M. trichosporium* OB3b wild type grown in the absence of any rare earth element (no REE) or in the presence of 25 µM Lanthanum (La), Praseodymium (Pr), Neodymium (Nd), or Samarium (Sm) with either 0 µM or 10 µM copper. Errors bars represent the standard deviation of triplicate samples. The values for columns within each plot labeled by different letters are significantly different ($P < 0.05$).

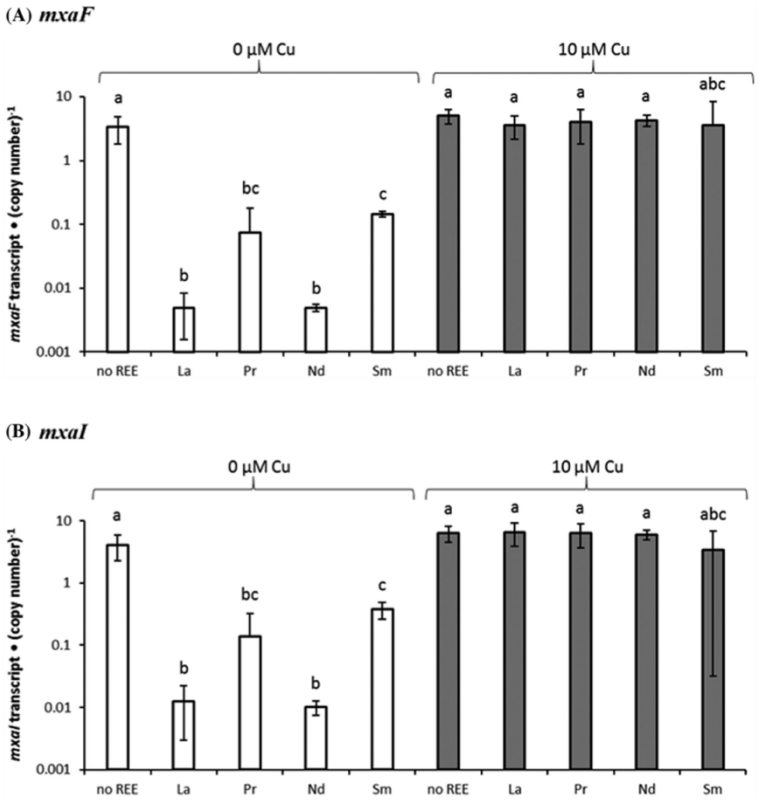

Figure 4.2. Expression analyses of *mxaF* (A) and *mxaI* (B) in the *M. trichosporium* OB3b wild type grown in the absence of any rare earth element (no REE) or in the presence of 25 µM Lanthanum (La), Praseodymium (Pr), Neodymium (Nd) or Samarium (Sm) with either 0 µM or 10 µM copper. Errors bars represent the standard deviation of triplicate cultures. Lower error bars are not visible for Pr with 0 µM Cu for both *mxaF* and *mxaI* and Sm with 10 µM Cu for *mxaF* as the standard deviation is larger than the mean. The values for columns within each plot labeled by different letters are signi cantly different ($P < 0.05$).

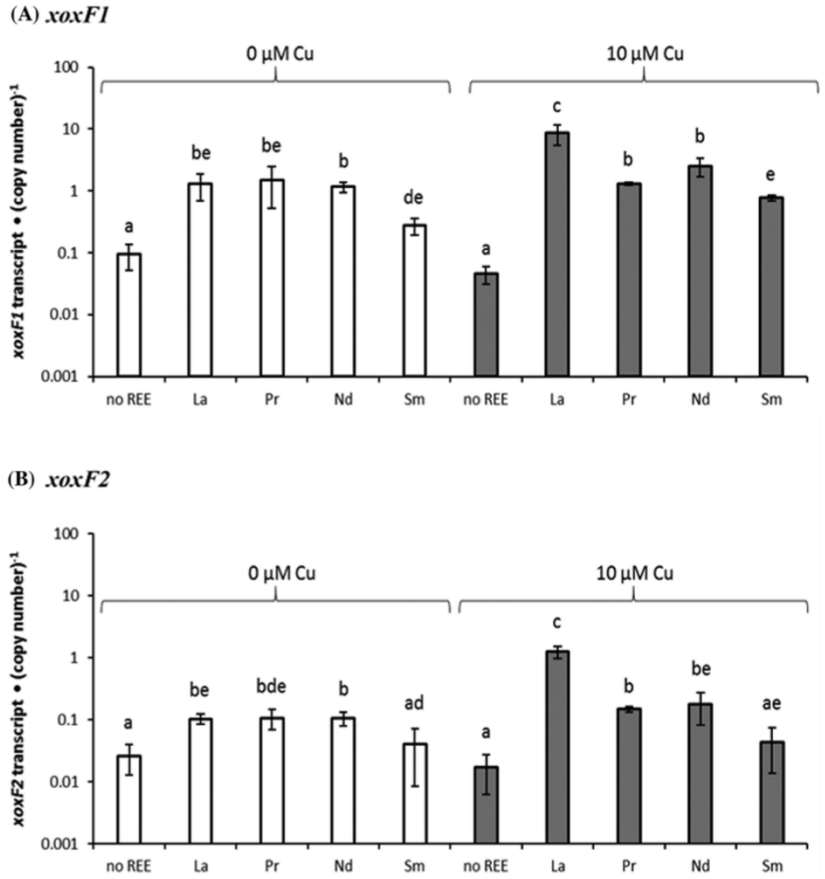

Figure 4.3. Expression analyses of *xoxF1* (A) and *xoxF2* (B) in the *M. trichosporium* OB3b wild type grown in the absence of any rare earth element (no REE) or in the presence of 25 µM Lanthanum (La), Praseodymium (Pr), Neodymium (Nd), or Samarium (Sm) with either 0 µM or 10 µM copper. Errors bars represent the standard deviation of triplicate samples. The values for columns within each plot labeled by different letters are significantly different ($P < 0.05$).

IV.1.4 Discussion

Here we extend an earlier finding that cerium serves to regulate expression of alternative methanol dehydrogenases in *M. trichosporium* OB3b (Farhan Ul Haque, et al., 2015) and show that other rare earth elements, i.e., lanthanum, praseodymium, neodymium, and samarium, also induce expression of Xox-MeDH and repress expression of Mxa-MeDH. Further, as found for cerium, such control was only evident in the absence of copper, i.e., the "copper-switch" appears to be of primary importance in controlling expression of genes involved in the conversion of not

only methane to methanol, but also methanol to formaldehyde. The cross-regulation by copper and rare earth elements on the expression of MMOs and MDHs is summarized in Figure 4.4.

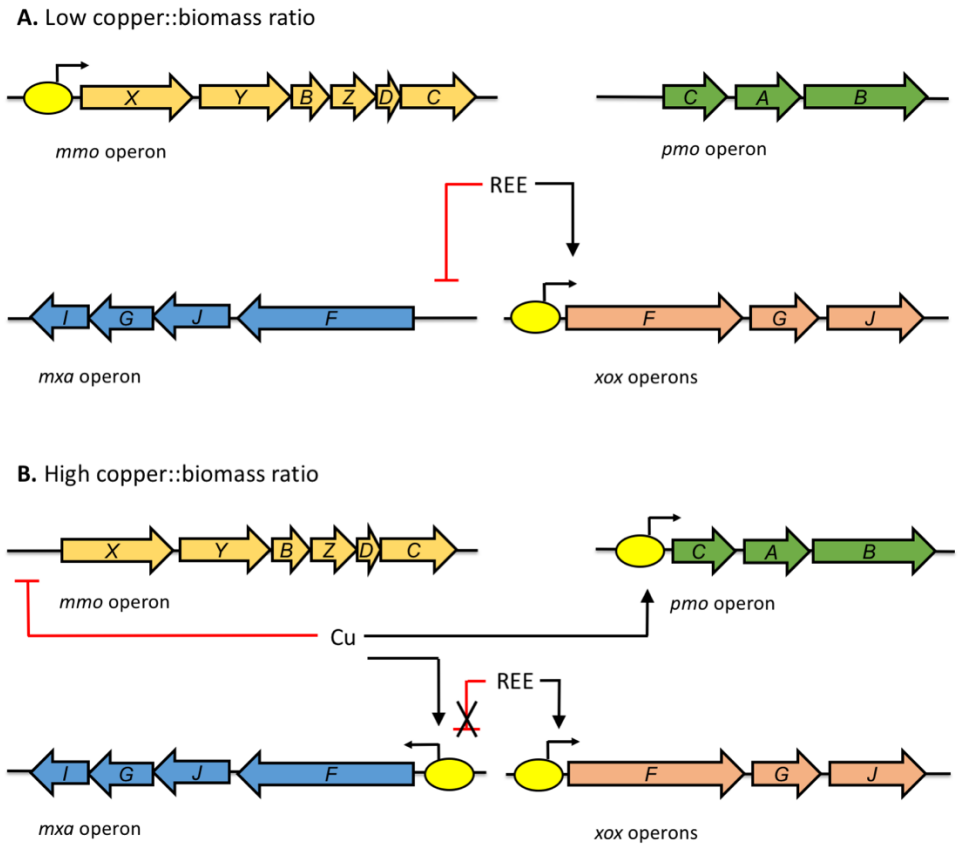

Figure 4.4. Cross-regulation on gene expression by copper and rare earth elements in *M. trichosporium* OB3b

Although samarium did affect expression of *mxaF* and *mxaI* in the absence of copper in *M. trichosporium* OB3b wildtype, its impact was comparatively less than that of lanthanum, praseodymium, and neodymium (Figure 4.2) and samarium also caused the lowest increase in expression of *xoxF1* and *xoxF2* (Figure 4.3). Further, the *mxaF*::Gm^r mutant was unable to grow in the presence of samarium. Similar findings have been reported in the *Methylobacterium extorquens* AM1 where samarium was also found to have relatively weaker effects on growth in Mxa-MeDH mutant strains (Vu, et al., 2016). It was suggested that the relatively greater ionic

radius of samarium vs. other rare earth elements may either limit uptake of samarium and/or insertion into Xox-MeDH. The ionic radius of an element, however, depends on a number of factors, including oxidation state and coordination number, and the ionic radii of the rare earth elements have great overlap (Shannon, 1976). Our finding that samarium was effectively taken up by both *M. trichosporium* OB3b wildtype and *mxaF*::Gm^r mutant suggest that reduced effect of samarium compared to other rare earth elements is not due to limited bioavailability but rather a reduced ability to correctly insert samarium into Xox-MeDH, i.e., poor coordination with residues that stabilize its localization within Xox-MeDH as well as ensure its effective coordination with POQ for electron transfer.

Although it is now apparent that methanotrophs strongly respond to the presence of rare earth elements, nothing is known as to how these metals are sensed, collected, or regulate gene expression. A review of the literature reveals that the question of uptake of rare earth elements is actually poorly understood, likely due to the fact it was initially believed that rare earth elements were non-essential as they had no established biological function (Nakamura, et al., 2006). Early studies found that cerium uptake varies widely, with some bacteria taking up more than 80% of added cerium (e.g., *Escherichia coli* and *Aerobacter aerogenes*) while others take up less than 25% (e.g., *Serretia marcescens* and *Pseudomonas vulgaris*). In fact, uptake can vary widely within specific genera, i.e., *Streptomyces flavovirens* has been shown to take up more than 75% of added cerium while *Streptomyces viridoflavus* collects less than 25% (Johnson and Kyker, 1961). It has been argued that such uptake is largely passive (Johnson and Kyker, 1961), but others have found that microbes can actively oxidize cerium (Moffett, 1990). This result, coupled with the finding that rare earth elements control the expression and activity of methanol

dehydrogenase in methanotrophs, and that most of the added rare earth elements are associated with biomass, however, suggest an uptake mechanism for rare earth elements exists in at least some microbes.

Equally unknown is the basis by which rare earth elements control gene expression in methanotrophs. At this time, expression of only four genes in *M. trichosporium* OB3b has been shown to be affected by the presence of rare earth elements, i.e., *mxaF* and *mxaI* (which are co-expressed on the same polycistronic transcript), and *xoxF1* and *xoxF2* (which have different transcripts). Scanning of the promoter regions of these genes indicates that there is one unique sequence found in all: CGA(T/C)(G/A)TGACC. This sequence has also been found in the promoter regions of over a dozen genes in the genome of *M. trichosporium* OB3b. The majority of these encode for proteins of unknown function. It is tempting to speculate that this sequence may serve as binding site for some regulatory protein that differentially regulates expression of genes encoding for Mxa- vs. Xox-MeDH (and perhaps other proteins) in response to rare earth elements.

It should be stressed that although *mxaF* and *mxaI* expression decreased in the presence of rare earth elements, this was only in the absence of copper. In the presence of copper, *mxaF* and *mxaI* expression was not reduced with the concurrent addition of a rare earth element, although *xoxF1* and *xoxF2* expression did increase. These data indicate that the *mxa* operon is controlled by both rare earth elements and copper, but that copper is the primary regulator. Scanning of the promoter regions of genes clearly shown to be upregulated with respect to copper, e.g., *pmoA*, *mxaF*, and *mxaI* finds one consensus sequence: TATT(G/T)CA(C/T)GT. Further, examination of

the entire genome of *M. trichosporium* OB3b indicates that this sequence is found in the promoter region of many genes encoding for proteins of unknown function. It is tempting to speculate that this sequence is important for the copper regulation of these genes. It is also interesting to note that the *mxa* operon was the only operon found to have both putative copper and cerium regulatory sequences.

IV.1.5 Conclusions and future perspectives

In conclusion, we demonstrate that a range of rare earth elements affect the expression of alternative methanol dehydrogenases in *M. trichosporium* OB3b, but such control is only apparent in the absence of copper. Further, growth of the *mxaF*::Gm^r mutant of *M. trichosporium* OB3b was not observed in the presence of samarium, but did occur in the presence of lanthanum, praseodymium and neodymium, suggesting that these metals enable Xox-MeDH to become active, but samarium cannot.

These findings open more questions as to how methanotrophs sense, transport, storage, and regulate REEs. Further experiments need to be done to understand the interaction between methanotrophs and REEs, which may include mutagenesis study to identify novel sensing, uptake, and storage mechanisms, the use of reporter vectors and DNA binding techniques to investigate genetic regulation elements, and structural characterization of more Xox-MeOH to better determine the nature of the metal-binding site in Xox-MeDH. To date only the Xox-MeDH from *Methylacidiphilum fumariolicum* SolV, an acidophilic methanotroph of the Verrucomicrobia, has been studied to any great extent (Pol, et al., 2014).

IV.2 Transcriptomic analysis of M. trichosporium OB3b in response to copper and/or cerium

IV.2.1 Introduction

The activity of methanotrophs is strongly affected by a number of environmental parameters, including the bioavailability of copper and REEs. As described before, methanotrophs have a well-known "copper-switch" where the expression and activity of sMMO and pMMO responds significantly to the availability of copper (Choi, et al., 2003; Semrau et al., 2010; Semrau, et al., 2013). More recently, rare earth elements have been shown to have a major effect on methanotrophs (Pol et al., 2014; Wu et al., 2015) by strongly regulating the activity and expression of alternative methanol dehydrogenases (MxaF-MeOH and XoxF-MeDH) that oxidize methanol to formaldehyde, signifying that a "REE-switch" also exists (Farhan Ul Haque, et al. 2015; Gu, et al., 2016; Vu, et al., 2016). Cross-regulation by these metals on gene expression has been observed as described above.

What is not clear, however, is if copper and/or cerium exert more global control over gene expression in methanotrophs. These metals clearly control expression of enzymes mediating the oxidation of methane and methanol - two key steps in the central pathway of methane oxidation- but do they regulate expression of genes in other metabolic pathways? Here we describe the effect of different concentrations of copper and/or cerium on the transcriptome of *M. trichosporium* OB3b using RNA-seq and RT-qPCR.

IV.2.2 Transcriptomic analysis by RNA-Seq

IV.2.2.1 General analyses of transcriptomic samples

To investigate the effect of copper and cerium on the transcriptome of *M. trichosporium* OB3b, this strain was grown under four different conditions: 0 μM copper + 0 μM cerium, 0 μM copper + 25 μM cerium, 10 μM copper + 0 μM cerium, and 10 μM copper + 25 μM cerium. The quality of the collected RNA from these cultures was very good (RIN ≥ 8.7 for each sample) with 23.1 – 42.8 x 10^6 reads per sample (Table 4.2). Of these, 7.3 - 15.2 x 10^6 reads per sample were assigned to regions encoding for proteins. To determine the reproducibility of biological replicates, principal component analysis of the normalized logarithmic transformed read counts of each transcriptome was performed using DESeq2 (Anders & Huber, 2010). High similarity was observed between triplicate biological replicates for three of the growth conditions - 0 μM copper + 0 μM cerium, 0 μM copper + 25 μM cerium, and 10 μM copper + 25 μM cerium (Figure 4.5). Transcriptomes of replicates of the fourth growth condition - 10 μM copper + 0 μM cerium - showed less uniformity (Figure 4.5). Despite the variability in the transcriptome of *M. trichosporium* OB3b when grown with 10 μM copper + 0 μM cerium, we could not reasonably conclude that any replicate in this condition was an outlier as: (1) the coverage and sequence of these replicates were comparable, and; (2) the Spearman's rank correlation coefficient between these three replicates was found to be > 0.93. As such, all replicates for all conditions were included in subsequent analyses of differential gene expression.

Table 4.2. General properties of transcriptome samples of *M. trichosporium* OB3b grown in the presence of varying amounts of copper and cerium.

Conditions	0 μM Cu 0 μM Ce			10 μM Cu 0 μM Ce			0 μM Cu 25 μM Ce			10 μM Cu 25 μM Ce		
RIN	9.1	9.0	9.1	9.0	9.0	8.9	9.2	9.2	9.3	8.7	9.0	9.1
Reads ($X10^6$)	32.7	29.9	23.9	30.6	33.4	41.4	29.7	23.1	38.3	42.8	41.1	39.1
Reads aligned ($X10^6$)	28.3	21.9	18.0	26.5	29.1	32.7	25.3	20.0	31.8	34.2	33.1	33.7
Reads assigned to coding features ($X10^6$)	11.8	8.7	7.3	11.2	11.7	14.3	10.3	8.2	12.7	15.2	14.6	14.8

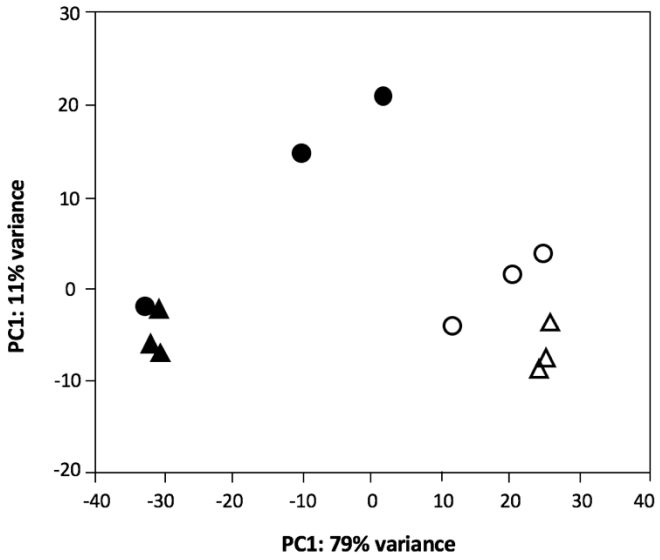

Figure 4.5. Principal component analysis of collected transcriptomic sequence data.
○ - 0 μM copper + 0 μM cerium; ● - 10 μM copper + 0 μM cerium; △ - 0 μM copper + 25 μM cerium; ▲ - 10 μM copper + 25 μM cerium.

IV.2.2.2 Differentially expressed genes in the presence or absence of copper

When comparing the transcriptome of *M. trichosporium* OB3b grown with 10 μM copper + 0 μM cerium vs. 0 μM copper + 0 μM cerium, 37 genes were found to have significantly increased expression in the presence of copper, i.e., $\log_2$ change ≥ 1.5 and Benjamini-Hochberg-adjusted p-value ≤ 1×10^{-3} (Table 4.3). As expected from previous RT-qPCR assays of *pmoA*, genes of the *pmo* operon were significantly upregulated ($\log_2 > 2$; $p < 3 \times 10^{-8}$). Further, a gene (locus tag ADVE02_v2_12455) encoding for a recently discovered copper storage protein, Csp1, (Vita et

al., 2015) was also significantly upregulated in the presence of copper but its homolog, Csp2 (locus tag ADVE02_v2_10455), did not vary with respect to copper. *cusA*, encoding for a copper efflux system (Munson et al., 2000), was also found to have increased expression in the presence vs. absence of copper. Very few other groups of genes were found to be upregulated, with the exception of genes encoding for 30S and 50S ribosomal proteins and genes of unknown function. Approximately twice as many genes (86 in total) were downregulated in the presence of copper (i.e., $\log_2$ change ≤ -1.5 and Benjamini-Hochberg-adjusted p-value ≤ 1 x 10^{-3}) in several general groups, e.g., *mmo* genes encoding for polypeptides of the sMMO as well as *mbn* genes involved in methanobactin synthesis. Many genes encoding for TonB-dependent transporters had reduced expression in the presence of copper, as did numerous putative σ factors and proteins of unknown function (Table 4.3).

IV.2.2.3 Differentially expressed genes in the presence or absence of cerium

Gene expression was also affected by the availability of cerium, but fewer genes showed differential expression in response to the addition of this rare earth element as compared to changes observed when copper was varied, i.e., 20 genes were upregulated and 15 downregulated in the presence vs. absence of cerium (Table 4.4). As expected from previous RT-qPCR assays (Farhan Ul Haque et al., 2015, Gu et al., 2016), when comparing the transcriptome of *M. trichosporium* OB3b grown with 0 μM copper + 0 μM cerium vs. 0 μM copper + 25 μM cerium, genes encoding for the rare earth element-containing methanol dehydrogenase (Xox-MeDH) increased in the presence of cerium. Interestingly, so did genes predicted to be involved in pyoverdine synthesis and uptake. The only other genes significantly upregulated by cerium were two genes encoding for a σ^{70} factor and an ABC transporter, as well as several genes

Table 4.3. Select genes differentially expressed in *M. trichosporium* OB3b grown with 10 μM copper + 0 μM cerium vs. 0 μM copper + 0 μM cerium.
(Benjamini-Hochberg-adjusted p-value < 1 x10^{-3}, $|\log_2| > 1.5$)

Function	Gene/Locus number
Up-regulated	
Particulate methane monooxygenase	*pmoAB12*
Metal transport and metabolism	*cusA*, *csp1*(ADVE02_v2_12455), *modA,* ADVE02_v2_14468
Ribosomal proteins	50S (*rplDWBVP, rpmC*), 30S (*rpsSQNH*)
Proteins of unknown function	ADVE02_v2_10901, 10902, 11082, 11143, 11164, 11568, 12042, 12128, 12492, 12978, 12979, 12980, 13152, 14285, 14468, 30055
Down-regulated	
Soluble methane monooxygenase	*mmoRGXYBDZC*
Methanobactin synthesis and transport	*mbnTABCMNPH*
TonB-dependent transporters	ADVE02_v2_10030, 10151, 11125, 11295, 11307, 11588, 12266, 12284, 13641, 13988, 14392, 20043
Transcription regulators	σ^{24} factors (ADVE02_v2_10149, 11305, 11827, 12264)
	σ^{54} factor (*mmoR*)
	σ^{70} factor (ADVE02_v2_13661)
	FecRI-like proteins (ADVE02_v2_10211&10212, 11296&11297, 11828, 13990, 14098, 14393&14394, 20042)
Proteins of unknown function	ADVE02_v2_10007, 10008, 10031, 10035, 11119, 11294, 11308, 11588, 12283, 12503, 12506, 12508, 13637, 13638, 13660, 13662, 13663, 13985, 13986, 14096, 14246, 20041

encoding for proteins of unknown function. Genes encoding for the calcium-containing methanol dehydrogenase (Mxa-MeDH) were downregulated in the presence of cerium (Table 4.4). Three

genes encoding for either a TonB dependent receptor, a pentapeptide repeat protein and a protein of unknown function were the only other genes to exhibit decreased expression when cerium was added in the absence of copper (Table 4.4).

Table 4.4. Select genes differentially expressed in *M. trichosporium* OB3b grown with 0 μM copper + 25 μM cerium vs. 0 μM copper + 0 μM cerium.
(Benjamini-Hochberg-adjusted p-value < 1 x10^{-3}, $|\log_2| > 1.5$)

Function	Gene/Locus number
Up-regulated	
Xox-type methanol dehydrogenase gene cluster	*xoxFG1, xoxGJF2*
Pyoverdine synthesis and transport	*aphA, pvdFAHL*, *fpvA, mbtH, macB*
ABC-type transporter	ADVE02_v2_11792
σ^{70} factor	ADVE02_v2_30017
Proteins of unknown function	ADVE02_v2_12116, 30014
Down-regulated	
Mxa-type methanol dehydrogenase	*mxaHDLKCASRIGJF*
TonB-dependent transporter	ADVE02_v2_10208
Pentapeptide repeat protein	ADVE02_v2_11208
Protein of unknown function	ADVE02_v2_12110

IV.2.2.4 Differentially expressed genes in the presence or absence of cerium and in the presence of copper

When comparing the transcriptome of *M. trichosporium* OB3b grown with 10 μM copper + 0 μM cerium vs. 10 μM copper + 25 μM cerium, only seven genes were upregulated when cerium was added in the presence of copper, i.e., genes encoding for the Xox-MeDH, ABC or TonB-

dependent transporters, or of unknown function (Table 4.5). 36 genes were found to be downregulated, most notably genes encoding for nitrogenase and hydrogenase (discussed in more detail below). Finally, no significant difference in the expression of genes involved in pyoverdine synthesis was observed, suggesting that iron uptake was not affected by the variation of cerium so long as copper was also present. As discussed below, it may be that an alternative copper-based iron uptake was operative in these conditions such that pyoverdine synthesis was not required for iron sequestration.

Table 4.5. Select genes differentially expressed in *M. trichosporium* OB3b grown with 10 μM copper + 25 μM cerium vs. 10 μM copper + 0 μM cerium.
(Benjamini-Hochberg-adjusted p-value < 1 x10^{-3}, $|\log_2| > 1.5$)

Function	Gene/Locus number
Up-regulated genes	
Xox-type methanol dehydrogenase	*xoxFG1*
ABC-type transporter	ADVE02_v2_11791, 11792
TonB-dependent transporter	ADVE02_v2_10208
Protein of unknown function	ADVE02_v2_12116
Down-regulated genes	
Hydrogenase	*hupH, hyaCB,* ADVE02_v2_10849
Nitrogenase	*nifBENXU, frxA*
Proteins of unknown function	ADVE02_v2_10223, 10394, 10643, 11076, 11428, 11580, 11714, 11715, 12128, 12519, 12756, 12823, 12824, 13014, 13310, 13674, 13996, 14333

IV.2.2.5 Differentially expressed genes in the presence or absence of copper and in the presence of cerium

When comparing the transcriptome of *M. trichosporium* OB3b grown with 0 µM copper + 25 µM cerium or 10 µM copper + 25 µM cerium, over 780 genes, approximately 15% of the entire genome, were found to be either up- or down-regulated. Figure 4.6 maps major shifts in gene expression for various metabolic pathways and uptake systems while Table 4.6 summarizes major changes in gene expression.

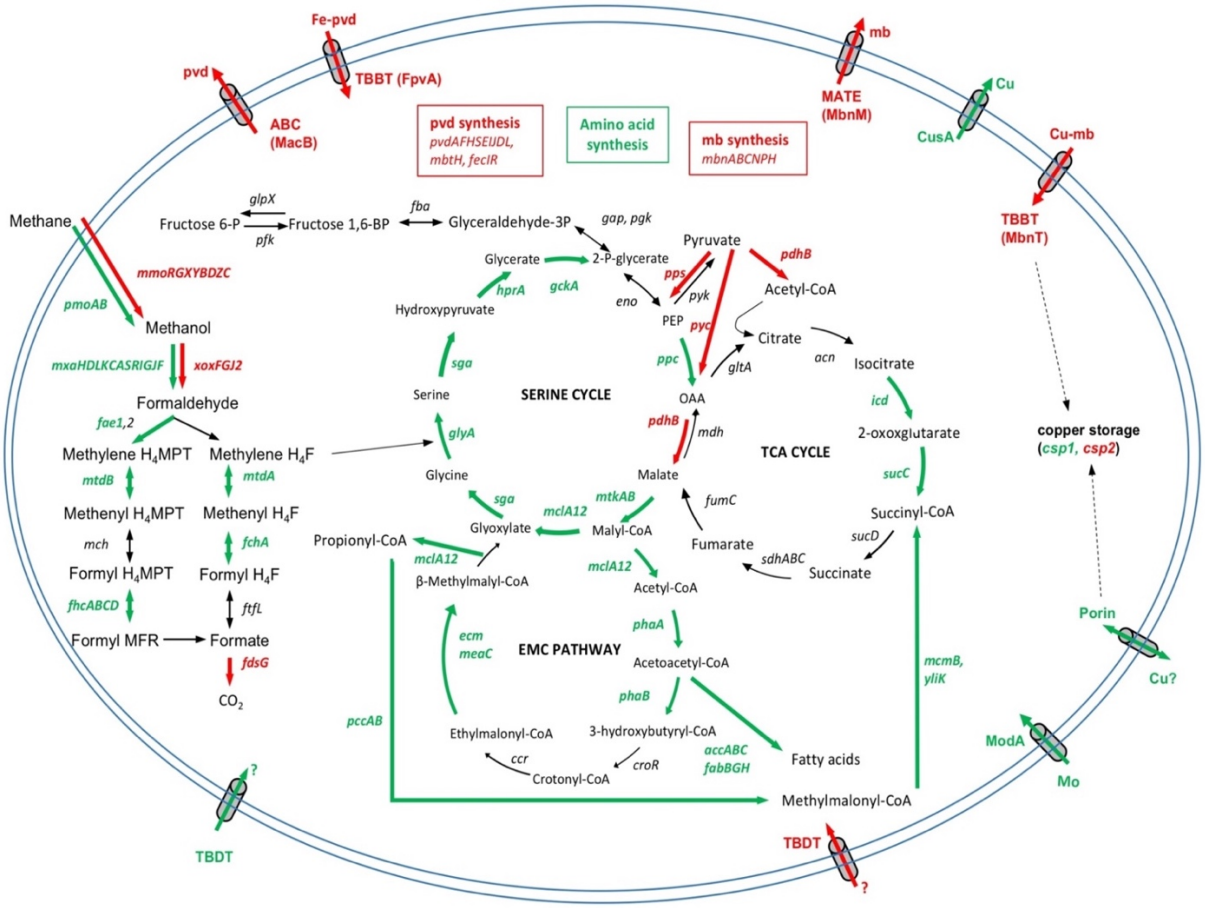

Figure 4.6. Central metabolism of *M. trichosporium* OB3b. Genes highlighted in green or red were significantly upregulated or downregulated, respectively, when *M. trichosporium* OB3b was grown in the presence of 10 µM copper + 25 µM cerium vs. in the presence of 0 µM copper + 25 µM cerium. (Green arrows indicate up-regulated genes, red arrows indicate down-regulated genes)

Table 4.6. Select genes differentially expressed in *M. trichosporium* OB3b grown with 10 µM copper + 25 µM cerium vs. 0 µM copper + 25 µM cerium.
(Benjamini-Hochberg-adjusted p-value < 1 x10^{-3}, $|\log_2| > 1.5$)

Function	Gene/Locus number
Up-regulated	
Methane oxidation	*pmoAB12, mxaHDLKCASRIGJF, fae1, mtdAB, fchA, fhcABCD*
Carbon assimilation	*glyA, sga, hprA, gckA, ppc, mtkAB, mclA12, phaAB, ecm, meaC, pccAB, mcmB, yliK, sucC, icd*
Fatty acid synthesis	*accABC, fabBGH*
Ribosomal proteins and rRNA maturation	30S (*rpsOPIFDBKSCQNH*), 50S (*rplIMLYQAKDWBVPNXEFRT*, *rpmCDHI*) *rlmJ, rsmD, rim, era*
tRNA synthetase	*tyrS, thrS, pheT, hisS, valS, alaS, queA, gatA, mtaB, tsaD, truB*
Cellular division	*ftsEX, parAB*
Amino acid synthetases	*hisACGH, pro, glnA, trpE, leuB, thrB, leuD, argBFJH, serC, ilvC*
NADH-quinone oxidoreductase	*nuoBCDEFGHIJKLMN*
Vitamin synthesis	*cobDQTONWFBMLJIH*, *bioB*
ATP synthase	*atpCBGAFEB*
Transcription regulators	TetR-like regulator (ADVE02_v2_12329), *oxyR*
Copper storage protein	*csp1*(ADVE02_v2_12455)
Function	Gene/Locus number
Cobalamine synthesis	*cobDQTONWFBMLJIH*
Flagella synthesis	*flhB,* ADVE02_v2_11202

Table 4.6 Continued

Function	Gene/Locus number
Transporters	*secBFD, hppA, cscA, modA, cusA*
	TonB-dependent transporters (ADVE02_v2_10208, 10688, 13035, 14446, 14451),
	MATE-type exporter (mdtA),
	ABC-type transporters (ADVE02_v2_12321, 12556, *yejF*),
	RND-type exporters (ADVE02_v2_11509, 11510, 11574)
	Down-regulated
Soluble methane monooxygenase	*mmoRGXYBDZC*
Xox-type methanol dehydrogenase	*xoxFGJ2*
Methanobactin synthesis and transport	*mbnTABCMNPH*
Pyoverdine synthesis and transport	*pvdAFHSEIJDLL*, *fpvA* ,*fecIR, mbtH, macB*
Nitrogenase	*nifBHDENUW, frxA*
Hydrogenase	*hypDCFB, hybF, hupJHGF, hyaDCBA, hydA,* ADVE02_v2_10849
Transcription regulators	σ^{24} factors (ADVE02_v2_11827, 12264, 14394),
	σ^{54} factor (*mmoR*),
	σ^{70} factor (ADVE02_v2_13661, 30017),
Transcription regulators	FecRI-like proteins (ADVE02_v2_10212, 11296&11297, 13990, 14098, 14393),
	sigH, *fixJ, rpoH*,
	LuxR-like protein (ADVE02_v2_12868),
	TetR-like protein (ADVE02_v2_10058)

Table 4.6 Continued

Function	Gene/Locus number
Transporters	TonB-dependent transporters (*mbnT*, *fpvA*, ADVE02_v2_10030, 10151, 11295, 11307, 11411, 12266, 11588, 12284, 12822, 13641, 13988, 14392, 20043), MATE-type transporters (*mbnM*, ADVE02_v2_12268), ABC-type transporters (ADVE02_v2_12305, 30003, 30018, 30146), RND-type exporters (ADVE02_v2_11413, 30009), *actP* (copper transporting ATPase)

As found when copper was added in the absence of cerium (Table 4.3), if copper was added in the presence of cerium, it again appears that copper homeostasis must be carefully managed given that genes involved in copper uptake decreased (*mbnA*) while those involved in copper efflux and storage increased (*cusA* and *csp1*, respectively), and only a fraction of the added copper was associated with biomass (see below). Similarly, genes involved in pyoverdine synthesis decreased when copper was added in the presence of cerium, again suggesting that a copper-dependent iron uptake system may exist in methanotrophs.

Further, as found when comparing the transcriptomes of cultures grown with 0 μM copper + 0 μM cerium vs. 10 μM copper + 0 μM cerium, expression of genes encoding for 30S and 50S ribosomal proteins increased for cultures grown in the presence of 10 μM copper + 25 μM cerium vs. 0 μM copper + 25 μM cerium. In addition, expression of genes involved in the conversion of formaldehyde to biomass via the serine cycle and ethylmalonyl-CoA pathway were upregulated as were genes for amino acid, tRNA, fatty acid and cobalamin synthesis, amongst many others (Figure 4.6, Table 4.6). In the presence of copper and cerium, Mxa-and

Xox-MeDH were both expressed, and as such, *M. trichosporium* OB3b is likely converting methanol to formaldehyde more rapidly. In doing so, however, it appears that the cell is also increasing the rate at which formaldehyde is assimilated to control the buildup of this toxic intermediate. Interestingly, expression of the NAD-linked formate dehydrogenase decreased in the presence of both copper and cerium, suggesting that carbon flow to carbon dioxide via formate oxidation was reduced under these conditions.

Expression of nitrogenase genes also decreased when copper was added in the presence of cerium. The finding of reduced nitrogenase expression when cerium and copper are both present is intriguing as nitrogenase activity was not expected under any condition as nitrate mineral salts (NMS) medium containing 9.9 mM NO_3^- was used for all cultures, and it has been shown that *M. trichosporium* OB3b has no N_2-fixation activity in this medium (Murrell & Dalton, 1983). Others have shown, however, low expression of nitrogenase genes in *M. trichosporium* OB3b when grown in NMS medium amended with copper (Matsen et al., 2013). Our data support these findings, and further indicate that nitrogenase expression is most affected when both copper and cerium are present, for reasons as yet unknown.

Finally, hydrogenase expression significantly decreased in the presence of copper and cerium. It has been observed that several methanotrophs, including *M. trichosporium* OB3b, *Methylococcus capsulatus* Bath and *Methylomicrobium album* BG8 can generate significant amounts of H_2, with production dependent on the oxidation of formate to carbon dioxide (Hanczár et al., 2002, Kawamura et al., 1983). H_2 generation may be used to balance the ratio of NAD^+ to NADH by regenerating NAD^+ consumed during formate oxidation (Kawamura et al.,

1983). We speculate that in the presence of copper and cerium, carbon flux through the serine cycle and ethylmalonyl-CoA pathway increased, reducing carbon flow to carbon dioxide through formate, and this is supported by the finding of reduced expression of the NAD-linked formate dehydrogenase under these conditions (Figure 4.6). As a result, there was reduced formate oxidation and subsequent formation of NADH, decreasing the need to generate H_2 to balance NAD^+: NADH ratios. It would be interesting to examine the proteome and metabolome of *M. trichosporium* OB3b under varying amounts of copper and cerium to determine if this indeed the case, but such experiments are beyond the scope of this research.

IV.2.3 RT-qPCR confirmation of differential gene expression

To confirm RNA-Seq findings that genes encoding for alternative MMOs (sMMO vs. pMMO), MeDHs (Mxa-MeDH vs Xox-MeDH), metal uptake systems (methanobactin and pyoverdine) and nitrogenase varied in response to varied concentrations of copper or cerium, more focused and accurate RT-qPCR assays of the following genes were performed: *mmoX* and *pmoA* (sMMO/pMMO)*, mxaF, xoxF1* and *xoxF2* (Mxa-MeDH/Xox-MeDH), *mbnA* and *pvdF* (methanobactin/pyoverdine), and *nifH* (nitrogenase). Three genes - *rrs* (16s rRNA), *clpX*, (a subunit of a ClpX-ClpP ATP-dependent serine protease), and *yjg* (a permease of the YjgP/YjgQ family) - were used as internal references. These were chosen as *rrs* was found earlier to be appropriate (Kalidass, et al., 2015; Farhan UI Haque et al., 2015; Gu et al., 2016), and expression of *clpX* and *yjg* were observed to be invariant under the growth conditions described examined here, i.e., $\log_2$ expression changes < 0.05 as determined via RNASeq. New primers were designed (Table 4.2) and calibration curves were measured as shown in Figure 4.7. Figure 4.8

shows changes in gene expression when the geometric mean of all three reference standards was used; similar trends were found when any one reference gene was used (Figure 4.9-4.11).

As expected from RNA-Seq data, expression of *mmoX* and *mbnA* significantly decreased when copper was added, while *pmoA* expression increased, and such changes occurred regardless if cerium was present or not ($p < 0.05$; Figure 4.7). Further, expression of *xoxF1* increased when cerium was added both in the absence and presence of copper. *mxaF* expression only decreased when cerium was added in the absence of copper (Figure 4.7, $p < 0.05$). *nifH* expression was also found to decrease in the presence of both copper and cerium as compared in the absence of both metals or in the presence of cerium only, i.e., there was no difference in *nifH* expression for *M. trichosporium* OB3b grown with 10 μM copper + 0 μM cerium and 10 μM copper + 25 μM cerium. Finally, *pvdF* was also found to be upregulated when cerium was added, but only in the absence of copper. Interestingly, RT-qPCR indicated that *pvdF* expression decreased slightly when copper was added but no significant changes were observed in the RNA-Seq data (Figure 4.7). Collectively the RT-qPCR data support the RNA-Seq data in that copper and cerium differentially affected gene expression in *M. trichosporium* OB3b.

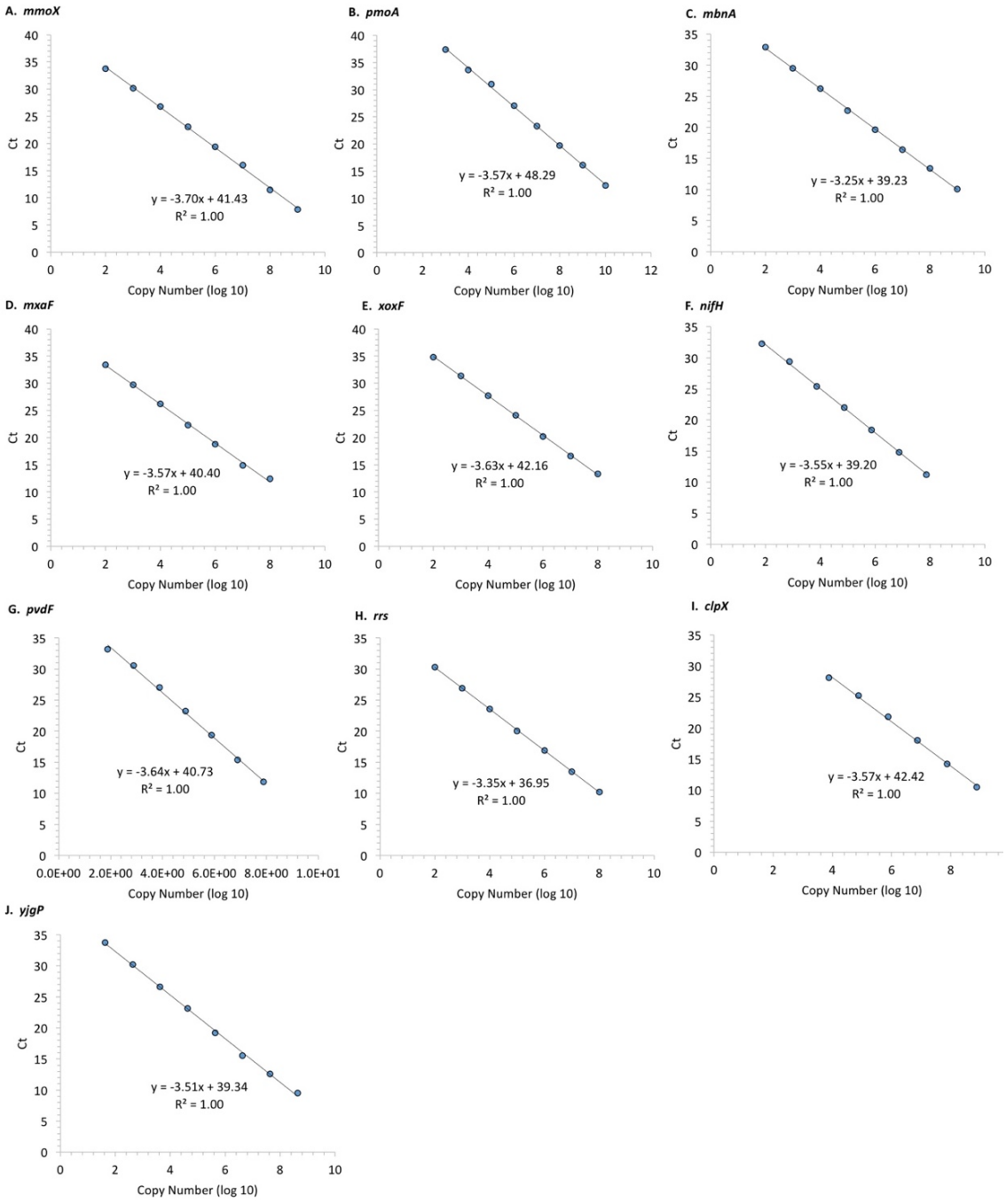

Figure 4.7. Calibration curves for qRT-PCR

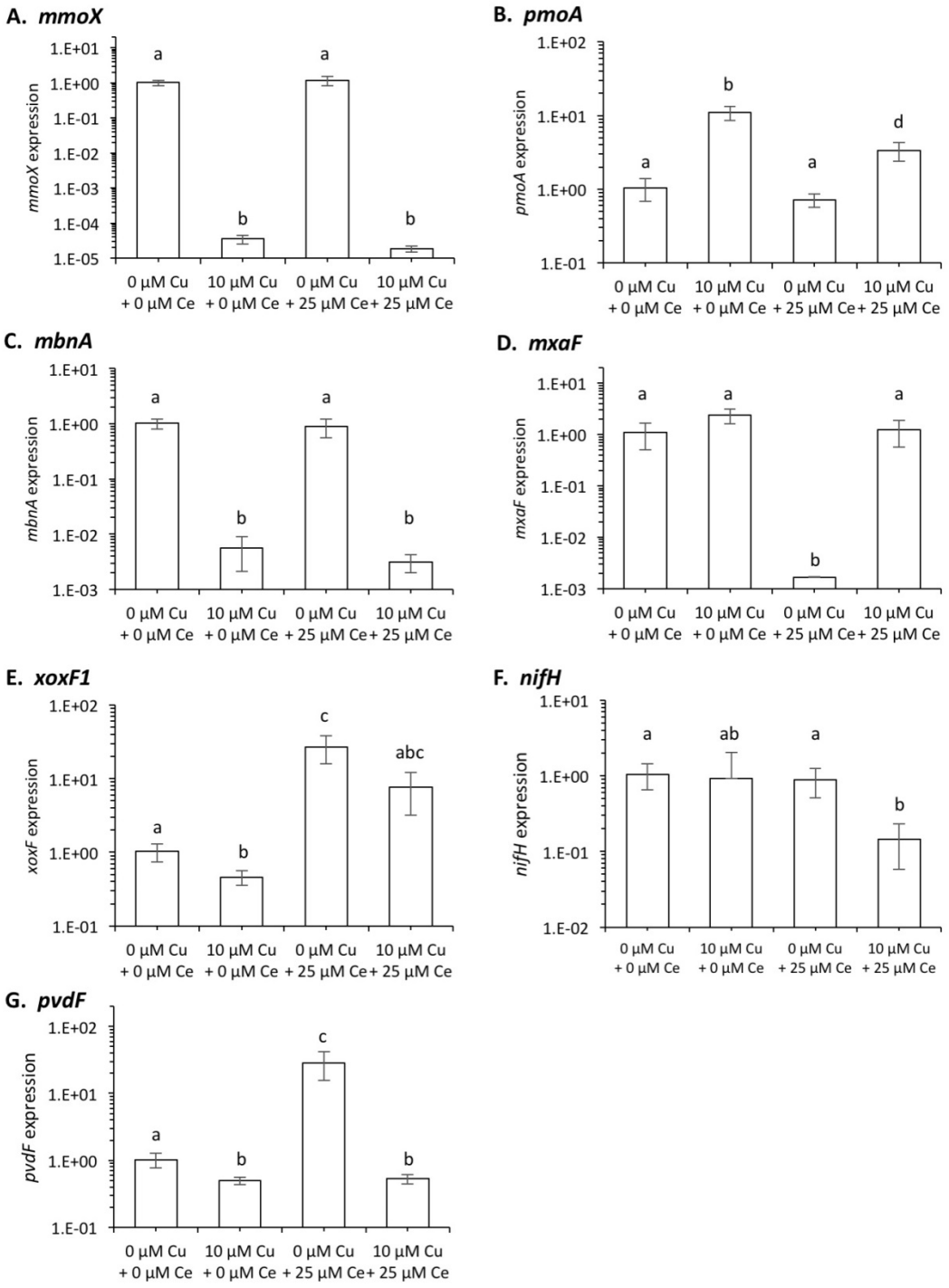

Figure 4.8. qRT-PCR using geometric mean of all reference genes for normalization. Each bar represents average of triplicate cultures; error bars represent standard deviation. Bars within each plot labeled by different letters are significantly different ($P < 0.05$).

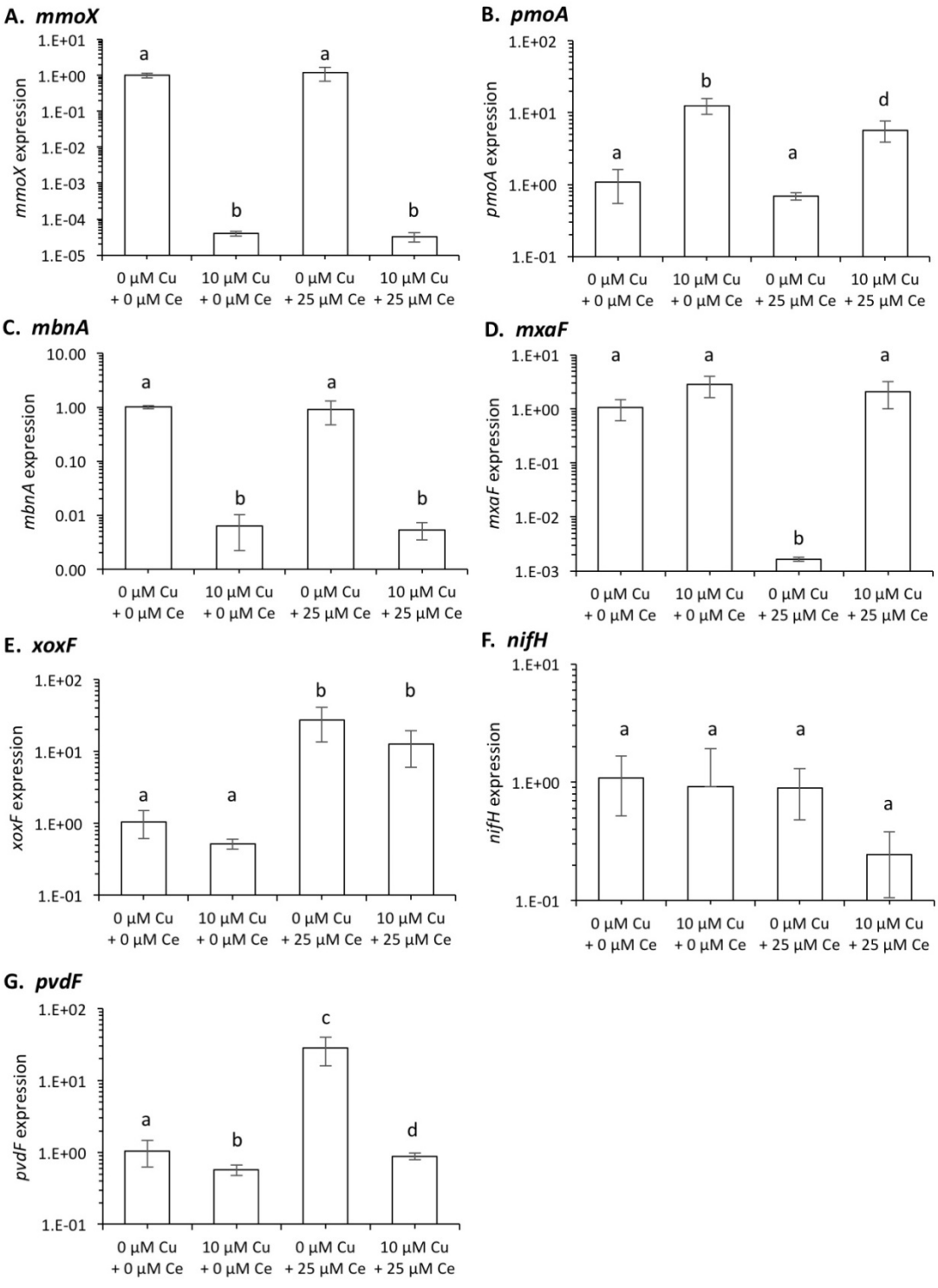

Figure 4.9. RT-qPCR using reference gene *rrs*

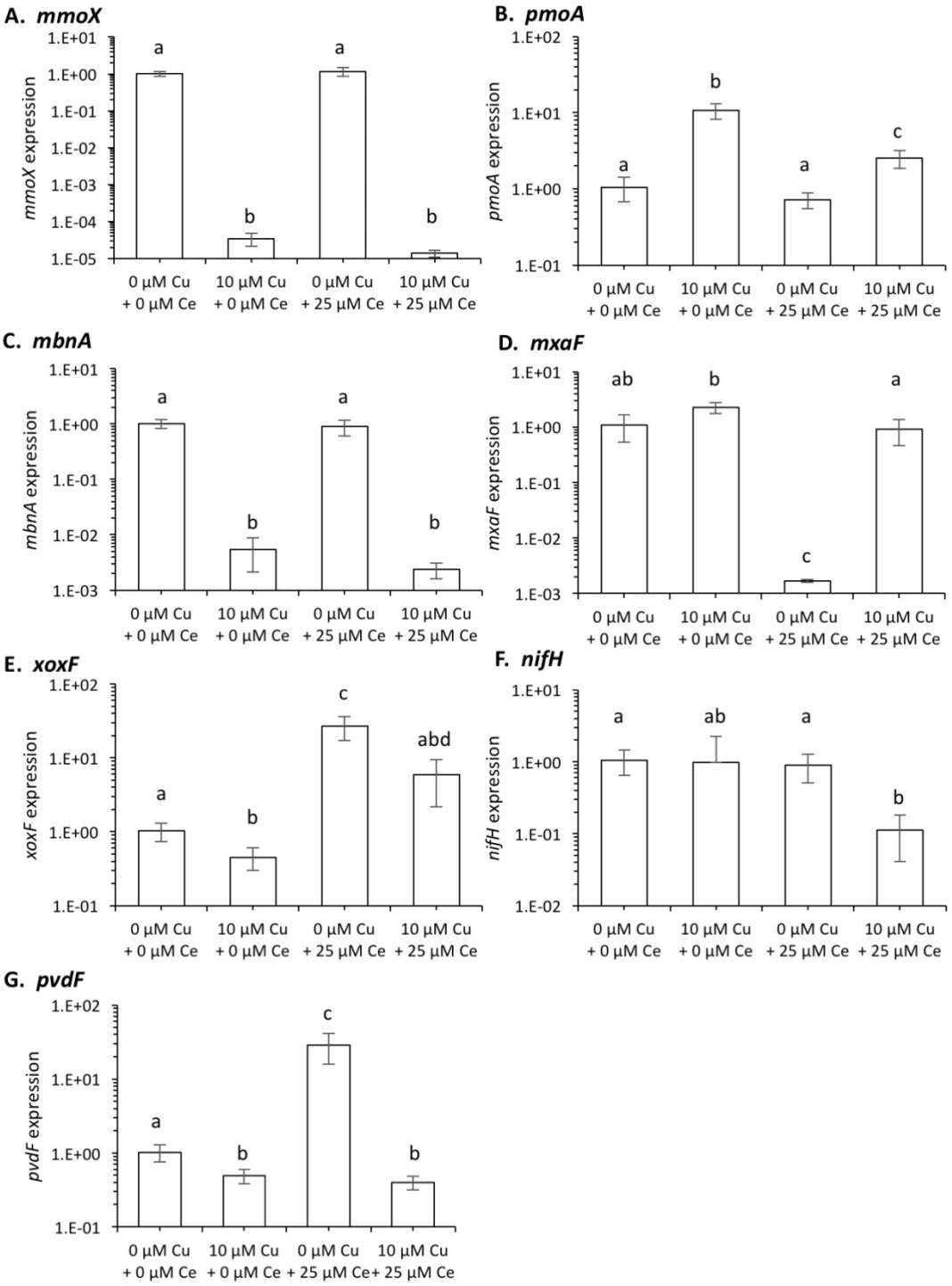

Figure 4.10. RT-qPCR using reference gene *clpX*

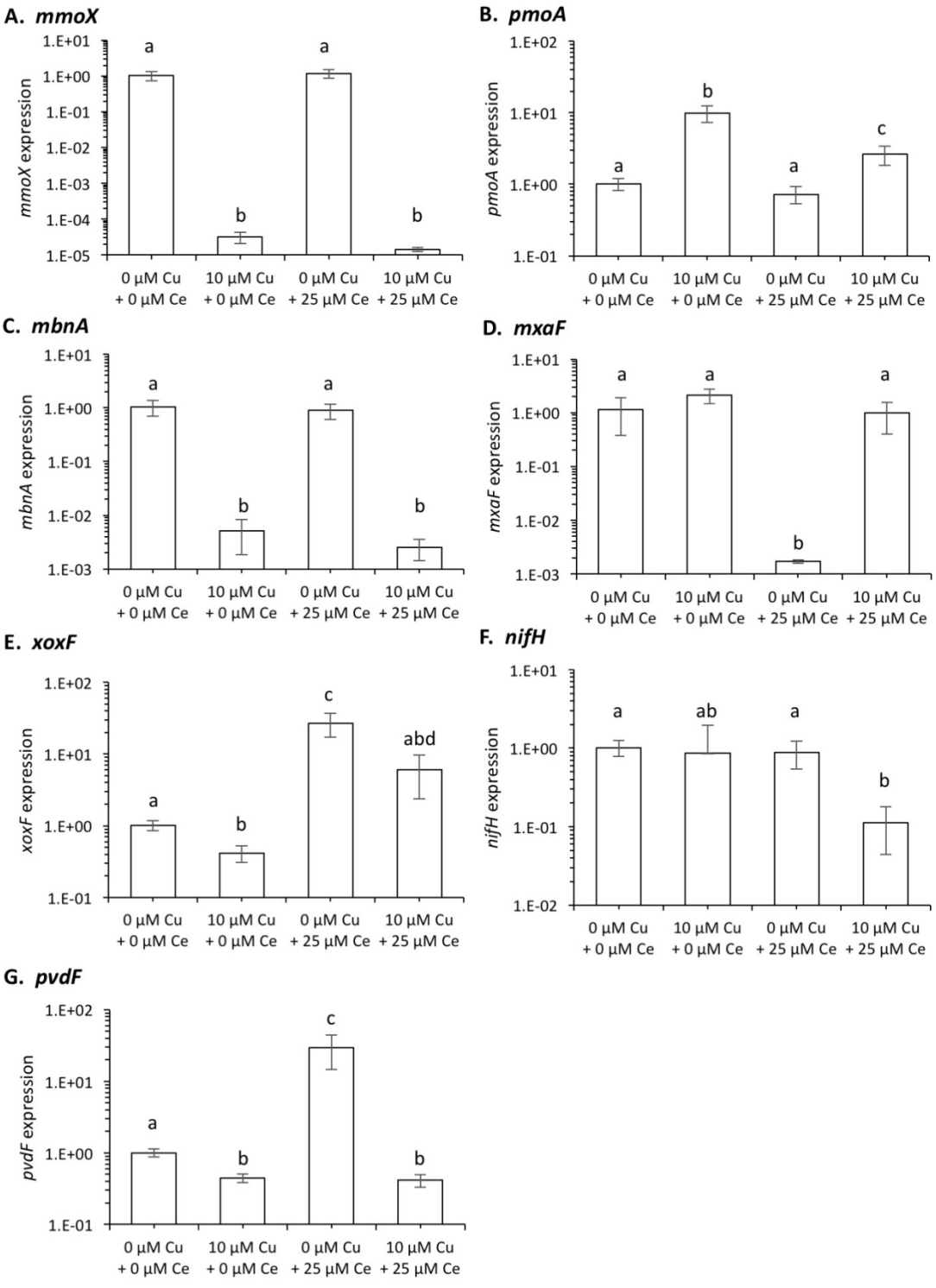

Figure 4.11. RT-qPCR using reference gene *yjpG*

IV.2.4 Metal analysis

Metal (including copper, cerium, and iron) associated with cells were measured by ICP-MS. When copper was added as $CuCl_2$, the amount of copper associated with biomass increased by ~70-fold, and copper uptake was ~50% greater in the presence of cerium than in its absence (Figure 4.12, $p < 0.05$). When 10 μM copper was added, however, only 10-15% of the added copper was found to be cell-associated, indicating that *M. trichosporium* OB3b has active mechanisms to regulate copper homeostasis, i.e., differential expression of genes involved in copper uptake (e.g., *mbnA*), copper storage (*csp1*), and efflux (*cusA*) was observed under different growth concentrations of copper (see above).

Unlike, copper, when cerium was added as $CeCl_3$, the majority of cerium was found to be cell-associated (~90%), suggesting that cerium is not toxic. Further, copper did not have any measurable effect on cerium uptake ($p > 0.05$), indicating that copper and cerium uptake are mediated by independent systems.

Iron uptake, however, was affected by the presence of copper (Figure 4.12). Iron associated with biomass increased ~ 2.5-fold when copper was increased from 0 (no added) to 10 μM ($p < 0.05$), suggesting that there may be a copper-dependent iron transport system in *M. trichosporium* OB3b. At this time, it is unclear what this uptake mechanism may be, but it is tempting to speculate that as multi-copper oxidases have been shown to serve as iron transporters in other bacteria (Dubbels et al., 2004; Huston et al., 2002), a similar mechanism may be utilized here. There is one annotated multi-copper oxidase in the genome of *M. trichosporium* OB3b (locus tag ADVE02_v2_10748), but expression of this oxidase did not change significantly with respect to

copper (data not shown). Thus, we hasten to stress that the role (if any) of this gene product in iron uptake is unclear. When one considers this uncertainty, and that many genes encoding for proteins of unknown function also had differential expression when copper was added, it is evident that much more work is required to determine how copper may enhance iron uptake in methanotrophs. Finally, cerium had no significant effect on iron uptake, either in the absence or presence of copper (Figure 4.12, $p > 0.05$), suggesting that cerium uptake is independent of iron uptake.

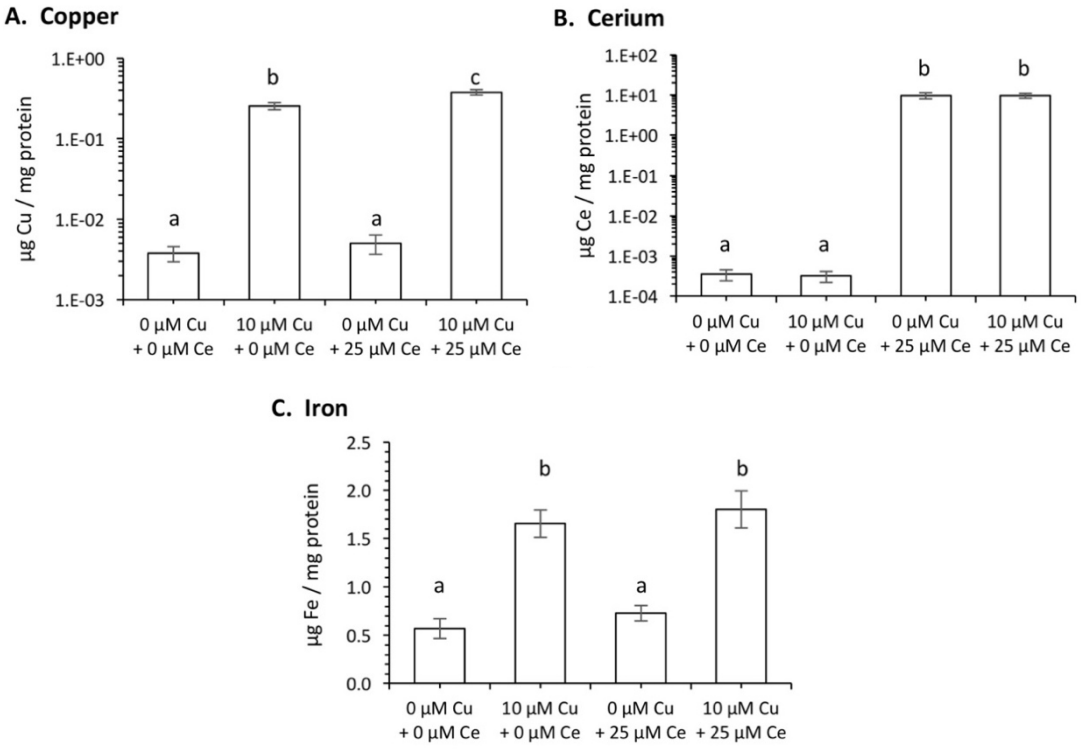

Figure 4.12. Metal associated with biomass.

IV.2.5 Discussion

We here investigate how the transcriptome of *M. trichosporium* OB3b varies in response to copper and cerium. These metals were chosen as it has been found that they control expression of key parts of methanotrophic metabolism, i.e., genes encoding for methane and methanol

oxidation, respectively (Choi, et al., 2003; Nielsen, et al., 1996, 1997). Interestingly, copper and cerium affected the expression of other genes, but such control was strongly dependent on if both metals were present.

In the absence of cerium, copper affected expression of genes encoding for sMMO, pMMO and methanobactin, as found earlier using more focused RT-qPCR assays (Semrau, et al., 2013; Farhan Ul Haque, et al., 2015; Gu, et al., 2016). Interestingly, although copper is an important component of methanotrophic metabolism, these microbes (like others) appear to carefully regulate the distribution and amount of copper *in vivo*. That is, only a fraction of the added copper was found to be cell-associated and expression of *mbn* genes (responsible for methanobactin synthesis) decreased in the presence of copper while expression *csp1* and *cusA* (encoding for a copper storage protein and a copper efflux system respectively) increased. Such data indicate that *M. trichosporium* OB3b actively controls the amount of copper *in vivo*, and suggests that methanotrophs have a complex, interconnected system whereby copper uptake, storage, and excretion pathways are tightly coupled to effectively utilize copper while minimizing its toxicity.

In addition to genes involved in methane oxidation and copper homeostasis being differentially expressed in the absence/presence of copper, genes encoding for ribosomal proteins had increased expression when copper was added. Many genes encoding for proteins of unknown function also had differential expression when copper was added, indicating the transcriptome of *M. trichosporium* OB3b is "tuned" to the availability of copper. Such a response may explain earlier findings that methanotrophic growth yields increase with increasing copper (Leak and

Dalton, 1986). It should be noted, however, that overall growth rates of *M. trichosporium* OB3b, however, do not change significantly with respect to copper (Farhan Ul Haque, et al., 2015). Thus it appears that changes in the transcriptome with respect to copper enable methanotrophs to enhance the efficiency of methane utilization, but does not alter the overall rate at which methane is converted into biomass.

Interestingly, in addition to changes in the transcriptome of *M. trichosporium* OB3b to the absence/presence of copper, significantly more iron was associated with biomass when copper was added (Figure 4.12), suggesting that there may be a copper-dependent iron transport system in *M. trichosporium* OB3b. At this time, it is unclear what this uptake mechanism may be, but it is tempting to speculate that as multicopper oxidases have been shown to serve as iron transporters in other bacteria (Dubbels, et al., 2007; Huston, et al., 2002), a similar mechanism may be utilized here. There is one annotated multicopper oxidase in the genome of *M. trichosporium* OB3b (locus tag ADVE02_v2_10748), but expression of this oxidase did not change significantly with respect to copper (data not shown). Thus, we hasten to stress that the role (if any) of this gene product in iron uptake is unclear. When one considers this uncertainty, and that many genes encoding for proteins of unknown function also had differential expression when copper was added, it is evident that much more work is required to determine how copper may enhance iron uptake in methanotrophs.

When cerium was varied in the absence of copper, expression of fewer genes was observed to vary as compared to when copper was varied in the absence of cerium, suggesting that cerium (and by extension other REEs) plays a less significant role in methanotrophic metabolism than

copper. Besides genes encoding for Xox-MeDH increased in expression, while those encoding for Mxa-MeDH had lower expression when cerium was added in the absence of copper, the finding of increased expression of pyoverdine synthesis genes in the presence of cerium, however, is novel and unexpected. Typically, expression of metal uptake systems increases with decreasing metal availability, suggesting that pyoverdine synthesis increased when cerium was added as this may have limited iron uptake. Iron speciation at equilibrium, however, was not significantly different in the absence vs. presence of cerium (Table 4.7), nor was the amount of iron associated with biomass appreciably different for *M. trichosporium* OB3b grown with either 0 μM copper + 0 μM cerium or 0 μM copper + 25 μM cerium (Figure 4.12). This suggests that increased pyoverdine synthesis when *M. trichosporium* OB3b was grown with 0 μM copper + 25 μM cerium was not due to iron limitation, but to a different stress. Remarkably, cerium, in addition to iron, can act as a catalyst to activate H_2O_2 via a Fenton-like mechanism (Bokare & Choi, 2014; Heckert, et al., 2008). That is, cerium can generate free radicals from the activation of H_2O_2 as follows:

$$Ce^{3+} + H_2O_2 \rightarrow Ce^{4+} + HO\bullet + OH^- \quad (1)$$

$$Ce^{4+} + H_2O_2 \rightarrow Ce^{3+} + HO_2\bullet + H^+ \quad (2)$$

Given that cerium can also serve as a Fenton reagent, it is possible that pyoverdine synthesis increased to limit free radical formation by reducing the free ion concentration of cerium. We cannot state with any certainty if this indeed the case, but it suggests that in addition to copper, methanotrophs must carefully control the speciation and distribution of cerium to effectively utilize use it in methanol oxidation while limiting its (possible) toxicity. We would like to highlight that this hypothesis implicitly assumes that pyoverdine binds cerium to such a degree that that it can alter cerium speciation. To the best of our knowledge, however, the affinity of

pyoverdine or any other siderophore to bind cerium has not been measured. It has been observed though, that siderophores can mobilize rare earth elements from igneous materials (Kraemer, et al., 2015; Bao, et al., 2013), suggesting that these biogenic chelating agents can bind rare earth elements in complex situations. Expression of pyoverdine, however, decreased when copper was added in addition to cerium, indicating that if cerium toxicity can be an issue, it was only important in the absence of copper.

Table 4.7. Predicted speciation of copper, iron, and cerium at equilibrium for all conditions as determined using Visual Minteq v3.1 (Gustafsson, 2011).

Component	Species name	% of total concentration			
		0 µM Cu + 0 µM Ce	10 µM Cu + 0 µM Ce	0 µM Cu + 25 µM Ce	10 µM Cu + 25 µM Ce
Fe^{3+}	$Fe_2(OH)_2(EDTA)_2^{4-}$	$4.5x10^{-2}$	$1.3x10^{-2}$	$4.5x10^{-2}$	$1.2x10^{-2}$
	$FeOH^{2+}$	0.0	$4.1x10^{-2}$	0.0	$4.1x10^{-2}$
	$Fe(OH)_2^+$	8.2	50	8.3	50
	$Fe(OH)_3$ (aq)	$5.0x10^{-2}$	$3.0x10^{-1}$	$5.0x10^{-2}$	$3.0x10^{-1}$
	$Fe(OH)_4^-$	$2.0x10^{-2}$	$1.2x10^{-1}$	$2.0x10^{-2}$	$1.2x10^{-1}$
	$FeHPO_4^+$	$2.1x10^{-1}$	1.3	$2.1x10^{-1}$	1.3
	$FeEDTA^-$	71	38	71	38
	$Fe(OH)EDTA^{2-}$	20	11	20	11
Cu^{2+}	Cu^{2+}	ND	5.7	ND	5.7
	$CuOH^+$	ND	1.4	ND	1.4
	$Cu(OH)_2$ (aq)	ND	$3.1x10^{-2}$	ND	$3.1x10^{-2}$
	$Cu_2(OH)_2^{2+}$	ND	$1.7x10^{-2}$	ND	$1.7x10^{-2}$
	$CuCl^+$	ND	$1.9x10^{-2}$	ND	$1.9x10^{-2}$
	$CuSO_4$ (aq)	ND	1.1	ND	1.1
	$CuNO_3^+$	ND	$8.7x10^{-2}$	ND	$8.8x10^{-2}$
	$CuHPO_4$ (aq)	ND	34	ND	34
	$CuEDTA^{2-}$	ND	58	ND	58
	$CuHEDTA^-$	ND	$1.1x10^{-2}$	ND	$1.1x10^{-2}$
Ce^{3+}	Ce^{3+}	ND	ND	$2.3x10^{-1}$	$2.3x10^{-1}$
	$Ce(SO_4)^{2-}$	ND	ND	$2.5x10^{-2}$	$2.5x10^{-2}$
	$CeSO_4^+$	ND	ND	$4.8x10^{-1}$	$4.8x10^{-1}$
	$CeH_2PO_4^{2+}$	ND	ND	$2.9x10^{-2}$	$2.9x10^{-2}$
	$CePO_4$ (aq)	ND	ND	99	99
	$CeEDTA^-$	ND	ND	$7.8x10^{-2}$	0.0

If copper was varied in the presence of cerium, expression of many genes was found to be affected (Figure 4.6; Table 4.6). As found when copper was varied in the absence of cerium, *cusA*, *pmo*, ribosomal protein genes and the gene encoding for a copper storage protein increased when copper was added in the presence of cerium. Expression of *mxa* genes and genes encoding for ATP synthases were also found to have increased expression when copper was added in the presence of cerium. Many steps for the conversion of formaldehyde to formate and biomass were also found to increase when copper was added in the presence of cerium, likely due to both Mxa- and Xox-MeDH being expressed. As such, in the presence of both copper and cerium, *M. trichosporium* OB3b appears to be able to more rapidly convert methanol to formaldehyde, but in so doing must also increase the rate at which formaldehyde is converted to either formate or assimilated into biomass to control the buildup of this toxic intermediate. It would be interesting to examine the proteome and metabolome of *M. trichosporium* OB3b under varying amounts of copper and cerium to determine if this indeed the case, but such experiments are beyond the scope of this research. Further, expression of nitrogenase and hydrogenase also decreased when both copper and cerium were present as opposed to just cerium. With the data presented here, we cannot state with any certainty as why expression of these systems would decrease, although it may be that enhanced growth efficiency is partly due to enhanced utilization of nitrogen, reducing the need for fixing nitrogen to meet growth requirements. In any event, the growth rate of *M. trichosporium* OB3b did not appreciably change when copper was varied in the presence of cerium (Farhan Ul Haque, et al., 2015), suggesting that the observed changes in gene expression *in M. trichosporium* OB3b do not translate to significant changes in the overall rate of growth.

IV.2.6 Conclusion and future perspectives

We show herein that both copper and cerium affect the expression of many genes in *M. trichosporium* OB3b, but that the greatest changes occurred when both metals were present. Such studies can be very informative for manipulating methanotrophic metabolism for the valorization of methane, considering that the presence of both copper and cerium may increase the rate of carbon assimilation in *M. trichosporium* OB3b. It would, however, be necessary to examine the proteome (and metabolome) of *M. trichosporium* OB3b under varying amounts of copper and cerium to determine if this is indeed the case. This study could also be extended with targeted physiological characterizations, which include measuring the rate of methanol oxidation and the activities of nitrogenase and hydrogenase in *M. trichosporium* OB3b under varying amounts of copper and cerium to verify some of the observations.

CHAPTER V INVESTIGATION OF ALTERNATIVE COPPER-UPTAKE MECHANISMS

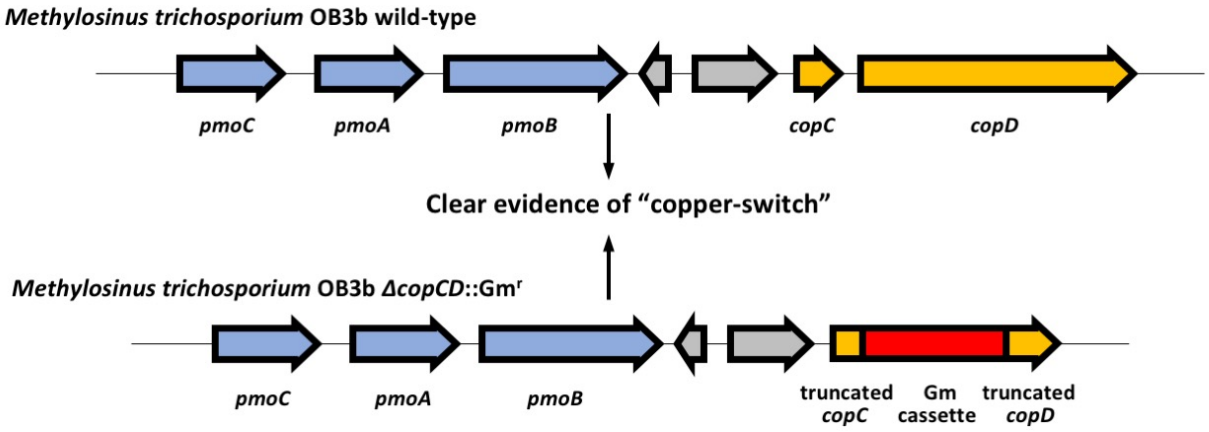

Figure 5.0 Elucidation of the role of CopCD in *M. trichosporium* OB3b

Accepted:

Characterization of the role of *copCD* in copper uptake and the "copper-switch" in *Methylosinus trichosporium* OB3b, FEMS Microbiology Letters.

V.1 Introduction

There is of great interest to understand the basis of the "copper-switch" as this could be key for greater control of methanotrophic activity, and thus for the valorization of methane. Currently, there are conflicting models for this switch. One model, proposed by us, is based on *mmoD*, a gene within the operon for the soluble methane monooxygenase (*mmo* operon). In prior work, it

was shown that when *mmoD* was knocked out in the methanotrophic type strain, *Methylosinus trichosporium* OB3b, expression of pMMO was inverted as compared to *M. trichosporium* OB3b wildtype, i.e., pMMO expression in the mutant was highest in the absence of copper and decreased with the addition of copper (Semrau et al., 2013). In this mutant, however, not only was *mmoD* deleted, so were genes encoding for polypeptides of sMMO. As such, independent assessment of sMMO expression was not possible. Subsequently, Yan et al., (2016) selectively removed *mmoD* from *Methylomicrobium buryatense* 5GB1C. In this mutant, no sMMO activity or expression was observed in the absence of copper, supporting our hypothesis that MmoD is a transcriptional activator for the sMMO operon.

Others disagree with this hypothesis. It has been reported that MmoD, when expressed and purified from *E. coli* does not bind either copper or DNA (Kenney et al., 2016). Instead, it has been suggested that *copD*, encoding for a copper importer may be involved in copper uptake and/or the copper switch in methanotrophs (Keeney et al., 2016). The rationale for this hypothesis was developed by comparing the genome of *M. trichosporium* OB3b wildtype to that of a mutant generated via random chemical mutagenesis that constitutively expressed sMMO (smmoC) in the presence of copper. Interestingly, the smmoC mutant did not collect copper, suggesting that the phenotype of this mutant was due to specific lesions in genes involved in copper uptake. Several differences were observed, perhaps most notably *copD* in smmoC has a 22 bp-deletion (Figure 5.1). *copD*, encoding for an inner membrane protein, has been found to be involved in copper uptake in other bacteria, and is commonly in an operon with *copC*, encoding for a periplasmic copper binding protein (Cha & Cooksey, 1993; Koay et al., 2005; Wijekoon et al., 2015). Thus it was speculated that *copD* may play a critical role in the "copper-switch"

and/or copper homeostasis in methanotrophs. Both conclusions are somewhat controversial, given that independent laboratories conclude MmoD is involved in the copper switch, and the role of methanobactin, a well-characterized copper binding agent shown to be important for copper uptake (Gu, et al., 2016) is not explicitly considered in this model. Here we describe the phenotype of specific mutants to elucidate the role of *copD* in both copper uptake and the "copper-switch" in *M. trichosporium* OB3b.

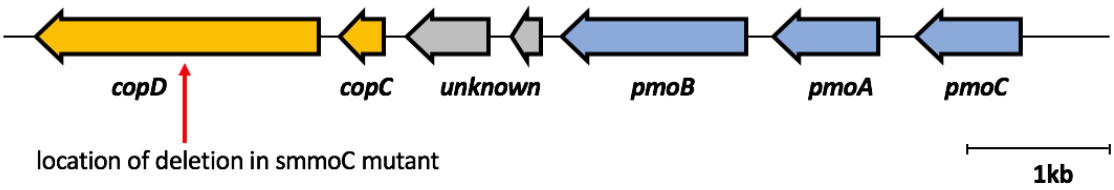

Figure 5.1. Gene arrangement of *copCD* in *M. trichosporium* OB3b.

V.2 Characterization of copCD::Gm^r and ΔmbnAN copCD::Gm^r

Using marker exchange mutagenesis, *copCD* from wildtype *M. trichosporium* OB3b and the Δ*mbnAN* mutant (Gu et al., 2017) was knocked-out creating *copCD*::Gm^r and Δ*mbnAN copCD*::Gm^r. The mutants are gentamicin-resistant, indicating successful insertion of the Gm cassette, and kanamycin-sensitive and sucrose-resistant, showing loss of the plasmid backbone. The genotypes of these mutants were verified by PCR (Figure 5.2) and Sanger sequencing.

The phenotype of the *copCD*::Gm^r and *mbnAN copCD*::Gm^r mutants were compared to that of wild-type *M. trichosporium* and the Δ*mbnAN* mutant. When grown in the presence of either 0 (no added) or 1 μM copper, all strains had similar amounts of copper associated with biomass (Figure 5.3). Further, gene expression in all three mutants, as well as in *M. trichosporium* OB3b wildtype showed clear evidence of the copper switch (Figure 5.4). Specifically, in the presence

of 1 μM copper, expression of *mmoX* decreased by several orders of magnitude as compared to when no copper was added. Further, *pmoA* expression increased by about an order of magnitude when copper was added. Interestingly, *mmoX* expression was slightly (but significantly) higher in the *copCD*::Gm^r and Δ*mbnAN copCD*::Gm^r mutants as compared to wildtype *M. trichosporium* and the Δ*mbnAN* mutant in the presence of 1 μM copper. It should be noted, however, that in the presence of copper *mmoX* expression was low for any strain, i.e., < 0.1 transcripts per gene copy number. Further, no sMMO activity was observed for any strain in the presence of copper as determined via the naphthalene assay (Brusseau, et al., 1990) (Figure 5.5). This strongly suggests that CopCD alone is not the cause of constitutive sMMO activity in the smmoC mutant.

To determine if expression of *copCD* was affected by the availability of copper, expression of both *copC* and *copD* was monitored via RT-qPCR. The qPCR calibration curves for *copCD* are presented in Figure 5.6. Expression of *copC* and *copD* did not change with increasing copper in wildtype *M. trichosporium* OB3b. *copC* and *copD* expression did increase slightly (~1.5-fold; $p < 0.05$) in Δ*mbnAN* with increasing copper, but expression was in any case very low (< 0.1 transcripts per gene copy number) (Figure 5.7).

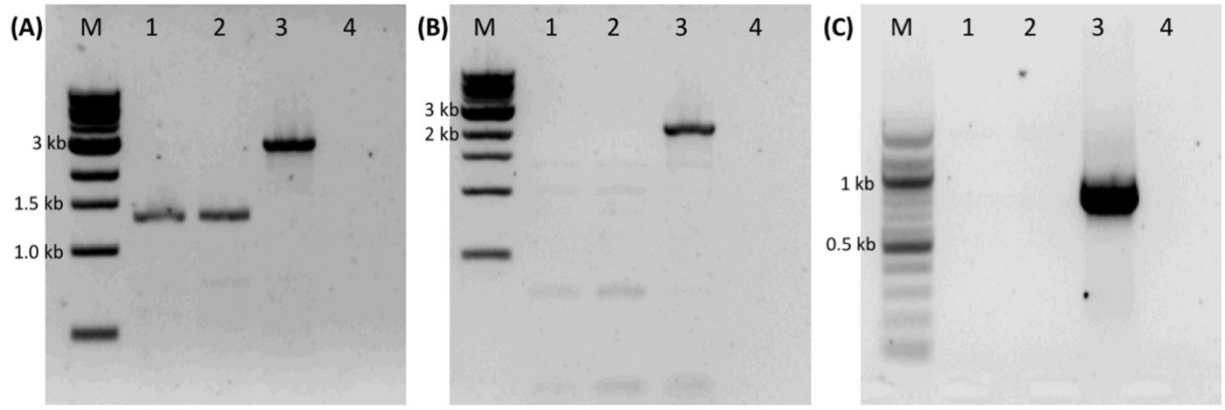

Figure 5.2. Knockout of *copCD* in *M. trichosporium* OB3b *copCD::*Gm^r and Δ*mbnAN copCD::*Gm^r mutants. (A) PCR products amplified using primers *copCD*_F/R from Lanes 1- *M. trichosporium* OB3b *copCD::*Gm^r (1.3 kb), 2 - Δ*mbnAN copCD::*Gm^r (1.3 kb), 3 – wildtype (2.8 kb), 4 - water (negative control); (B) using primers qcopC_FO/qcopD_RO from Lanes 1- *M. trichosporium* OB3b *copCD::*Gm^r, 2 - Δ*mbnAN copCD::*Gm^r, 3 - wildtype (2.1 kb), 4 - water (negative control); (C) PCR of plasmid backbone of pK18*mobsacB* from Lanes 1- *M. trichosporium* OB3b *copCD::*Gm^r, 2 - Δ*mbnAN copCD::*Gm^r, 3 - pK18*mobsacB* (0.8 kb, positive control), 4 - water (negative control)

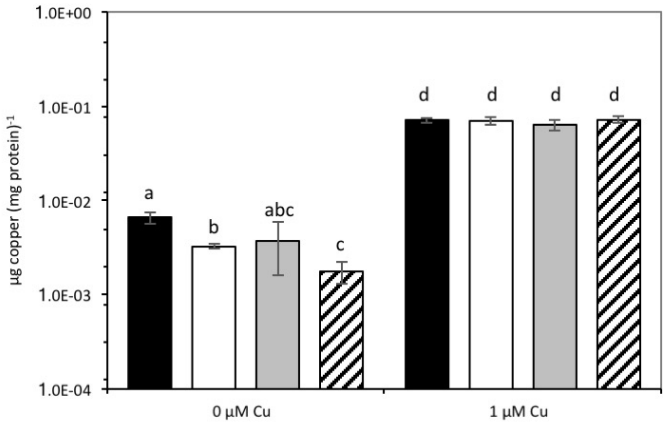

Figure 5.3. Copper associated with *M. trichosporium* OB3b wild type (black), Δ*mbnAN* (white), *copCD*::Gm^r (grey) and Δ*mbnAN copCD*::Gm^r (striped) grown in the presence of either 0 or 1 µM copper. Columns indicated by different letters are significantly different ($p < 0.05$)

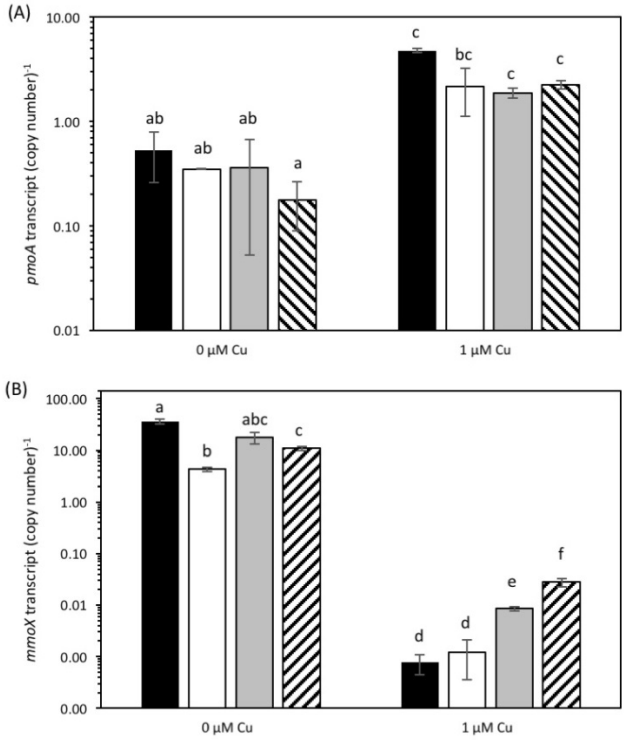

Figure 5.4. Expression of (A) *pmoA* and (B) *mmoX* in *M. trichosporium* OB3b wild type (black), Δ*mbnAN* (white), *copCD*::Gm^r (gray) and Δ*mbnAN copCD*:Gm^r (striped) grown in the presence of either 0 or 1 µM copper.

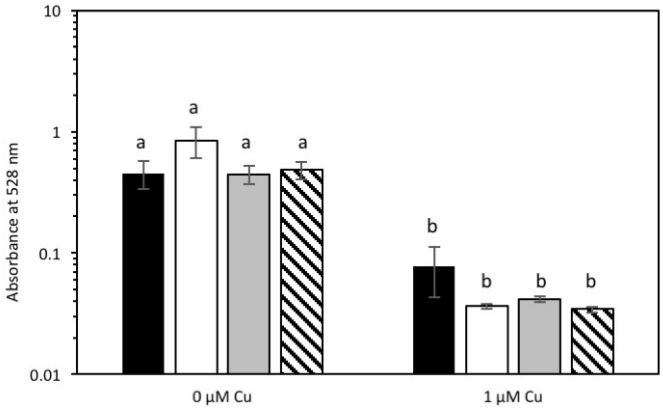

Figure 5.5. sMMO activities as determined via naphthalene oxidation. *M. trichosporium* OB3b wild type (black), Δ*mbnAN* (white), *copCD*::Gm^r (gray) and Δ*mbnAN copCD*::Gm^r (striped) grown in the presence of either 0 or 1 µM copper.

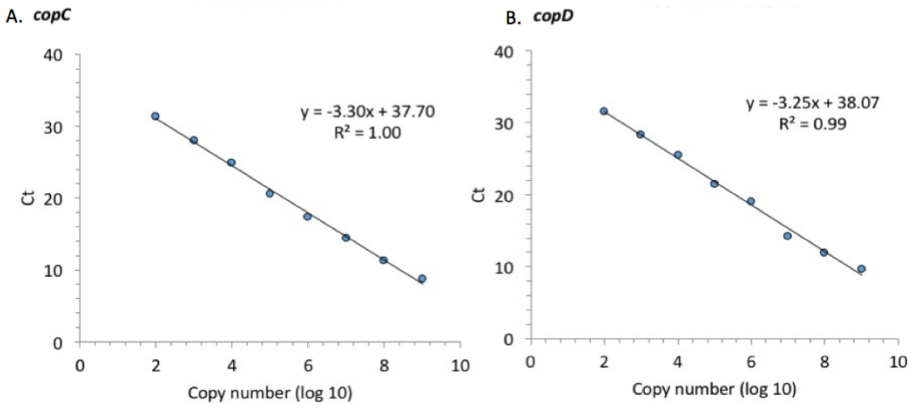

Figure 5.6. qPCR calibration curve for (A) *copC* and (B) *copD*

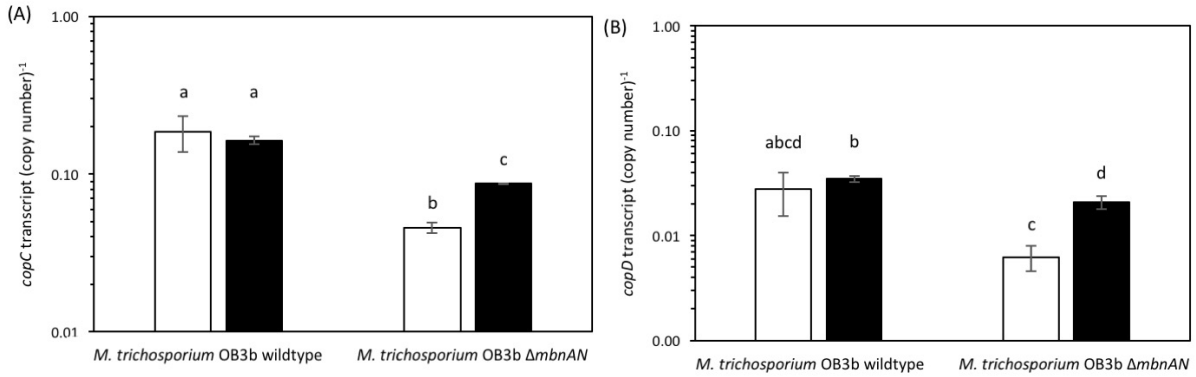

Figure 5.7. Expression of (A) *copC* and (B) *copD* in *M. trichosporium* OB3b wild type and Δ*mbnAN* grown at 0 μM (open) and 1 μM (filled) copper conditions.

V.3 Conclusion and future perspectives

Via genomic sequencing of a constitutive sMMO-expressing mutant created by Phelps et al. (1992), a 22 bp deletion in *copD* was observed by Keeney et al. (2016). Given that this mutant not only expresses sMMO in the presence of copper but also has reduced copper uptake as compared to *M. trichosporium* OB3b, it was speculated that CopD may be involved in both copper uptake and the "copper-switch" of *M. trichosporium* OB3b. To test these hypotheses, we constructed a specific knockout of *copCD* in both wildtype *M. trichosporium* OB3b and a previously constructed mutant where genes encoding for methanobactin synthesis were removed

(*ΔmbnAN*). All strains exhibited similar responses to copper, i.e., all strains were still able to sequester copper and all strains exhibited the copper switch. These data indicate that CopD likely does not play a role in the copper-switch. Further, as discussed earlier, it is apparent that in addition to methanobactin, methanotrophs have a second mechanism for copper uptake (Gu, et al., 2016; Balusabramian, et al., 2011). Given that the mutants defective in *copCD* still collected copper suggest that CopD and its partner CopC do not play a significant role in copper uptake, or that there is a third (unknown) mechanism by which *M. trichosporium* OB3b collects copper.

Further, we did not observe any changes in *copC* or *copD* expression with respect to copper in either wildtype *M. trichosporium* OB3b or the *ΔmbnAN* mutant. This is in contrast to the findings of Keeney, et al. (2016) where mild upregulation in the presence of copper was reported. We can not explain this difference, but the fact that at most mild increases have been observed in *copCD* gene expression in response to copper suggests that it may have a limited role in the copper-switch and/or copper uptake.

In conclusion, our selective knockout of *copCD* in *M. trichosporium* OB3b indicates that these genes, on their own, do not play a significant role in the "copper-switch". Further, if CopCD are involved in copper uptake, there is remarkable redundancy of copper uptake systems in *M. trichosporium* OB3b as copper uptake was observed when *copCD* was knocked out in either wildtype *M. trichosporium* OB3b or the *ΔmbnAN* mutant. Nonetheless, it is must be kept in mind that the smmoC mutant has no copper-switch. As such, it cannot be stated unequivocally that *copD* is not involved, but rather, the constitutive expression of sMMO in smmoC is likely due to a suite of mutations. In addition to the 22 bp deletion in copD, several other lesions were noted in

the genome of the smmoC mutant, including in two kinases that may (or may not) be involved in copper uptake/sensing, as well as several hypothetical proteins. It may be that these mutations in concert are responsible for the phenotype of the smmoC mutant

CHAPTER VI CONCLUSIONS AND FUTURE WORK

VI.1 Conclusions

The general objective of this study was to understand how various metals and methanobactin (mb) impact gene expression in the methanotrophic type strain, *Methylosinus trichosporium* OB3b. Such information is critical to enhance our ability to utilize methanotrophs for a suite of medical, industrial and environmental applications.

First, the uptake mechanism of methanobactin was investigated. The gene encoding the polypeptide precursor of mb, *mbnA*, is part of a gene cluster that also includes several genes encoding proteins of unknown function (but speculated to be involved in mb formation) as well as *mbnT*, which encodes a TonB-dependent transporter hypothesized to be responsible for mb uptake. A knockout of *mbnT* was constructed in *M. trichosporium* OB3b using marker exchange mutagenesis. The resulting *M. trichosporium mbnT*::Gm^r mutant was found to be able to produce mb but was unable to internalize it. Further, if this mutant was grown in the presence of copper and exogenous mb, copper uptake was significantly reduced. Expression of *mmoX* and *pmoA*, encoding polypeptides of the soluble methane monooxygenase (sMMO) and particulate methane monooxygenase (pMMO), respectively, also changed significantly when mb was added, which indicates that the mutant was unable to collect copper under these conditions. Copper uptake and gene expression, however, were not affected in wild-type *M. trichosporium* OB3b, indicating that the TonB-dependent transporter encoded by *mbnT* is responsible for mb uptake and that mb

is a key mechanism used by methanotrophs for copper uptake. When the *mbnT*::Gm^r mutant was grown under a range of copper concentrations in the absence of mb, however, the phenotype of the mutant was indistinguishable from that of wild-type *M. trichosporium* OB3b, indicating that this methanotroph has multiple mechanisms for copper uptake.

Second, to begin to elucidate the function of other genes in the mb gene cluster, we constructed an unmarked deletion of *mbnABCMN* in *Methylosinus trichosporium* OB3b and then homologously expressed *mbnABCM* using a broad-host-range cloning vector to determine the function of *mbnN*, annotated as coding for an aminotransferase. Methanobactin produced by this strain was found to be substantially different from wild-type methanobactin in that the C-terminal methionine was missing and only one of the two oxazolone rings was formed. Rather, in place of the N-terminal 3-methylbutanoyl-oxazolone-thioamide group, a leucine and a thioamide-containing glycine (Gly-Ψ) were found, indicating that MbnN is used for deamination of the N-terminal leucine of mb and that this posttranslational modification is critical for closure of the N-terminal oxazolone ring in *M. trichosporium* OB3b. Mb not only plays a key role in controlling methanotrophic activity, it has also been shown to be effective in the treatment of Wilson disease, an autosomal recessive disorder where the human body cannot correctly assimilate copper. Thus, it is important to characterize the mb biosynthesis pathway to understand how methanotrophs respond to their environment as well as to optimize the use of mb for the treatment of copper-related diseases such as Wilson disease.

Besides the genetic regulation of alternative forms of methane monooxygenases by copper, more recently, it has been discovered that *M. trichosporium* OB3b also has multiple types of methanol

dehydrogenase (MeDH), i.e. the Mxa-type MeDH (Mxa-MeDH) and Xox-type MeDH (Xox-MeDH), and the expression of these two forms is regulated by the availability of the rare earth element (REE), cerium (Farhan UI Haque, et al., 2016). We first extended these studies by showing that lanthanum, praseodymium, neodymium and samarium also regulate expression of alternative forms of MeDH. The effect of these REEs on MeDH expression, however, was only observed in the absence of copper. Further, a mutant of *M. trichosporium* OB3b, where the Mxa-MeDH was knocked out (Farhan UI Haque, et al., 2016), was able to grow in the presence of lanthanum, praseodymium and neodymium, but was not able to grow in the presence of samarium. Collectively, these data suggest that multiple levels of gene regulation by metals exist in *M. trichosporium* OB3b, but that copper overrides the effect of other metals by an as yet unknown mechanism.

To further investigate the effect of copper and REEs on gene expression in *M. trichosporium* OB3b, RNA-Seq analysis was performed to compare the transcriptome of *M. trichosporium* OB3b grown in the presence of varying amounts of copper and cerium. We found that when copper was added in the absence of cerium, expression of genes encoding for both soluble and particulate methane monooxygenases varied as expected. Genes encoding for copper uptake, storage, and efflux also increased, indicating that methanotrophs must carefully control copper homeostasis. When cerium was added in the absence of copper, expression of genes encoding for alternative methanol dehydrogenases varied as expected, but few other genes were found have differential expression. When cerium concentrations were varied in the presence of copper, few genes were found to be either up or downregulated, indicating that copper over rules any regulation by cerium. When copper was added in the presence of cerium, however, many genes

were upregulated, most notably multiple steps of the central methane oxidation pathway, the serine cycle, and the ethylmalonyl-CoA pathway. Such studies can be very informative for manipulating methanotrophic metabolism for the valorization of methane.

Lastly, efforts to further elucidate the molecular basis of "copper-switch" were made. Recently it was suggested via characterization of a mutant of *M. trichosporium* OB3b that expresses sMMO in the presence of copper (smmoC mutant) that the "copper-switch" may be based on *copCD* (Kenney et al., 2016). These genes encode for a periplasmic copper-binding protein and an inner membrane protein, and are used by other bacteria for copper uptake. Specific knockouts of *copCD* in *M. trichosporium* OB3b wildtype, however, show these genes are not part of the "copper-switch" in methanotrophs, nor do they appear to be critical for copper uptake. Rather, it appears that the constitutive expression of sMMO in the smmoC mutant of *M. trichosporium* OB3b may be due to multiple lesions as smmoC was generated via random chemical mutagenesis.

VI.2 Future work

From this study, it is evident that metals, copper and REEs, play a key role in regulating gene expression in *M. trichosporium* OB3b. However, much is unknown for developing a complete model for these "metal switches", particularly how they might be used to enhance methanotrophic applications. Future efforts should include, but are not limited to the following.

1. As shown in Figure 2.5 and Table 2.3, a series of methanobactin mutants have been created in *M. trichosporium* OB3b. By now, only the *mbnT*::Gm^r and *ΔmbnN* are

characterized. The phenotypes for other mutants will be investigated in the near future. Downstream of *mbnA*, there are *mbnB* and *mbnC*, two putative genes with no significant homologues in the current database. They are conserved in all identified mb gene clusters and are speculated to be involved in the maturation of mb. Thus, *ΔmbnB* and *ΔmbnC* mutants are expected to produce the mb precursor polypeptide while not modified as a mature product. Following *mbnC*, there is *mbnM* encoding for a multi-antimicrobial extrusion protein and is proposed to export mb out of cell. The *ΔmbnM* mutant may be able to synthesize a mature product of mb-OB3b but not secrete it out of the cell. Downstream of *mbnN* are *mbnP* and *mbnH*, encoding for a di-heme cytochrome c peroxidase homologue and its partner, respectively. Similar pairs of proteins are found in *M. capsulatus* Bath and *M. album* BG8 and are believed to be alternative copper sensing system (Berson & Lidstrom, 1997; Fjellbirkeland et al., 2001). The copper uptake of *M. trichosporium* OB3b *ΔmbnAH* mutant (*mbnABCMNPH* were all knocked out), however, does not seem to be affected (preliminary data not shown). It is thus proposed that MbnPH in the mb gene cluster are involved in the oxidation steps required for ring formation (DiSpirito et al., 2016). *ΔmbnPH* mutant may produce an immature form of mb.

2. Besides mb from *M. trichosporium* OB3b, there is also interest in studying the synthesis of mb in *Methylocystis* sp. strain SB2. The size of mb-SB2 (851 Da) is 30% less than mb-OB3b (1154 Da) (Figure 1.10). It may be a more effective treatment for Wilson disease as it may enter the cells more easily (Lichtmannegger J, et al. 2016). To study the synthesis pathway of mb-SB2, one must first develop genetic systems, e.g., transferrable

expression and suicidal vectors, for this strain. Subsequently, similar mutation work can be carried out as done in *M. trichosporium* OB3b.

3. Another task to achieve the application of mb is to enhance its production. One way to realize this goal is to heterologously express mb genes in robust host like *E. coli*. Succeussful production of mb heterologously requires (1) all the genes required for the production and maturation of mb to be expressed; (2) all the genes expressed to be translated into active enzymes. Another way to realize the enhancement of mb production is to do so in its native host by increasing the copy number of the mb genes or increasing their expression by manipulating their genetic regulatory system. For example, the *mbnT*::Gm^r mutant may be a good start as it can secret but not take mb back up.

4. Besides methanobactin, the genetic regulation in methanotrophs in response to metals will be investigated as the building blocks for developing regulatory models for enhanced metabolic engineering of methanotrophs. Based on our recent transcriptomic studies, there are candidate genes, including putative transporters and regulatory kinases that may be involved in copper and rare earth metals' sensing and regulation. Especially, two kinases were found to have point mutation in the smmoC mutant. The mutation of a histine kinase, MxaY, in *Methylomicrobium buryatense* 5GB1C disrupted the regulation of Mxa-/Xox- types of MeDHs by REEs. It is not unreasonable to assume that the sensor-kinase system also plays a role in the "copper-switch" in methanotrophs. The two mutated kinases may be the reason for the sMMO-constitutive phenotype. To elucidate the roles and involvement of different molecular elements in metal sensing, genetic

mutation, quantitative reverse transcription PCR, and other molecular biological techniques can be applied.

5. The long-term goal of understanding the genetics and metabolism in methanotrophs is to apply methanotrophs for valorizing methane to different products in engineered systems. To achieve this, it is proposed here that bioinformatic tools and molecular biological techniques can be applied to realize the redirection of carbon flux in methanotrophs to desired products. For example, stoichiometric model can be constructed to evaluate metabolic capcity of methanotrophs (Van Dien and Lidstrom, 2001) and as a guildline for metabolic engineering. Analysis of metabolic flux and proteome can be carried out to validate the reconstructed models. Further, efforts can be put forward into constructing pilot bioreactors and developing robust mathematical models to characterize methanotrophic growth and optimize for higher methane conversion. One important goal is to increase mass transfer of methane between gas and liquid phases. Novel bioreactor designs such as hollow fiber membrane bioreactors can be tested to achieve this goal.

6. It may also be interesting to revisit bioremediation by methanotrophs *in situ*. Methane monooxygenase (MMO) in methanotrophs has been found to be nonspecific and can oxidize organic compounds like alkanes, cyclic alkanes, aromatic hydrocarbons, chlorinated hydrocarbons, etc., as non-growth substrates. Methanotrophs have been applied for *in situ* bioremediation of polluted sites, however, the predominant form of methane monooxygenase expressed by *in situ* communities is difficult to control. Recent works in our and other labs have discovered many interesting interactions of metals and

methanotrophs. For example, gold competitively bind to mb over copper and affect the expression and activity of MMO (Kalidass, et al., 2015). Several strains of methanotrophs have been found to detoxify mercury (Vorobev et al., 2013; Boden and Murrell, 2011; Xia et al., *in review*) which may benefit microbial community. Rare earth metals may enhance methanotrophic activity (Farhan UI Haque et al., 2015, Gu et al., 2016; Chu and Lidstrom, 2016). Methantorophs compete with othe microbes for copper via the mediation of mb (Jin et al., *in preparation*). With our expanding knowledge of the ecological role of methanotrophs, especially in its interaction with metals and other microbes, it will be interesting to revisit its application in bioremediation from the microbial community point of view using meta-omics techniques and with better characterization of the environment, especially of metal content.

REFERENCES

Ala, A., Walker, A. P., Ashkan, K., Dooley, J. S., & Schilsky, M. L. (2007). Wilson's disease. *The Lancet*, *369*(9559), 397-408.

Ali, H., & Murrell, J. C. (2009). Development and validation of promoter-probe vectors for the study of methane monooxygenase gene expression in *Methylococcus capsulatus* Bath. *Microbiology*, *155*(3), 761-771.

Ali, H., Scanlan, J., Dumont, M. G., & Murrell, J. C. (2006). Duplication of the *mmoX* gene in *Methylosinus sporium*: cloning, sequencing and mutational analysis. *Microbiology*, *152*(10), 2931-2942.

Anders, S., & Huber, W. (2010). Differential expression analysis for sequence count data. *Genome biology*, *11*(10), R106.

Anders, S., Pyl, P. T., & Huber, W. (2014). HTSeq - a Python framework to work with high-throughput sequencing data. *Bioinformatics*, btu638.

Andrews, S. (2010). FastQC: a quality control tool for high throughput sequence data. http://www.bioinformatics.babraham.ac.uk/projects/fastqc/

Anthony, C. (1982). *Biochemistry of methylotrophs*. Academic Press.

Anthony, C. (1992). The structure of bacterial quinoprotein dehydrogenases. *International journal of biochemistry*, *24*(1), 29-39.

Anthony, C., & Williams, P. (2003). The structure and mechanism of methanol dehydrogenase. *Biochimica et Biophysica Acta (BBA)-Proteins and Proteomics*, *1647*(1), 18-23.

AOAC International. (1994) Official Methods of Analysis. Gaithersburg, MD, USA, *Official method 994*.12.

Asenjo, J. A., & Suk, J. S. (1986). Microbial conversion of methane into poly-β-hydroxybutyrate (PHB): growth and intracellular product accumulation in a type II methanotroph. *Journal of fermentation technology*, *64*(4), 271-278.

Baani, M., & Liesack, W. (2008). Two isozymes of particulate methane monooxygenase with different methane oxidation kinetics are found in *Methylocystis* sp. strain SC2. *Proceedings of the national academy of sciences*, *105*(29), 10203-10208.

Balasubramanian, R., Kenney, G. E., & Rosenzweig, A. C. (2011). Dual pathways for copper uptake by methanotrophic bacteria. *Journal of biological chemistry*, 286(43), 37313-37319.

Balasubramanian, R., & Rosenzweig, A. C. (2008). Copper methanobactin: a molecule whose time has come. *Current opinion in chemical biology*, *12*(2), 245-249.

Bandow, N. L., Gallagher, W. H., Behling, L., Choi, D. W., Semrau, J. D., Hartsel, S. C., ... & DiSpirito, A. A. (2011). Isolation of methanobactin from the spent media of methane-oxidizing bacteria. *Methods enzymol*, *495*, 259-269.

Baneyx, F. (1999) Recombinant protein expression in *Escherichia coli*. *Current opinion in biotechnology* 10: 411-421.

Barrios, H., Valderrama, B., & Morett, E. (1999) Compilation and analysis of σ54-dependent promoter sequences. *Nucleic acids research* 27: 4305-4313.

Piku, B. A. S. U., Katterle, B., Andersson, K. K., & Dalton, H. (2003). The membrane-associated form of methane monooxygenase from *Methylococcus capsulatus* (Bath) is a copper/iron protein. *Biochemical journal*, *369*(2), 417-427.

Behling, L. A., Hartsel, S. C., Lewis, D. E., DiSpirito, A. A., Choi, D. W., Masterson, L. R., ... & Gallagher, W. H. (2008). NMR, mass spectrometry and chemical evidence reveal a different chemical structure for methanobactin that contains oxazolone rings. *Journal of the American chemical society*, *130*(38), 12604-12605.

Belova, S. E., Baani, M., Suzina, N. E., Bodelier, P. L., Liesack, W., & Dedysh, S. N. (2011). Acetate utilization as a survival strategy of peat-inhabiting *Methylocystis* spp. *Environmental microbiology reports*, *3*(1), 36-46.

Berson, O., & Lidstrom, M. E. (1997). Cloning and characterization of *corA*, a gene encoding a copper-repressible polypeptide in the type I methanotroph, *Methylomicrobium albus* BG8. *FEMS microbiology letters*, *148*(2), 169-174.

Boden, R., & Murrell, J. C. (2011). Response to mercury (II) ions in *Methylococcus capsulatus* (Bath). *FEMS microbiology letters*, 324(2), 106-110.

Borodina, E., Nichol, T., Dumont, M. G., Smith, T. J. & Murrell, J. C. (2007) Mutagenesis of the "leucine gate" to explore the basis of catalytic versatility in soluble methane monooxygenase. *Applied and environmental microbiology* 73: 6460-6467.

Bowman, J. P. (1998) *Pseudoalteromonas prydzensis* sp. nov., a psychrotrophic, halotolerant bacterium from Antarctic sea ice. *International journal of systematic bacteriology* 48: 1037-1041.

Braun, V., & Mahren, S., (2005) Transmembrane transcriptional control (surface signalling) of the *Escherichia coli* Fec type. *FEMS microbiology reviews* 29: 673-684.

Brooks, B.E. & Buchanan, S. K. (2008) Signaling mechanisms for activation of extracytoplasmic function (ECF) sigma factors. *Biochimica et Biophysica Acta (BBA)-Biomembranes* 1778: 1930-1945.

Brusseau, G. A., Tsien, H-C, Hanson, R. S., Wackett, L. P. (1990) Optimization of trichloroethylene oxidation by methanotrophs and the use of a colorimetric assay to detect soluble methane monooxygenase activity. *Biodegradation*; 1:19-29.

Burrows, K. J., Cornish, A., Scott, D. & Higgins, I. J. (1984) Substrate specificities of the soluble and particulate methane monooxygenases of *Methylosinus trichosporium* OB3b. *Journal of general microbiology* 130: 3327-3333.

Caetano, T., Krawczyk, J. M., Mösker, E., Süssmuth, R. D., & Mendo, S. (2011). Heterologous expression, biosynthesis, and mutagenesis of type II lantibiotics from *Bacillus licheniformis* in *Escherichia coli*. *Chemistry & biology*, *18*(1), 90-100.

Cardy, D. L. N., Laidler, V., Salmond, G. P. C., & Murrell, J. C. (1991). The methane monooxygenase gene cluster of *Methylosinus trichosporium*: cloning and sequencing of the mmoC gene. *Archives of microbiology*, *156*(6), 477-483.

Castaldi, S., & Tedesco, D. (2005). Methane production and consumption in an active volcanic environment of Southern Italy. *Chemosphere*, *58*(2), 131-139.

Cha JS, Cooksey DA. Copper hypersensitivity and uptake in *Pseudomonas syringae* containing cloned components of the copper resistance operon. *Applied and environmental microbiology* 1993; 59:1671-4.

Chen, R. (2012). Bacterial expression systems for recombinant protein production: *E. coli* and beyond. *Biotechnology advances*, *30*(5), 1102-1107.

Chen, Y. P., & Yoch, D. C. (1988). Reconstitution of the electron transport system that couples formate oxidation to nitrogenase in *Methylosinus trichosporium* OB3b. *Microbiology*, *134*(12), 3123-3128.

Chistoserdova, L. (2011) Modularity of methylotrophy, revisited. *Environmental microbiology* 13: 2603-2622.

Chistoserdova, L., & Lidstrom, M. E. (1997). Molecular and mutational analysis of a DNA region separating two methylotrophy gene clusters in *Methylobacterium extorquens* AM1. *Microbiology*, *143*(5), 1729-1736.

Chistoserdova, L., Chen, S. W., Lapidus, A., & Lidstrom, M. E. (2003). Methylotrophy in *Methylobacterium extorquens* AM1 from a genomic point of view. *Journal of bacteriology*, *185*(10), 2980-2987.

Chistoserdova, L., Kalyuzhnaya, M. G., & Lidstrom, M. E. (2009). The expanding world of methylotrophic metabolism. *Annual review of microbiology*, *63*, 477-499.

Chistoserdova, L., Laukel, M., Portais, J. C., Vorholt, J. A., & Lidstrom, M. E. (2004). Multiple formate dehydrogenase enzymes in the facultative methylotroph *Methylobacterium extorquens* AM1 are dispensable for growth on methanol. *Journal of bacteriology*, *186*(1), 22-28.

Choi, D. W., Kunz, R. C., Boyd, E. S., Semrau, J. D., Antholine, W. E., Han, J. I., ... & DiSpirito, A. A. (2003). The membrane-associated methane monooxygenase (pMMO) and pMMO-NADH: quinone oxidoreductase complex from *Methylococcus capsulatus* Bath. *Journal of bacteriology*, *185*(19), 5755-5764.

Choi, D. W., Bandow, N. L., McEllistrem, M. T., Semrau, J. D., Antholine, W. E., Hartsel, S. C., ... & DiSpirito, A. A. (2010). Spectral and thermodynamic properties of methanobactin from γ-proteobacterial methane oxidizing bacteria: A case for copper competition on a molecular level. *Journal of inorganic biochemistry*, *104*(12), 1240-1247.

Choi, D. W., Do, Y. S., Zea, C. J., McEllistrem, M. T., Lee, S. W., Semrau, J. D., ... & Boyd, E. S. (2006). Spectral and thermodynamic properties of Ag (I), Au (III), Cd (II), Co (II), Fe (III), Hg (II), Mn (II), Ni (II), Pb (II), U (IV), and Zn (II) binding by methanobactin from *Methylosinus trichosporium* OB3b. *Journal of inorganic biochemistry*, *100*(12), 2150-2161.

Choi, D. W., Kunz, R. C., Boyd, E. S., Semrau, J. D., Antholine, W. E., Han, J. I., ... & DiSpirito, A. A. (2003). The membrane-associated methane monooxygenase (pMMO) and pMMO-NADH: quinone oxidoreductase complex from *Methylococcus capsulatus* Bath. *Journal of bacteriology*, *185*(19), 5755-5764.

Choi, D. W., Semrau, J. D., Antholine, W. E., Hartsel, S. C., Anderson, R. C., Carey, J. N., ... & Van Gorden, G. S. (2008). Oxidase, superoxide dismutase, and hydrogen peroxide reductase activities of methanobactin from types I and II methanotrophs. *Journal of inorganic biochemistry*, *102*(8), 1571-1580.

Choi, D. W., Zea, C. J., Do, Y. S., Semrau, J. D., Antholine, W. E., Hargrove, M. S., ... & Shafe, P. H. (2006). Spectral, kinetic, and thermodynamic properties of Cu (I) and Cu (II) binding by methanobactin from *Methylosinus trichosporium* OB3b. *Biochemistry*, *45*(5), 1442-1453.

Choi, J. M., Kim, H. G., Kim, J. S., Youn, H. S., Eom, S. H., Yu, S. L., ... & Lee, S. H. (2011). Purification, crystallization and preliminary X-ray crystallographic analysis of a methanol dehydrogenase from the marine bacterium *Methylophaga aminisulfidivorans* MPT. *Acta crystallographica section F: structural biology and crystallization communications*, *67*(4), 513-516.

Choi, Y. J., Gringorten, J. L., Bélanger, L., Morel, L., Bourque, D., Masson, L., ... & Míguez, C. B. (2008). Production of an insecticidal crystal protein from Bacillus thuringiensis by the methylotroph *Methylobacterium extorquens*. *Applied and environmental microbiology*, *74*(16), 5178-5182.

Chu, F., & Lidstrom, M. E. (2016). XoxF acts as the predominant methanol dehydrogenase in the type I methanotroph *Methylomicrobium buryatense*. *Journal of bacteriology*, *198*(8), 1317-1325.

Chubiz, L. M., Purswani, J., Carroll, S. M., & Marx, C. J. (2013). A novel pair of inducible expression vectors for use in *Methylobacterium extorquens*. *BMC research notes*, *6*(1), 183.

Cohen, S. N., Chang, A. C., & Hsu, L. (1972). Nonchromosomal antibiotic resistance in bacteria: genetic transformation of Escherichia coli by R-factor DNA. *Proceedings of the national academy of sciences*, *69*(8), 2110-2114.

Colby, J., Stirling, D. I., & Dalton, H. O. W. A. R. D. (1977). The soluble methane mono-oxygenase of *Methylococcus capsulatus* (Bath). Its ability to oxygenate n-alkanes, n-alkenes, ethers, and alicyclic, aromatic and heterocyclic compounds. *Biochemical journal*, *165*(2), 395-402.

Collins, M. L. P., Buchholz, L. A., & Remsen, C. C. (1991). Effect of copper on *Methylomonas albus* BG8. *Applied and environmental microbiology*, *57*(4), 1261-1264.

Conrado, R. J., & Gonzalez, R. (2014). Envisioning the bioconversion of methane to liquid fuels. *Science*, 343(6171), 621-623.

Costello, A. M., & Lidstrom, M. E. (1999). Molecular characterization of functional and phylogenetic genes from natural populations of methanotrophs in lake sediments. *Applied and environmental microbiology*, *65*(11), 5066-5074.

Csaki, R., Bodrossy, L., Klem, J., Murrell, J. C., & Kovacs, K. L. (2003). Genes involved in the copper-dependent regulation of soluble methane monooxygenase of *Methylococcus capsulatus* (Bath): cloning, sequencing and mutational analysis. *Microbiology*, *149*(7), 1785-1795.

Dalton, H. (2005). The Leeuwenhoek Lecture 2000 the natural and unnatural history of methane-oxidizing bacteria. *Philosophical transactions of the royal society B: biological sciences*, *360*(1458), 1207-1222.

Dalton, H., Prior, S. D., Leak, D. J., & Stanley, S. H. (1984). Regulation and control of methane monooxygenase. *Microbial growth on C1 compounds. American society for microbiology, Washington, DC*, 75-82.

Dedysh, S. N., Knief, C., & Dunfield, P. F. (2005). *Methylocella* species are facultatively methanotrophic. *Journal of bacteriology*, *187*(13), 4665-4670.

Dedysh, S. N., Liesack, W., Khmelenina, V. N., Suzina, N. E., Trotsenko, Y. A., Semrau, J. D., ... & Tiedje, J. M. (2000). Methylocella palustris gen. nov., sp. nov., a new methane-oxidizing acidophilic bacterium from peat bogs, representing a novel subtype of serine-pathway methanotrophs. *International journal of systematic and evolutionary microbiology*, *50*(3), 955-969.

Delaney, N. F., Kaczmarek, M. E., Ward, L. M., Swanson, P. K., Lee, M. C., & Marx, C. J. (2013). Development of an optimized medium, strain and high-throughput culturing methods for *Methylobacterium extorquens*. *PLoS One*, *8*(4), e62957.

Delmotte, N., Knief, C., Chaffron, S., Innerebner, G., Roschitzki, B., Schlapbach, R., ... & Vorholt, J. A. (2009). Community proteogenomics reveals insights into the physiology of phyllosphere bacteria. *Proceedings of the national academy of sciences*, *106*(38), 16428-16433.

Dennis, J. J., & Zylstra, G. J. (1998). Plasposons: modular self-cloning minitransposon derivatives for rapid genetic analysis of gram-negative bacterial genomes. *Applied and environmental microbiology*, *64*(7), 2710-2715.

DiSpirito, A. A., Semrau, J. D., Murrell, J. C., Gallagher, W. H., Dennison, C., & Vuilleumier, S. (2016). Methanobactin and the link between copper and bacterial methane oxidation. *Microbiology and molecular biology reviews*, *80*(2), 387-409.

Dubbels, B. L., DiSpirito, A. A., Morton, J. D., Semrau, J. D., Neto, J. N. E., & Bazylinski, D. A. (2004). Evidence for a copper-dependent iron transport system in the marine, magnetotactic bacterium strain MV-1. *Microbiology*, *150*(9), 2931-2945.

Dunfield, P. F., Belova, S. E., Vorob'ev, A. V., Cornish, S. L., & Dedysh, S. N. (2010). *Methylocapsa aurea* sp. nov., a facultative methanotroph possessing a particulate methane monooxygenase, and emended description of the genus *Methylocapsa*. *International journal of systematic and evolutionary microbiology*, *60*(11), 2659-2664.

Dunfield, P. F., Khmelenina, V. N., Suzina, N. E., Trotsenko, Y. A., & Dedysh, S. N. (2003). *Methylocella silvestris* sp. nov., a novel methanotroph isolated from an acidic forest cambisol. *International journal of systematic and evolutionary microbiology*, *53*(5), 1231-1239.

Dunfield, P. F., Yimga, M. T., Dedysh, S. N., Berger, U., Liesack, W., & Heyer, J. (2002). Isolation of a *Methylocystis* strain containing a novel pmo A-like gene. *FEMS microbiology ecology*, *41*(1), 17-26.

Dunfield, P. F., Yuryev, A., Senin, P., Smirnova, A. V., Stott, M. B., Hou, S., ... & Wang, J. (2007). Methane oxidation by an extremely acidophilic bacterium of the phylum Verrucomicrobia. *Nature*, *450*(7171), 879-882.

Eccleston, M., & Kelly, D. P. (1973). Inhibition by L-threonine of aspartokinase as a cause of threonine toxicity to *Methylococcus capsulatus*. *Microbiology*, *75*(1), 223-226.

El Ghazouani, A., Baslé, A., Gray, J., Graham, D. W., Firbank, S. J., & Dennison, C. (2012). Variations in methanobactin structure influences copper utilization by methane-oxidizing bacteria. *Proceedings of the national academy of sciences*, *109*(22), 8400-8404.

Ettwig, K. F., Butler, M. K., Le Paslier, D., Pelletier, E., Mangenot, S., Kuypers, M. M., ... & Gloerich, J. (2010). Nitrite-driven anaerobic methane oxidation by oxygenic bacteria. *Nature*, *464*(7288), 543-548.

Farhan UI Haque, M., Gu, W., DiSpirito, A. A., & Semrau, J. D. (2014). Marker Exchange Mutagenesis of *mxaF*, Encoding the Large Subunit of the Mxa Methanol Dehydrogenase, in *Methylosinus trichosporium* OB3b. *Applied and environmental microbiology*, *82*(5), 1549-1555.

Farhan UI Haque, M., Kalidass, B., Bandow, N., Turpin, E. A., DiSpirito, A. A., & Semrau, J. D. (2015). Cerium regulates expression of alternative methanol dehydrogenases in *Methylosinus trichosporium* OB3b. *Applied and environmental microbiology*, *81*(21), 7546-7552.

Farhan Ul Haque, M., Kalidass, B., Vorobev, A., Baral, B. S., DiSpirito, A. A., & Semrau, J. D. (2015). Methanobactin from *Methylocystis* sp. Strain SB2 Affects Gene Expression and Methane Monooxygenase Activity in *Methylosinus trichosporium* OB3b. *Applied and environmental microbiology*, *81*(7), 2466-2473.

Fei, Q., Guarnieri, M. T., Tao, L., Laurens, L. M., Dowe, N., & Pienkos, P. T. (2014). Bioconversion of natural gas to liquid fuel: opportunities and challenges. *Biotechnology advances*, *32*(3), 596-614.

Fitzgerald, K. A., & Lidstrom, M. E. (2003). Overexpression of a heterologous protein, haloalkane dehalogenase, in a poly-β-hydroxybutyrate-deficient strain of the facultative methylotroph *Methylobacterium extorquens* AM1. *Biotechnology and bioengineering*, *81*(3), 263-268.

Fjellbirkeland, A., Torsvik, V., & Øvreås, L. (2001). Methanotrophic diversity in an agricultural soil as evaluated by denaturing gradient gel electrophoresis profiles of *pmoA*, *mxaF* and 16S rDNA sequences. *Antonie van Leeuwenhoek*, *79*(2), 209-217.

Geymonat, E., Ferrando, L., & Tarlera, S. E. (2011). *Methylogaea oryzae* gen. nov., sp. nov., a mesophilic methanotroph isolated from a rice paddy field. *International journal of systematic and evolutionary microbiology*, *61*(11), 2568-2572.

Gilbert, B., McDonald, I. R., Finch, R., Stafford, G. P., Nielsen, A. K., & Murrell, J. C. (2000). Molecular analysis of the pmo (particulate methane monooxygenase) operons from two type II methanotrophs. *Applied and environmental microbiology*, *66*(3), 966-975.

Goodwin, P. M., & Anthony, C. (1995). The biosynthesis of periplasmic electron transport proteins in methylotrophic bacteria. *Microbiology*, *141*(5), 1051-1064.

Goodwin, P. M., & Anthony, C. (1998). The biochemistry, physiology and genetics of PQQ and PQQ-containing enzymes. *Advances in microbial physiology*, *40*, 1-80.

Graham, D. W., & Kim, H. J. (2011). 15 Production, Isolation, Purification, and Functional Characterization of Methanobactins. *Methods in enzymology*, *495*, 227.

Green, J., & Dalton, H. (1985). Protein B of soluble methane monooxygenase from *Methylococcus capsulatus* (Bath). A novel regulatory protein of enzyme activity. *Journal of biological chemistry*, *260*(29), 15795-15801.

Griffiths, R. I., Whiteley, A. S., O'Donnell, A. G., & Bailey, M. J. (2000). Rapid method for coextraction of DNA and RNA from natural environments for analysis of ribosomal DNA-and rRNA-based microbial community composition. *Applied and environmental microbiology*, *66*(12), 5488-5491.

Grosse, S., Laramee, L., Wendlandt, K. D., McDonald, I. R., Miguez, C. B., & Kleber, H. P. (1999). Purification and Characterization of the Soluble Methane Monooxygenase of the Type II Methanotrophic Bacterium *Methylocystis* sp. Strain WI 14. *Applied and environmental microbiology*, *65*(9), 3929-3935.

Gu, W., Baral, B. S., DiSpirito, A. A., & Semrau, J. D. (2017). An Aminotransferase is Responsible for the Deamination of the N-terminal Leucine and Required for Formation of Oxazolone Ring A in Methanobactin of *Methylosinus trichosporium* OB3b. *Applied and environmental microbiology*, *83*(1), e02619-16.

Gu, W., Haque, M. F. U., DiSpirito, A. A., & Semrau, J. D. (2016). Uptake and effect of rare earth elements on gene expression in *Methylosinus trichosporium* OB3b. *FEMS microbiology letters*, *363*(13), fnw129.

Gu, W., Haque, M. F. U., Baral, B. S., Turpin, E. A., Bandow, N. L., Kremmer, E., ... & Semrau, J. D. (2016). A TonB-dependent transporter is responsible for methanobactin uptake by *Methylosinus trichosporium* OB3b. *Applied and environmental microbiology*, *82*(6), 1917-1923.

Gutiérrez, J., Bourque, D., Criado, R., Choi, Y. J., Cintas, L. M., Hernández, P. E., & Míguez, C. B. (2005). Heterologous extracellular production of enterocin P from *Enterococcus faecium* P13 in the methylotrophic bacterium *Methylobacterium extorquens*. *FEMS microbiology letters*, *248*(1), 125-131.

Hakemian, A. S., & Rosenzweig, A. C. (2007). The biochemistry of methane oxidation. *Annu. Rev. Biochem.*, *76*, 223-241.

Hakemian, A. S., Kondapalli, K. C., Telser, J., Hoffman, B. M., Stemmler, T. L., & Rosenzweig, A. C. (2008). The metal centers of particulate methane monooxygenase from *Methylosinus trichosporium* OB3b. *Biochemistry*, *47*(26), 6793-6801.

Hanczár, T., Csáki, R., Bodrossy, L., Murrell, C. J., & Kovács, K. L. (2002). Detection and localization of two hydrogenases in *Methylococcus capsulatus* (Bath) and their potential role in methane metabolism. *Archives of microbiology*, *177*(2), 167-172.

Hanson, R. S., & Hanson, T. E. (1996). Methanotrophic bacteria. *Microbiological reviews*, *60*(2), 439-471.

Haroon, M. F., Hu, S., Shi, Y., Imelfort, M., Keller, J., Hugenholtz, P., ... & Tyson, G. W. (2013). Anaerobic oxidation of methane coupled to nitrate reduction in a novel archaeal lineage. *Nature*, *500*(7464), 567-570.

Harvey, A. L., Edrada-Ebel, R., & Quinn, R. J. (2015). The re-emergence of natural products for drug discovery in the genomics era. *Nature reviews drug discovery*, *14*(2), 111-129.

Heidrich, C., Pag, U., Josten, M., Metzger, J., Jack, R. W., Bierbaum, G., ... & Sahl, H. G. (1998). Isolation, characterization, and heterologous expression of the novel lantibiotic epicidin 280 and analysis of its biosynthetic gene cluster. *Applied and environmental microbiology*, *64*(9), 3140-3146.

Helm, J., Wendlandt, K. D., Jechorek, M., & Stottmeister, U. (2008). Potassium deficiency results in accumulation of ultra-high molecular weight poly -β-hydroxybutyrate hydroxybutyrate in a methane-utilizing mixed culture. *Journal of applied microbiology,* 105(4), 1054-1061.

Hibi, Y., Asai, K., Arafuka, H., Hamajima, M., Iwama, T., & Kawai, K. (2011). Molecular structure of La^{3+}-induced methanol dehydrogenase-like protein in *Methylobacterium radiotolerans*. *Journal of bioscience and bioengineering*, *111*(5), 547-549.

Holmes, A. J., Costello, A., Lidstrom, M. E., & Murrell, J. C. (1995). Evidence that participate methane monooxygenase and ammonia monooxygenase may be evolutionarily related. *FEMS microbiology letters*, *132*(3), 203-208.

Hou, S., Makarova, K. S., Saw, J. H., Senin, P., Ly, B. V., Zhou, Z., ... & Wolf, Y. I. (2008). Complete genome sequence of the extremely acidophilic methanotroph isolate V4, *Methylacidiphilum infernorum*, a representative of the bacterial phylum Verrucomicrobia. *Biology direct*, *3*(1), 26.

Huston, W. M., Jennings, M. P., & McEwan, A. G. (2002). The multicopper oxidase of *Pseudomonas aeruginosa* is a ferroxidase with a central role in iron acquisition. *Molecular microbiology*, *45*(6), 1741-1750.

Hutchens, E., Radajewski, S., Dumont, M. G., McDonald, I. R., & Murrell, J. C. (2004). Analysis of methanotrophic bacteria in Movile Cave by stable isotope probing. *Environmental Microbiology*, *6*(2), 111-120.

Im, J., Lee, S. W., Yoon, S., DiSpirito, A. A., & Semrau, J. D. (2011). Characterization of a novel facultative *Methylocystis* species capable of growth on methane, acetate and ethanol. *Environmental microbiology reports*, *3*(2), 174-181.

Islam, T., Jensen, S., Reigstad, L. J., Larsen, Ø., & Birkeland, N. K. (2008). Methane oxidation at 55C and pH 2 by a thermoacidophilic bacterium belonging to the Verrucomicrobia phylum. *Proceedings of the national academy of sciences*, *105*(1), 300-304.

Jenkins, M. B., Chen, J. H., Kadner, D. J., & Lion, L. W. (1994). Methanotrophic bacteria and facilitated transport of pollutants in aquifer material. *Applied and environmental microbiology*, *60*(10), 3491-3498.

Jiang, H., Chen, Y., Jiang, P., Zhang, C., Smith, T. J., Murrell, J. C., & Xing, X. H. (2010). Methanotrophs: multifunctional bacteria with promising applications in environmental bioengineering. *Biochemical Engineering Journal*, *49*(3), 277-288.

Johnson, G. T., & Kyker, G. C. (1961). Fission-product and cerium uptake by bacteria, yeasts, and molds. *Journal of bacteriology*, *81*(5), 733.

Joshi NA, Fass JN. (2011) Sickle: A sliding-window, adaptive, quality-based trimming tool for FastQ files.

Kaler, S. G. (2016). Microbial peptide de-coppers mitochondria: implications for Wilson disease. *Journal of clinical investigation*, *126*(7), 2412.

Kalidass, B., Ul-Haque, M. F., Baral, B. S., DiSpirito, A. A., & Semrau, J. D. (2015). Competition between metals for binding to methanobactin enables expression of soluble methane monooxygenase in the presence of copper. *Applied and environmental microbiology*, *81*(3), 1024-1031.

Kalidass, B., Ul-Haque, M. F., Baral, B. S., DiSpirito, A. A., & Semrau, J. D. (2015). Competition between metals for binding to methanobactin enables expression of soluble methane monooxygenase in the presence of copper. *Applied and environmental microbiology*, *81*(3), 1024-1031.

Kaluzhnaya, M., Khmelenina, V., Eshinimaev, B., Suzina, N., Nikitin, D., Solonin, A., ... & Trotsenko, Y. (2001). Taxonomic characterization of new alkaliphilic and alkalitolerant methanotrophs from soda lakes of the Southeastern Transbaikal region and description of *Methylomicrobium buryatense* sp. nov. *Systematic and applied microbiology*, *24*(2), 166-176.

Kalyuzhnaya, M. G., Puri, A. W., & Lidstrom, M. E. (2015). Metabolic engineering in methanotrophic bacteria. *Metabolic engineering*, *29*, 142-152.

Kalyuzhnaya, M. G., Yang, S., Rozova, O. N., Smalley, N. E., Clubb, J., Lamb, A., ... & Vuilleumier, S. (2013). Highly efficient methane biocatalysis revealed in a methanotrophic bacterium. *Nature communications*, *4*.

Karlsen, O. A., Ramsevik, L., Bruseth, L. J., Larsen, Ø., Brenner, A., Berven, F. S., ... & Lillehaug, J. R. (2005). Characterization of a prokaryotic haemerythrin from the methanotrophic bacterium *Methylococcus capsulatus* (Bath). *FEBS Journal*, *272*(10), 2428-2440.

Kawamura, S., O'Neil, J. G., Wilkinson, J. F. (1983) Hydrogen production by methylotrophs under anaerobic conditions. *Journal of fermentation technology*, *61*(2), 151-156.

Keltjens, J. T., Pol, A., Reimann, J., & den Camp, H. J. O. (2014). PQQ-dependent methanol dehydrogenases: rare-earth elements make a difference. *Applied microbiology and biotechnology*, *98*(14), 6163-6183.

Kenney, G. E., & Rosenzweig, A. C. (2013). Genome mining for methanobactins. *BMC biology*, *11*(1), 17.

Kenney, G. E., Sadek, M., & Rosenzweig, A. C. (2016). Copper-responsive gene expression in the methanotroph *Methylosinus trichosporium* OB3b. *Metallomics*, *8*(9), 931-940.

Khmelenina, V. N., Rozova, O. N., But, S. Y., Mustakhimov, I. I., Reshetnikov, A. S., Beschastnyi, A. P., & Trotsenko, Y. A. (2015). Biosynthesis of secondary metabolites in methanotrophs: Biochemical and genetic aspects (Review). *Applied biochemistry and microbiology*, *51*(2), 150.

Khmelenina, V. N., Rozova, O. N., But, S. Y., Mustakhimov, I. I., Reshetnikov, A. S., Beschastnyi, A. P., & Trotsenko, Y. A. (2015). Biosynthesis of secondary metabolites in methanotrophs: Biochemical and genetic aspects (Review). *Applied biochemistry and microbiology*, *51*(2), 150.

Kim, H. J., Graham, D. W., DiSpirito, A. A., Alterman, M. A., Galeva, N., Larive, C. K., ... & Sherwood, P. M. (2004). Methanobactin, a copper-acquisition compound from methane-oxidizing bacteria. *Science*, *305*(5690), 1612-1615.

Kim, B. S. (2000). Production of poly (3-hydroxybutyrate) from inexpensive substrates. *Enzyme and microbial technology*, *27*(10), 774-777.

Kim, H. J., Galeva, N., Larive, C. K., Alterman, M., & Graham, D. W. (2005). Purification and Physical− Chemical Properties of Methanobactin: A Chalkophore from Methylosinus trichosporium OB3b. *Biochemistry*, *44*(13), 5140-5148.

Kim, S. W., Kim, P., & JUNG, H. K. (1998). PHB accumulation stimulated by ammonium ions in potassium-limited cultures of *Methylobacterium organophilum*. *Journal of microbiology and biotechnology*, *8*(4), 301-304.

Kitmitto, A., Myronova, N., Basu, P., & Dalton, H. (2005). Characterization and structural analysis of an active particulate methane monooxygenase trimer from *Methylococcus capsulatus* (Bath). *Biochemistry*, *44*(33), 10954-10965.

Knapp, C. W., Fowle, D. A., Kulczycki, E., Roberts, J. A., & Graham, D. W. (2007). Methane monooxygenase gene expression mediated by methanobactin in the presence of mineral copper sources. *Proceedings of the National Academy of Sciences*, *104*(29), 12040-12045.

Knittel, K., & Boetius, A. (2009). Anaerobic oxidation of methane: progress with an unknown process. *Annual review of microbiology*, *63*, 311-334.

Koay, M., Zhang, L., Yang, B., Maher, M. J., Xiao, Z., & Wedd, A. G. (2005). CopC Protein from *Pseudomonas syringae*: Intermolecular Transfer of Copper from Both the Copper (I) and Copper (II) Sites. *Inorganic chemistry*, *44*(15), 5203-5205.

Koebnik, R. (2005). TonB-dependent trans-envelope signalling: the exception or the rule?. *Trends in microbiology*, *13*(8), 343-347.

Krawczyk, J. M., Völler, G. H., Krawczyk, B., Kretz, J., Brönstrup, M., & Süssmuth, R. D. (2013). Heterologous expression and engineering studies of labyrinthopeptins, class III lantibiotics from *Actinomadura namibiensis*. *Chemistry & biology*, *20*(1), 111-122.

Krentz, B. D., Mulheron, H. J., Semrau, J. D., DiSpirito, A. A., Bandow, N. L., Haft, D. H., ... & Gallagher, W. H. (2010). A comparison of methanobactins from *Methylosinus trichosporium* OB3b and *Methylocystis* strain SB2 predicts methanobactins are synthesized from diverse peptide precursors modified to create a common core for binding and reducing copper ions. *Biochemistry*, *49*(47), 10117-10130.

Kuhad, R. C., Singh, A., & Eriksson, K. E. L. (1997). Microorganisms and enzymes involved in the degradation of plant fiber cell walls. In *Biotechnology in the pulp and paper industry* (pp. 45-125). Springer Berlin Heidelberg.

Lamont, I. L., Beare, P. A., Ochsner, U., Vasil, A. I., & Vasil, M. L. (2002). Siderophore-mediated signaling regulates virulence factor production in *Pseudomonas aeruginosa. Proceedings of the National Academy of Sciences*, *99*(10), 7072-7077.

Lane, D. J. (1991) 16S/23S rRNA sequencing. Nucleic acid techniques in bacterial systematics 125-175.

Langmead, B., & Salzberg, S. L. (2012). Fast gapped-read alignment with Bowtie 2. *Nature methods*, *9*(4), 357-359.

Law, C. W., Chen, Y., Shi, W., & Smyth, G. K. (2014). Voom: precision weights unlock linear model analysis tools for RNA-seq read counts. *Genome biology*, *15*(2), R29.

Leak, D. J., Stanley, S. H., & Dalton, H. (1985). Implications of the nature of methane monooxygenase on carbon assimilation in methanotrophs. *Microbial gas metabolism, mechanistic, metabolic, and biotechnological aspects. Academic, London*, 201-208.

Lechevalier, M. P., & Moss, C. W. (1977). Lipids in bacterial taxonomy-a taxonomist's view. *CRC critical reviews in microbiology*, *5*(2), 109-210.

Lee, S. J., McCormick, M. S., Lippard, S. J., & Cho, U. S. (2013). Control of substrate access to the active site in methane monooxygenase. *Nature*, *494*(7437), 380-384.

Lee, S. W., Keeney, D. R., Lim, D. H., Dispirito, A. A., & Semrau, J. D. (2006). Mixed pollutant degradation by *Methylosinus trichosporium* OB3b expressing either soluble or particulate methane monooxygenase: can the tortoise beat the hare? *Applied and environmental microbiology*, *72*(12), 7503-7509.

Lee, S. Y., & Chang, H. N. (1994). Effect of complex nitrogen source on the synthesis and accumulation of poly (3-hydroxybutyric acid) by recombinant *Escherichia coli* in flask and fed-batch cultures. *Journal of environmental polymer degradation*, *2*(3), 169-176.

Lee, S. Y., Park, S. J., Park, J. P., Lee, Y., & Lee, S. H. (2005). Economic aspects of biopolymer production. *Biopolymers Online*.

Li, H., & Durbin, R. (2009). Fast and accurate short read alignment with Burrows-Wheeler transform. *Bioinformatics*, *25*(14), 1754-1760.

Li, H., Handsaker, B., Wysoker, A., Fennell, T., Ruan, J., Homer, N., ... & Durbin, R. (2009). The sequence alignment/map format and SAMtools. *Bioinformatics*, *25*(16), 2078-2079.

Lichtmannegger, J., Leitzinger, C., Wimmer, R., Schmitt, S., Schulz, S., Kabiri, Y., ... & Straub, B. K. (2016). Methanobactin reverses acute liver failure in a rat model of Wilson disease. *The Journal of clinical investigation*, *126*(7), 2721-2735.

Lidstrom, M. E. (1990). Genetics of carbon metabolism in methylotrophic bacteria. *FEMS microbiology reviews*, *7*(3-4), 431-436.

Lidstrom-Oconnor, M. E., Fulton, G. L., & Wopat, A. E. (1983). "*Methylobacterium ethanolicum*": a Syntrophic Association of Two Methylotrophic Bacteria. *Microbiology*, *129*(10), 3139-3148.

Lieberman, R. L., & Rosenzweig, A. C. (2005). Crystal structure of a membrane-bound metalloenzyme that catalyses the biological oxidation of methane. *Nature*, *434*(7030), 177-182.

Lindner, A. S., Adriaens, P., & Semrau, J. D. (2000). Transformation of ortho-substituted biphenyls by *Methylosinus trichosporium* OB3b: substituent effects on oxidation kinetics and product formation. *Archives of microbiology*, *174*(1), 35-41.

Lloyd, J. S., De Marco, P., Dalton, H., & Murrell, J. C. (1999). Heterologous expression of soluble methane monooxygenase genes in methanotrophs containing only particulate methane monooxygenase. *Archives of microbiology*, *171*(6), 364-370.

Lontoh, S., & Semrau, J. D. (1998). Methane and Trichloroethylene Degradation by *Methylosinus trichosporium* OB3b Expressing Particulate Methane Monooxygenase. *Applied and environmental microbiology*, *64*(3), 1106-1114.

Makino, T., Skretas, G., & Georgiou, G. (2011). Strain engineering for improved expression of recombinant proteins in bacteria. *Microbial cell factories*, *10*(1), 32.

Mandel, M., & Higa, A. (1970). Calcium-dependent bacteriophage DNA infection. *Journal of molecular biology*, *53*(1), 159-162.

Martin, H., & Murrell, J. C. (1995). Methane monooxygenase mutants of *Methylosinus trichosporium* constructed by marker-exchange mutagenesis. *FEMS microbiology letters*, *127*(3), 243-248.

Marx, C. J., Chistoserdova, L., & Lidstrom, M. E. (2003). Formaldehyde-detoxifying role of the tetrahydromethanopterin-linked pathway in *Methylobacterium extorquens* AM1. *Journal of bacteriology*, *185*(24), 7160-7168.

Matsen, J. B., Yang, S., Stein, L. Y., Beck, D. A., & Kalyuzhanaya, M. G. (2013). Global molecular analyses of methane metabolism in methanotrophic alphaproteobacterium, *Methylosinus trichosporium* OB3b. Part I: transcriptomic study. *Frontiers in microbiology*, *4*, 40.

McDonald, I. R., Bodrossy, L., Chen, Y., & Murrell, J. C. (2008). Molecular ecology techniques for the study of aerobic methanotrophs. *Applied and environmental microbiology*, *74*(5), 1305-1315.

Merkx, M., Kopp, D. A., Sazinsky, M. H., Blazyk, J. L., Müller, J., & Lippard, S. J. (2001). Dioxygen activation and methane hydroxylation by soluble methane monooxygenase: a tale of two irons and three proteins. *Angewandte chemie international edition*, *40*(15), 2782-2807.

Miller, M. B., & Bassler, B. L. (2001). Quorum sensing in bacteria. *Annual reviews in microbiology*, *55*(1), 165-199.

Moffett, J. W. (1990). Microbially mediated cerium oxidation in sea water. *Nature*, *345*(6274), 421.

Munson, G. P., Lam, D. L., Outten, F. W., & O'Halloran, T. V. (2000). Identification of a copper-responsive two-component system on the chromosome of *Escherichia coli* K-12. *Journal of bacteriology*, *182*(20), 5864-5871.

Murrell, J. C., & Dalton, H. (1983). Nitrogen fixation in obligate methanotrophs. *Microbiology*, *129*(11), 3481-3486.

Murrell, J. C., Gilbert, B., & McDonald, I. R. (2000). Molecular biology and regulation of methane monooxygenase. *Archives of microbiology*, *173*(5), 325-332.

Myronova, N., Kitmitto, A., Collins, R. F., Miyaji, A., & Dalton, H. (2006). Three-dimensional structure determination of a protein supercomplex that oxidizes methane to formaldehyde in *Methylococcus capsulatus* (Bath). *Biochemistry*, *45*(39), 11905-11914.

Nakagawa, T., Mitsui, R., Tani, A., Sasa, K., Tashiro, S., Iwama, T., ... & Kawai, K. (2012). A catalytic role of XoxF1 as La^{3+}-dependent methanol dehydrogenase in *Methylobacterium extorquens* strain AM1. *PloS one*, *7*(11), e50480.

Nakamaru, Y., Tagami, K., & Uchida, S. (2006). Effect of nutrient uptake by plant roots on the fate of REEs in soil. *Journal of alloys and compounds*, *408*, 413-416.

Nguyen, H. H. T., Elliott, S. J., Yip, J. H. K., & Chan, S. I. (1998). The Particulate Methane Monooxygenase from *Methylococcus capsulatus* (Bath) Is a Novel Copper-containing Three-subunit Enzyme Isolation and Characterization. *Journal of biological chemistry*, *273*(14), 7957-7966.

Nichol, T., Murrell, J. C., & Smith, T. J. (2015). Controlling the activities of the diiron centre in bacterial monooxygenases: Lessons from mutagenesis and biodiversity. *European journal of inorganic chemistry*, *2015*(21), 3419-3431.

Nielsen, A. K., Gerdes, K., & Murrell, J. C. (1997). Copper-dependent reciprocal transcriptional regulation of methane monooxygenase genes in *Methylococcus capsulatus* and *Methylosinus trichosporium*. *Molecular microbiology*, *25*(2), 399-409.

Nielsen, A. K., Gerdes, K., Degn, H., & Colin, M. J. (1996). Regulation of bacterial methane oxidation: transcription of the soluble methane mono-oxygenase operon of *Methylococcus capsulatus* (Bath) is repressed by copper ions. *Microbiology*, *142*(5), 1289-1296.

Omote, H., Hiasa, M., Matsumoto, T., Otsuka, M., & Moriyama, Y. (2006). The MATE proteins as fundamental transporters of metabolic and xenobiotic organic cations. *Trends in pharmacological sciences*, *27*(11), 587-593.

Ongley, S. E., Bian, X., Neilan, B. A., & Müller, R. (2013). Recent advances in the heterologous expression of microbial natural product biosynthetic pathways. *Natural product reports*, *30*(8), 1121-1138.

Op den Camp, H. J., Islam, T., Stott, M. B., Harhangi, H. R., Hynes, A., Schouten, S., ... & Dunfield, P. F. (2009). Environmental, genomic and taxonomic perspectives on methanotrophic Verrucomicrobia. *Environmental microbiology reports*, *1*(5), 293-306.

Paszczynski, A. J., Paidisetti, R., Johnson, A. K., Crawford, R. L., Colwell, F. S., Green, T., ... & Conrad, M. (2011). Proteomic and targeted qPCR analyses of subsurface microbial communities for presence of methane monooxygenase. *Biodegradation*, *22*(6), 1045-1059.

Patel, R. N., Hou, C. T., & Felix, A. (1978). Microbial oxidation of methane and methanol: isolation of methane-utilizing bacteria and characterization of a facultative methane-utilizing isolate. *Journal of bacteriology*, *136*(1), 352-358.

Patt, T. E., Cole, G. C., Bland, J., & Hanson, R. S. (1974). Isolation and characterization of bacteria that grow on methane and organic compounds as sole sources of carbon and energy. *Journal of Bacteriology*, *120*(2), 955-964.

Phelps, P. A., Agarwal, S. K., Speitel, G. E., & Georgiou, G. (1992). *Methylosinus trichosporium* OB3b mutants having constitutive expression of soluble methane monooxygenase in the presence of high levels of copper. *Applied and environmental microbiology*, *58*(11), 3701-3708.

Pol, A., Barends, T. R., Dietl, A., Khadem, A. F., Eygensteyn, J., Jetten, M. S., & Op den Camp, H. J. (2014). Rare earth metals are essential for methanotrophic life in volcanic mudpots. *Environmental microbiology*, *16*(1), 255-264.

Pol, A., Heijmans, K., Harhangi, H. R., Tedesco, D., Jetten, M. S., & Den Camp, H. J. O. (2007). Methanotrophy below pH 1 by a new Verrucomicrobia species. *Nature*, *450*(7171), 874-878.

Postle, K., & Larsen, R. A. (2007). TonB-dependent energy transduction between outer and cytoplasmic membranes. *Biometals*, *20*(3-4), 453.

Puri, A. W., Owen, S., Chu, F., Chavkin, T., Beck, D. A., Kalyuzhnaya, M. G., & Lidstrom, M. E. (2015). Genetic tools for the industrially promising methanotroph Methylomicrobium buryatense. *Applied and environmental microbiology*, *81*(5), 1775-1781.

Quayle, J. R. (1980). Microbial assimilation of C1 compounds.

Ricke, P., Erkel, C., Kube, M., Reinhardt, R., & Liesack, W. (2004). Comparative analysis of the conventional and novel pmo (particulate methane monooxygenase) operons from *Methylocystis* strain SC2. *Applied and environmental microbiology*, *70*(5), 3055-3063.

Roberts, E. A. (2011). Wilson's disease. *Medicine*, *39*(10), 602-604.

Rockne, K. J., & Strand, S. E. (1998). Biodegradation of bicyclic and polycyclic aromatic hydrocarbons in anaerobic enrichments. *Environmental science & technology*, *32*(24), 3962-3967.

Rosano, G. L., & Ceccarelli, E. A. (2014). Recombinant protein expression in *Escherichia coli*: advances and challenges. *Recombinant protein expression in microbial systems*, *7*.

Nordlund, P. (1993). Crystal structure of a bacterial non-haem iron hydroxylase that catalyses the biological oxidation of methane. *Nature*, *366*, 9.

Rozova, O. N., Khmelenina, V. N., Mustakhimov, I. I., Reshetnikov, A. S., & Trotsenko, Y. A. (2010). Characterization of recombinant fructose-1, 6-bisphosphate aldolase from *Methylococcus capsulatus* Bath. *Biochemistry (Moscow)*, *75*(7), 892-898.

Sambrook, J., & Russell, D. W. (2001). Molecular Cloning A Laboratory Manual Thirdth edition.

Scanlan, J., Dumont, M. G., & Murrell, J. C. (2009). Involvement of MmoR and MmoG in the transcriptional activation of soluble methane monooxygenase genes in *Methylosinus trichosporium* OB3b. *FEMS microbiology letters*, *301*(2), 181-187.

Schäfer, A., Tauch, A., Jäger, W., Kalinowski, J., Thierbach, G., & Pühler, A. (1994). Small mobilizable multi-purpose cloning vectors derived from the *Escherichia coli* plasmids pK18 and pK19: selection of defined deletions in the chromosome of *Corynebacterium glutamicum*. *Gene*, *145*(1), 69-73.

Schmidt, S., Christen, P., Kiefer, P., & Vorholt, J. A. (2010). Functional investigation of methanol dehydrogenase-like protein XoxF in *Methylobacterium extorquens* AM1. *Microbiology*, *156*(8), 2575-2586.

Schmittgen, T. D., & Livak, K. J. (2008). Analyzing real-time PCR data by the comparative CT method. *Nature protocols*, *3*(6), 1101-1108.

Semprini, L. (1997). Strategies for the aerobic co-metabolism of chlorinated solvents. *Current Opinion in Biotechnology*, *8*(3), 296-308.

Semrau, J. D., Chistoserdov, A., Lebron, J., Costello, A., Davagnino, J., Kenna, E., ... & Lidstrom, M. E. (1995). Particulate methane monooxygenase genes in methanotrophs. *Journal of Bacteriology*, *177*(11), 3071-3079.

Semrau, J. D., DiSpirito, A. A., & Vuilleumier, S. (2011). Facultative methanotrophy: false leads, true results, and suggestions for future research. *FEMS microbiology letters*, *323*(1), 1-12.

Semrau, J. D., DiSpirito, A. A., & Yoon, S. (2010). Methanotrophs and copper. *FEMS microbiology reviews*, *34*(4), 496-531.

Semrau, J. D., Jagadevan, S., DiSpirito, A. A., Khalifa, A., Scanlan, J., Bergman, B. H., ... & Haft, D. H. (2013). Methanobactin and MmoD work in concert to act as the 'copper-switch'in methanotrophs. *Environmental microbiology*, *15*(11), 3077-3086.

Semrau, J. (2011). Bioremediation via methanotrophy: overview of recent findings and suggestions for future research. *Frontiers in microbiology*, *2*, 209.

Shah, N. N., Hanna, M. L., & Taylor, R. T. (1996). Batch cultivation of *Methylosinus trichosporium* OB3b: V. Characterization of poly-β-hydroxybutyrate production under methane-dependent growth conditions. *Biotechnology and bioengineering*, *49*(2), 161-171.

Shannon, R. T. (1976). Revised effective ionic radii and systematic studies of interatomic distances in halides and chalcogenides. *Acta crystallographica section A: crystal physics, diffraction, theoretical and general crystallography*, *32*(5), 751-767.

Shukla, A. K., Vishwakarma, P., Upadhyay, S. N., Tripathi, A. K., Prasana, H. C., & Dubey, S. K. (2009). Biodegradation of trichloroethylene (TCE) by methanotrophic community. *Bioresource technology*, *100*(9), 2469-2474.

Simon, R. (1984). High frequency mobilization of gram-negative bacterial replicons by the in vitro constructed Tn5-Mob transposon. *Molecular and General Genetics MGG*, *196*(3), 413-420.

Skovran, E., Palmer, A. D., Rountree, A. M., Good, N. M., & Lidstrom, M. E. (2011). XoxF is required for expression of methanol dehydrogenase in *Methylobacterium extorquens* AM1. *Journal of bacteriology*, *193*(21), 6032-6038.

Smith, D. D. S. & Dalton, H. (1989) Solubilisation of methane monooxygenase from *Methylococcus capsulatus* (Bath). European Journal of Biochemistry 182: 667-671.

Smith, S. M., Balasubramanian, R., & Rosenzweig, A. C. (2011). Metal reconstitution of particulate methane monooxygenase and heterologous expression of the pmoB subunit. *Methods in enzymology*, *495*, 195.

Smith, T. J., Slade, S. E., Burton, N. P., Murrell, J. C., & Dalton, H. (2002). Improved system for protein engineering of the hydroxylase component of soluble methane monooxygenase. *Applied and environmental microbiology*, *68*(11), 5265-5273.

Söhngen, N. L. (1906). Über bakterien, welche methan als kohlenstoffnahrung und energiequelle gebrauchen. *Zentrabl Bakteriol Parasitenk Infektionskr*, *15*, 513-517.

Solovyev, V., & Salamov, A. (2011). Automatic annotation of microbial genomes and metagenomic sequences. *Metagenomics and its applications in agriculture, biomedicine and environmental studies*, 61-78.

Sowell, S. M., Abraham, P. E., Shah, M., Verberkmoes, N. C., Smith, D. P., Barofsky, D. F., & Giovannoni, S. J. (2011). Environmental proteomics of microbial plankton in a highly productive coastal upwelling system. *The ISME journal*, *5*(5), 856-865.

Stafford, G. P., Scanlan, J., McDonald, I. R., & Murrell, J. C. (2003). *rpoN, mmoR* and *mmoG*, genes involved in regulating the expression of soluble methane monooxygenase in *Methylosinus trichosporium* OB3b. *Microbiology*, *149*(7), 1771-1784.

Stainthorpe, A. C., Lees, V., Salmond, G. P., Dalton, H., & Murrell, J. C. (1990). The methane monooxygenase gene cluster of *Methylococcus capsulatus* (Bath). *Gene*, *91*(1), 27-34.

Stanley, S. H., & Dalton, H. (1982). Role of ribulose-1, 5-bisphosphate carboxylase/oxygenase in *Methylococcus capsulatus* (Bath). *Microbiology*, *128*(12), 2927-2935.

Stanley, S. H., Prior, S. D., Leak, D. J., & Dalton, H. (1983). Copper stress underlies the fundamental change in intracellular location of methane mono-oxygenase in methane-oxidizing organisms: studies in batch and continuous cultures. *Biotechnology letters*, *5*(7), 487-492.

Stanley, S. H., Prior, S. D., Leak, D. J., & Dalton, H. (1983). Copper stress underlies the fundamental change in intracellular location of methane mono-oxygenase in methane-oxidizing organisms: studies in batch and continuous cultures. *Biotechnology letters*, *5*(7), 487-492.

Stirling, D. I., & Dalton, H. (1979). Properties of the methane monooxygenase from extracts of *Methylosinus trichosporium* OB3b and evidence for its similarity to the enzyme from *Methylococcus capsulatus* (Bath). *European journal of biochemistry*, *96*(1), 205-212.

Stoecker, K., Bendinger, B., Schöning, B., Nielsen, P. H., Nielsen, J. L., Baranyi, C., ... & Wagner, M. (2006). Cohn's Crenothrix is a filamentous methane oxidizer with an unusual methane monooxygenase. *Proceedings of the national academy of sciences, 103*(7), 2363-2367.

Stolyar, S., Costello, A. M., Peeples, T. L., & Lidstrom, M. E. (1999). Role of multiple gene copies in particulate methane monooxygenase activity in the methane-oxidizing bacterium *Methylococcus capsulatus* Bath. *Microbiology*, *145*(5), 1235-1244.

Stolyar, S., Franke, M., & Lidstrom, M. E. (2001). Expression of individual copies of *Methylococcus capsulatu*s Bath particulate methane monooxygenase genes. *Journal of bacteriology*, *183*(5), 1810-1812.

Strong, P. J., Xie, S., & Clarke, W. P. (2015). Methane as a resource: can the methanotrophs add value? *Environmental science & technology*, *49*(7), 4001-4018.

Summer, K. H., Lichtmannegger, J., Bandow, N., Choi, D. W., DiSpirito, A. A., & Michalke, B. (2011). The biogenic methanobactin is an effective chelator for copper in a rat model for Wilson disease. *Journal of trace elements in medicine and biology*, *25*(1), 36-41.

Tavormina, P. L., Orphan, V. J., Kalyuzhnaya, M. G., Jetten, M. S., & Klotz, M. G. (2011). A novel family of functional operons encoding methane/ammonia monooxygenase-related proteins in gammaproteobacterial methanotrophs. *Environmental microbiology reports*, *3*(1), 91-100.

Taylor, S. C., Dalton, H. & Dow, C. S. (1981) Ribulose-1, 5-bisphosphate carboxylase/oxygenase and carbon assimilation in *Methylococcus capsulatus* (Bath). *Journal of general microbiology,*122: 89-94.

Trotsenko, Y. A., & Murrell, J. C. (2008). Metabolic aspects of aerobic obligate methanotrophy. *Advances in applied microbiology*, *63*, 183-229.

Ukaegbu, U. E., & Rosenzweig, A. C. (2009). Structure of the redox sensor domain of *Methylococcus capsulatus* (Bath) MmoS. *Biochemistry*, *48*(10), 2207-2215.

Vekeman, B., Speth, D., Wille, J., Cremers, G., De Vos, P., den Camp, H. J. O., & Heylen, K. (2016). Genome characteristics of two novel type I Methanotrophs enriched from North Sea

sediments containing exclusively a Lanthanide-eependent XoxF5-type methanol dehydrogenase. *Microbial ecology*, *72*(3), 503-509.

Visca, P., Leoni, L., Wilson, M. J., & Lamont, I. L. (2002). Iron transport and regulation, cell signalling and genomics: lessons from *Escherichia coli* and *Pseudomonas*. *Molecular microbiology*, *45*(5), 1177-1190.

Vita, N., Platsaki, S., Baslé, A., Allen, S. J., Paterson, N. G., Crombie, A. T., ... & Dennison, C. (2015). A four-helix bundle stores copper for methane oxidation. *Nature*, *525*(7567), 140-143.

Vorholt, J. A. (2002). Cofactor-dependent pathways of formaldehyde oxidation in methylotrophic bacteria. *Archives of microbiology*, *178*(4), 239-249.

Vorobev, A., Jagadevan, S., Baral, B. S., DiSpirito, A. A., Freemeier, B. C., Bergman, B. H., ... & Semrau, J. D. (2013). Detoxification of mercury by methanobactin from *Methylosinus trichosporium* OB3b. *Applied and environmental microbiology*, *79*(19), 5918-5926.

Vorobev, A. V., Baani, M., Doronina, N. V., Brady, A. L., Liesack, W., Dunfield, P. F., & Dedysh, S. N. (2011). *Methyloferula stellata* gen. nov., sp. nov., an acidophilic, obligately methanotrophic bacterium that possesses only a soluble methane monooxygenase. *International journal of systematic and evolutionary microbiology*, *61*(10), 2456-2463.

Vu, H. N., Subuyuj, G. A., Vijayakumar, S., Good, N. M., Martinez-Gomez, N. C., & Skovran, E. (2016). Lanthanide-dependent regulation of methanol oxidation systems in *Methylobacterium extorquens* AM1 and their contribution to methanol growth. *Journal of bacteriology*, *198*(8), 1250-1259.

Vuilleumier, S., Khmelenina, V. N., Bringel, F., Reshetnikov, A. S., Lajus, A., Mangenot, S., ... & Dunfield, P. (2012). Genome sequence of the haloalkaliphilic methanotrophic bacterium *Methylomicrobium alcaliphilum* 20Z. *Journal of bacteriology*, *194*(2), 551-552.

Ward, N., Larsen, Ø., Sakwa, J., Bruseth, L., Khouri, H., Durkin, A. S., ... & Lewis, M. (2004). Genomic insights into methanotrophy: the complete genome sequence of *Methylococcus capsulatus* (Bath). *PLoS biol*, *2*(10), e303.

Wartiainen, I., Hestnes, A. G., McDonald, I. R., & Svenning, M. M. (2006). *Methylocystis rosea* sp. nov., a novel methanotrophic bacterium from Arctic wetland soil, Svalbard, Norway (78 N). *International journal of systematic and evolutionary microbiology*, *56*(3), 541-547.

Weaver, P. F., Wall, J. D., & Gest, H. (1975). Characterization of *Rhodopseudomonas capsulata*. *Archives of microbiology*, *105*(1), 207-216.

West, A. H., & Stock, A. M. (2001). Histidine kinases and response regulator proteins in two-component signaling systems. *Trends in biochemical sciences*, *26*(6), 369-376.

Westrick, J. J., Mello, J. W., & Thomas, R. F. (1984). The groundwater supply survey. *Journal (American Water Works Association)*, 52-59.

Whittenbury, R., Phillips, K. C., & Wilkinson, J. F. (1970). Enrichment, isolation and some properties of methane-utilizing bacteria. *Microbiology*, *61*(2), 205-218.

Wijekoon, C. J., Young, T. R., Wedd, A. G., & Xiao, Z. (2015). CopC protein from *Pseudomonas fluorescens* SBW25 features a conserved novel high-affinity Cu (II) binding site. *Inorganic chemistry*, *54*(6), 2950-2959.

Willey, J. M., & Van Der Donk, W. A. (2007). Lantibiotics: peptides of diverse structure and function. *Annual review of microbiology*, *61*, 477-501.

Williams, P. A., Coates, L., Mohammed, F., Gill, R., Erskine, P. T., Coker, A., ... & Cooper, J. B. (2005). The atomic resolution structure of methanol dehydrogenase from *Methylobacterium extorquens*. *Acta Crystallographica Section D: Biological Crystallography*, *61*(1), 75-79.

Wilson, J. T., & Wilson, B. H. (1985). Biotransformation of trichloroethylene in soil. *Applied and environmental microbiology*, *49*(1), 242.

Wilson, S. M., Gleisten, M. P., & Donohue, T. J. (2008). Identification of proteins involved in formaldehyde metabolism by *Rhodobacter sphaeroides*. *Microbiology*, *154*(1), 296-305.

Wu, M. L., Ettwig, K. F., Jetten, M. S., Strous, M., Keltjens, J. T., & van Niftrik, L. (2011). A new intra-aerobic metabolism in the nitrite-dependent anaerobic methane-oxidizing bacterium *Candidatus* 'Methylomirabilis oxyfera'. *Biochemical Society Transactions, 39(1),*243-8.

Wu, M. L., Wessels, H. J., Pol, A., den Camp, H. J. O., Jetten, M. S., van Niftrik, L., & Keltjens, J. T. (2015). XoxF-Type Methanol Dehydrogenase from the Anaerobic Methanotroph "*Candidatus* Methylomirabilis oxyfera". *Applied and environmental microbiology*, *81*(4), 1442-1451.

Xia, Z. X., Dai, W. W., He, Y. N., White, S. A., Mathews, F. S., & Davidson, V. L. (2003). X-ray structure of methanol dehydrogenase from *Paracoccus denitrificans* and molecular modeling of its interactions with cytochrome c-551i. *Journal of biological inorganic chemistry*, *8*(8), 843-854.

Xia, Z. X., He, Y. N., Dai, W. W., White, S. A., Boyd, G. D., & Mathews, F. S. (1999). Detailed active site configuration of a new crystal form of methanol dehydrogenase from *Methylophilus* W3A1 at 1.9 Å Resolution. *Biochemistry*, *38*(4), 1214-1220.

Xin, J. Y., Cheng, D. D., Zhang, L. X., Lin, K., Fan, H. C., Wang, Y., & Xia, C. G. (2013). Methanobactin-mediated one-step synthesis of gold nanoparticles. *International journal of molecular sciences*, *14*(11), 21676-21688.

Yan, X., Chu, F., Puri, A. W., Fu, Y., & Lidstrom, M. E. (2016). Electroporation-based genetic manipulation in type I methanotrophs. *Applied and environmental microbiology*, *82*(7), 2062-2069.

Yimga, M. T., Dunfield, P. F., Ricke, P., Heyer, J., & Liesack, W. (2003). Wide distribution of a novel *pmoA*-like gene copy among type II methanotrophs, and its expression in *Methylocystis* strain SC2. *Applied and environmental microbiology*, *69*(9), 5593-5602.

Yoch, D. C., Chen, Y. P., & Hardin, M. G. (1990). Formate dehydrogenase from the methane oxidizer *Methylosinus trichosporium* OB3b. *Journal of bacteriology*, *172*(8), 4456-4463.

Yoon, S., Carey, J. N., & Semrau, J. D. (2009). Feasibility of atmospheric methane removal using methanotrophic biotrickling filters. *Applied microbiology and biotechnology*, *83*(5), 949-956.

Yoon, S., DiSpirito, A. A., Kraemer, S. M., & Semrau, J. D. (2011). A simple assay for screening microorganisms for chalkophore production. *Methods enzymology*, *495*, 247-258.

Yu, S. S. F., Chen, K. H. C., Tseng, M. Y. H., Wang, Y. S., Tseng, C. F., Chen, Y. J., ... & Chan, S. I. (2003). Production of high-quality particulate methane monooxygenase in high yields from *Methylococcus capsulatus* (Bath) with a hollow-fiber membrane bioreactor. *Journal of bacteriology*, *185*(20), 5915-5924.

Zahn, J. A., & DiSpirito, A. A. (1996). Membrane-associated methane monooxygenase from *Methylococcus capsulatus* (Bath). *Journal of bacteriology*, *178*(4), 1018-1029.

Zhang, Y., Xin, J., Chen, L., Song, H., & Xia, C. (2008). Biosynthesis of poly-3-hydroxybutyrate with a high molecular weight by methanotroph from methane and methanol. *Journal of natural gas chemistry*, *17*(1), 103-109.

Zischka, H., Lichtmannegger, J., Schmitt, S., Jägemann, N., Schulz, S., Wartini, D., ... & Chajes, V. (2011). Liver mitochondrial membrane crosslinking and destruction in a rat model of Wilson disease. *The Journal of clinical investigation*, *121*(4), 1508-1518.